Role of small GTP-binding protein Arl8b and its RUN domain-containing interaction partners in regulating cargo trafficking to lysosomes

Rituraj Marwaha

Thesis submitted for the partial fulfillment of the degree of

DOCTOR OF PHILOSOPHY

Department of Biological Sciences
Indian Institute of Science Education and Research Mohali
June 2019

Certificate

The work presented in this thesis has been carried out by me under the supervision of Dr. Mahak Sharma at the Department of Biological Sciences, Indian Institute of Science Education and Research (IISER) Mohali.

This work has not been submitted in part or full for a degree, diploma or fellowship to other university or institute.

Whenever contributions of others are involved, every effort is made to indicate this clearly, with due acknowledgment of collaborative research and discussions. This thesis is a bonafide record of original work done by me and all sources listed within have been detailed in the bibliography.

Date – 24.06.2019   **Place - Mohali**   **Rituraj Marwaha**

In my capacity as the supervisor of the candidate's thesis work, I certify that the above statements made by the candidate are true to the best of my knowledge.

Dr. Mahak Sharma

(Supervisor)

Acknowledgements

List of Publications

Rituraj Marwaha*, Subhash B. Arya*, Divya Jagga, Harmeet Kaur, Amit Tuli and Mahak Sharma. The Rab7 effector PLEKHM1 binds Arl8b to promote cargo traffic to lysosomes. **The Journal Cell Biology** March 2017, jcb.201607085; DOI: 10.1083/jcb.201607085 *Equal Contribution

Rituraj Marwaha and Mahak Sharma. DQ-Red BSA trafficking assay in cultured cells to assess cargo delivery to lysosomes. **Bio-protocol** Vol 7, Issue 19, October 05, 2017

Rituraj Marwaha, Devashish Dwivedi and Mahak Sharma. Emerging roles of Arf-like GTP-binding proteins: from membrane trafficking to cytoskeleton dynamics and beyond. *Proceedings of the Indian National Science Academy* (*accepted*, 2019)

<div align="center">**Thesis synopsis**</div>

Title – Role of small GTP-binding protein Arl8b and its RUN domain-containing interaction partners in regulating cargo trafficking to lysosomes

Thesis Supervisor – Dr. Mahak Sharma

Department – Department of Biological Sciences

Institute – Indian Institute of Science Education and Research, Mohali

Chapter 1: Introduction

The eukaryotic endocytic system is a complex network of membrane-bound compartments, constantly exchanging material via vesicular structures. Vesicle motility, tethering, and fusion are regulated by small GTP-binding (G) proteins and their downstream effectors. Small G proteins of the Rab, Arf, and Arl (Arf-like) families are key regulators of the membrane trafficking pathways in eukaryotes. They act as molecular switches that shuttle between the inactive GDP-bound state and membrane-localized, GTP-bound active state, recruiting their downstream effectors to target membranes in their GTP-bound state. The small G proteins localize to specific intracellular organelles and regulate trafficking to and from these compartments. The primary focus of my research is to study the role of small G proteins in regulating cargo trafficking to late endosomes and lysosomes that are the terminal degradative organelle of the endocytic pathway. Apart from its intracellular degradative function, lysosomes also regulate diverse processes such as nutrient sensing, plasma membrane repair, bone resorption, antigen presentation, tumor invasion, cell adhesion, and migration. Lysosomes are emerging as crucial regulators of cellular homeostasis, as their dysfunction leads to lysosomal storage disorders, but more recent studies have found lysosome dysfunction to be associated with common diseases such as neurodegeneration, and cancer.

The small G proteins of the Rab and Arl family, Rab7 and Arl8b, respectively, have emerged as crucial regulators of transport towards lysosome and lysosome function. Rab7 regulates

late endosome/lysosome fusion by binding to its effectors; RILP and PLEKHM1 that assist in recruitment of the multisubunit tethering factor- HOPS complex to vesicle contact sites. HOPS (HOmotypic fusion and Protein Sorting) complex is an evolutionarily conserved hexameric multisubunit tethering factor that promotes tethering of vesicles destined for fusion with lysosomes. HOPS complex also mediates trans-SNARE complex assembly that directly mediates the fusion of late-endosomes/autophagosomes with lysosomes. Besides its role in cargo delivery, Rab7 also mediates the positioning of late endosomes/lysosomes (by recruiting RILP and FYCO1 that bind to dynein and kinesin motor proteins, respectively to mediate anterograde and retrograde vesicle motility on the microtubule tracks.

The more recently characterized of the two G proteins, Arl8b, regulates both anterograde motility and fusion of lysosomes with late endosomes/autophagosomes by recruiting its downstream effectors-SKIP/PLEKHM2 and HOPS complex, respectively. Arl8b recruits SKIP/PLEKHM2, which in turn binds to kinesin motor protein to regulate anterograde motility of lysosomes on microtubule tracks. Arl8b-SKIP mediated lysosome motility is implicated in tumor invasion, cell migration, tubular lysosome formation and antigen presentation in dendritic cells. Previous studies from our group have shown that Arl8b directly interacts with one of the subunits of HOPS complex and recruits HOPS complex on lysosomes in mammalian cells, which in turn is a pre-requisite for HOPS-mediated endocytic/phagocytic cargo degradation. Rab7 is a very well characterized coordinator of endolysosome function; whereas the importance of Arl8b-mediated regulation of lysosome function is being recognized lately. We steered our efforts to further our understanding of the regulatory mechanisms of lysosome function mediated by Arl8. To this end, we have identified RUN domain-containing proteins, PLEKHM1 and Rabip4'/RUFY1, as potential Arl8b interaction partners, and elucidated the physiological relevance of these interactions.

Chapter 2: Rab7 effector PLEKHM1 binds to Arl8b to promote cargo traffic to lysosomes.

Although Rab7 and Arl8b have overlapping distribution and function in regulating cargo trafficking to lysosomes, it remains unknown if there is crosstalk and coordination between the two small G proteins to regulate lysosome positioning and function. In line with this, we

investigated the role of a known Rab7 effector, PLEKHM1 (Pleckstrin Homology domain containing Family M member-1) as a plausible interaction partner of Arl8b. The reasoning behind this hypothesis was that PLEKHM1 shares 40% identity over the length of its RUN domain with SKIP/PLEKHM2, a known Arl8b interaction partner that binds to Arl8b via its RUN domain. While the RUN domain is at the N-terminus of PLEKHM1, the binding site for Rab7 involves the PH and C1 domain, at the C-terminal end of this protein. We tested the interaction of PLEKHM1 with Arl8b and investigated its role in mediating endocytic and autophagic cargo trafficking to lysosomes. Our results demonstrate that PLEKHM1 interacts with Arl8b via its N-terminal RUN domain and serves as a linker between the two small G protein. We also identified a stretch of conserved basic residues within the RUN domain that were essential for mediating PLEKHM1's interaction with Arl8b. Using Arl8b binding-defective mutants of PLEKHM1 and siRNA-mediated Arl8b depletion approach, we show that 1) Arl8b mediates PLEKHM1 localization to lysosomes but not to Rab7–positive endosomes and 2) binding to Arl8b is required for HOPS complex recruitment to PLEKHM1/Rab7-positive compartments. Cells lacking PLEKHM1 have impaired endocytic and autophagic cargo degradation, which is rescued using wild-type PLEKHM1, but Arl8b binding-defective mutants of PLEKHM1 are unable to do so. Together, our results put forth a crucial role for PLEKHM1 as a bridging factor between Rab7- and Arl8b-positive vesicles and orchestrate assembly of vesicle fusion machinery required for endocytic and autophagic cargo clearance in lysosomes. (Marwaha R, Arya S et.al. JCB, 2017)

Chapter 3: PLEKHM1 and SKIP/PLEKHM2 compete for binding to Arl8b and regulate lysosome positioning.

SKIP/PLEKHM2 has been previously reported to interact with Arl8b via its N-terminal RUN domain and further bind to kinesin-1 motor protein to assist anterograde motility of lysosomes on microtubule tracks. Arl8b-SKIP dependent movement of lysosomes results in the peripheral distribution of the organelle. Our results show that similar to SKIP/PLEKHM2, PLEKHM1 binds to Arl8b via its N-terminal RUN domain but instead, PLEKHM1 mediates perinuclear positioning of late endosomes/lysosomes. We find that increasing the amount of either the RUN domain-containing region of SKIP or the full-length SKIP/PLEKHM2 wild-type disrupts PLEKHM1 binding to Arl8b, as demonstrated by both

Figure1: The model is representing the differential lysosome distribution mediated by SKIP/PLEKHM2 and PLEKHM1 and their physiological functions. (Marwaha R, Arya S et.al. JCB, 2017

purified protein interaction assay and co-immunoprecipitation assay. Cells depleted of PLEKHM1 or SKIP displayed lysosome accumulation in the cell periphery and cell center respectively, opposite to what was observed in the case of over-expression of these proteins, and the effect was rescued using siRNA-resistant constructs. Our results show that PLEKHM1 and SKIP/PLEKHM2 compete for binding to Arl8b and regulate opposing lysosome distribution in mammalian cells. (**Figure 1**) (**Marwaha R, Arya S et.al. JCB, 2017**)

Chapter 4: RUFY1/Rabip4' interacts with lysosomal small GTP-binding protein Arl8b and regulates cargo trafficking to lysosomes.

RUN domain and FYVE domain containing family of proteins (RUFYs), consisting of four members, namely RUFY1, RUFY2, RUFY3, and RUFY4, are reported to act as interaction partners for multiple small G proteins of the Rab and Rap families and regulate a range of cellular processes such as, endocytic cargo trafficking/recycling, macroautophagy, neurite growth, and cell migration. The family shares common domain architecture with an amino-terminal RUN domain, coiled-coil domains, and carboxy-terminal FYVE domain. Two isoforms of RUFY1, shorter (600 amino acids) and longer (708 amino acids) (Rabip4 and Rabip4', respectively) are known to bind Rab4 and Rab14 via their C-terminal region and localize to the early endosomes. At the early endosomes, RUFY1 regulate transferrin and glucose transporter recycling to the plasma membrane and Rab4a mediated organization of recycling endosomes.

Interestingly, a recent study had identified Rabip4'/RUFY1 as a regulator of lysosome subcellular distribution. Depletion of RUFY1 led to the accumulation of lysosomes to the cell periphery. Furthermore, in another study it was shown that RUFY1 depletion leads to longer retention and a subsequent delay in EGFR trafficking to lysosomes. However, the mechanism of Rabip4'/RUFY1-mediated lysosome positioning and receptor trafficking remains unknown. It was intriguing to note that the RUN domain of RUFY1 shares 38% and 35% similarity with that of known Arl8b effectors, PLEKHM1 and SKIP/PLEKHM2. Prompted by the likely role of Rabip4'/RUFY1 in mediating lysosome function, we investigated its role as a potential Arl8b interaction partner. We show that Rabip4'/RUFY1 interacts with Arl8b via its N-terminal RUN domain and conserved basic residues (R206 and R208) within the RUN domain were required for this interaction. While majority of Arl8b was localized to LAMP1-positive membranes, colocalization with Rabip4' was observed on EEA1- and Rab14-positive early endosomal/recycling endosomes. Arl8b depletion led to striking redistribution of endogenous Rabip4' from the endosomal membranes to the cytosol, which was rescued in cells expressing siRNA-resistant Arl8b. Thus, Arl8b expression is required for stable association of Rabip4' with endosomes; however the underlying mechanism is still under investigation. We also noted that RUFY1 depletion led to enlarged size of LAMP1 compartment and accordingly enhanced uptake of lysotracker dye that accumulates in the acidic compartments was observed upon RUFY1 depletion. siRNA-resistant Rabip4' WT, but not an Arl8b binding-defective mutant, restored the lysosome size back to the levels in control cells, suggesting that Arl8b-binding was required for maintaining endolysosomal morphology. We next investigated Rabip4' role in regulating replication and survival of *Salmonella enterica* serovar Typhimurium, an intracellular pathogen that resides in a vacuolar niche (SCVs or *Salmonella*-containing vacuoles) in host cells and interacts with the endolysosomal compartments of the host cells. We noted that Rabip4' regulates LAMP1 acquisition on SCVs and its depletion led to defective *Salmonella* replication in HeLa and RAW264.7 cells. Here we propose that Rabip4' and Arl8b interaction is important for ensuring typical endolysosomal morphology and regulating cargo trafficking to lysosomes including maturation of pathogen-containing vacuole.

Overall, my thesis work has revealed that PLEKHM1 and Rabip4' are novel interaction partners of the lysosomal small G protein Arl8b and via binding to Arl8b, the two proteins regulate lysosomal distribution and cargo trafficking to lysosomes.

Table of contents

Abbreviations

ARF	ADP Ribosylation Factor
ARL	ARF-like
Rab	Ras-like in Rat Brain
LAMP1/2	Lysosome Associated Membrane Protein-1/2
EEA1	Early Endosome Antigen-1
TGN	Trans Golgi Network
LE	Late Endosome
CME	Clathrin Mediated Endocytosis
CIE	Clathrin Independent Endocytosis
EGF	Epidermal Growth Factor
EGFR	Epidermal Growth Factor Receptor
LDL	Low Density Lipoprotein
DiI-LDL	DiI- Labeled Low Density Lipoprotein
DQ-BSA	De-quenched-Bovine Serum Albumin
GTP	Guanosine Triphosphate
GDP	Guanosine Diphosphate
GEF	Guanine Exchange Factor
GAP	GTPase-Activating Protein
BORC	BLOC-one-related Complex
SNARE	Soluble N-Ethylmale-imide-sensitive factor Attachment Protein Receptors
HOPS	HOmotypic Protein Sorting Complex

PLEKHM1/2	Pleckstrin Homology Domain Containing Family M Member 1/2
SKIP	SifA & Kinesin Interacting Protein
RILP	Rab Interacting Lysosomal Protein
ORP1L	Oxysterol-Binding Protein-Related Protein 1L
FYCO1	FYVE & coiled-coil Domain Containing 1
RUFY	RUN & FYVE domain containing Protein
VPS	Vacuolar Protein Sorting
LC3	Microtubule Associated Light Chain 3
GABARAP	Gamma Amino-butyric Acid receptor associated protein
ATG	Autophagy-related genes
mTORC1	Mammalian Target of Rapamycin Complex 1
TFEB	Transcription Factor EB
RUN	RPIP8, UNC-14, NESCA
PH	Pleckstrin Homology
C1	N-terminal region of Protein Kinase C
FYVE	Fab1, YOTB, Vac1 & EEA1
RPIP8	Rab2-interacting protein 8
UNC-14	Uncoordinated-14
NESCA	New Molecule containing SH3 at the carboxy terminus
KLC2	Kinesin Light Chain 2
WD-40	Tryptophan-Aspartic acid di-peptide repeats
ETK	E.coli EC 2.7.10.2 tyrosine kinase
GLUT-1	Glucose transferrin transporter 1

AP-3   Adapter Protein 3

PX   Phox homology Domain

HeLa cells   Henrietta Lacks cells

HEK cells   Human Embryonic kidney cells

SCV   *Salmonella*-Containing Vacuoles

Sifs   *Salmonella*-induced Filaments

qRT-PCR   Quantitative Real Time-Polymerase Chain Reaction

GST   Glutathione S-Transferase

NK   Natural Killer

GFP   Green Fluorescent Protein

Chapter 1

Introduction

(Parts of Section 1.2 and 1.2.2 are derived from Marwaha et.al, PINSA, 2019)

CHAPTER 1

1. Introduction

1.1 Lysosomes: Centre for cellular degradation and a dynamic metabolic signaling hub

Lysosomes are membrane-bound organelles present in eukaryotic cells responsible for the digestion and recycling of intracellular and extracellular cargo. Lysosomes were discovered back in the 1950s by Christian De Duve and his colleagues while studying the distribution of cellular enzymes using subcellular fractionation. Lysosome lumen houses nearly 60 different types of hydrolytic enzymes that have optimum activity in the acidic environment of lysosomes maintained at a pH of 4.5-5.0 by the action of proton pumping V-ATPases (Xu and Ren, 2015). Lysosomes make upto 5% of the total cell volume and are heterogeneous in size and morphology. Electron microscopy showed that lysosomes are electron dense compartments that appear multi-lamellar due to membranous folds (Luzio et al., 2007). The lysosomal membrane is a single lipid bilayer composed of integral and peripheral proteins, and the internal face is lined with glycocalyx which protects the membrane from the acidic interior of the lysosomes (Settembre et al., 2013). Till date, up to hundred lysosome resident proteins such as ion channels, transporters, nutrient sensing machinery, catabolic enzymes, structural proteins, and trafficking and fusion regulators are known. The structural proteins LAMP1 and LAMP2 (Lysosomal membrane-associated proteins) are the most abundant class of proteins present on lysosomes and are essential factors regulating trafficking events (Settembre et al., 2013). Newly synthesized lysosomal acid hydrolases, tagged with mannose-6-phosphate bind to MPRs (Mannose-6-Phosphate receptors) in TGN (Trans Golgi Network) and traffic to endosomes. Upon reaching the endosomes, the enzyme is dissociated from MPR, making MPRs free for another round of enzyme transport and the acid hydrolases are further delivered to lysosomes by vesicle maturation and fusion (Doray et al., 2002). The lysosomal membrane proteins lack the mannose-6-phosphate modification and traffic to lysosomes either directly or take the indirect path from the plasma membrane to endosomes (Ihrke et al., 2004; Luzio et al., 2007). Lysosomes are crucial for maintaining cellular

homeostasis, and any dysfunction such as mutations in the genes encoding lysosomal enzymes and other proteins involved in lysosome function can lead to at least 50 known lysosomal storage disorders, characterized by the accumulation of undigested material in lysosomes. Impaired degradative capacity due to such mutations can also cause accumulation of autophagic substrate and protein aggregates leading to neurodegeneration (Ballabio, 2016).

Lysosomes are a hub of cellular degradation, constantly exchanging cargo with endosomes for digestion and act as recycling units for cellular waste. Three major pathways are known to deliver cargo to lysosomes for degradation namely, Endocytosis, Phagocytosis, and Autophagy (**Fig 1.1**). Endocytosis is the process by which extracellular macromolecules, receptors, nutrients, fluid phase cargo, and integral membrane proteins are internalized at the plasma membrane in either clathrin-dependent (or CME – Clathrin-mediated endocytosis) or clathrin-independent manner (or CIE – Clathrin-independent endocytosis) and delivered to early endosomes. Early endosomes sort the cargo and either recycle it back to the plasma membrane or direct it towards late endosomes which eventually fuse transiently or completely with lysosomes forming endolysosomes and leading to subsequent degradation of the cargo (Luzio et al., 2007). Endocytosis is a tightly regulated process involving adaptor proteins (AP 1 to 5), clathrin coat proteins, dynamin in case of CME and caveolae, flotillin, endophilins, Rho, RacA, Cdc42 and Arf6 proteins in case of CIE as key molecular regulators (Kaksonen and Roux, 2018; Sandvig et al., 2011). Ligand-bound growth factor receptors such as EGFR, LDL bound to its receptor, parts of the membrane, fluid from the extracellular environment, viruses and toxins are few examples out of a plethora of macromolecules internalized by cells via endocytosis. Endocytic trafficking is essential for maintaining the nutrient pool of the cell, regulating receptor-mediated signaling and plasma membrane homeostasis (Kumari et al., 2010).

In mammals uptake of extracellular material typically larger than 0.5μm by specialized cells such as macrophages, dendritic cells, neutrophils, and monocytes is known as phagocytosis. Microbes, dead cells and cellular debris are the primary cargo taken up by phagocytosis (Luzio et al., 2007). Initiation of phagocytosis occurs at the plasma membrane by repeated interactions of the cargo with phagocytic receptors (Pattern recognition

receptors, Opsonic receptors, and receptors for apoptotic corpses), followed by reorganization of host cell actin cytoskeleton to form membrane protrusions that eventually engulf the particulate matter in a membrane-enclosed structure known as phagosome. The phagosome communicates extensively with the components of the endocytic pathway and matures to ultimately fuse with lysosomes, forming phagolysosomes which are responsible for clearing out the unwanted particulate matter (Flannagan et al., 2012). Phagocytosis is essential for mediating innate and adaptive immune responses in mammalian systems.
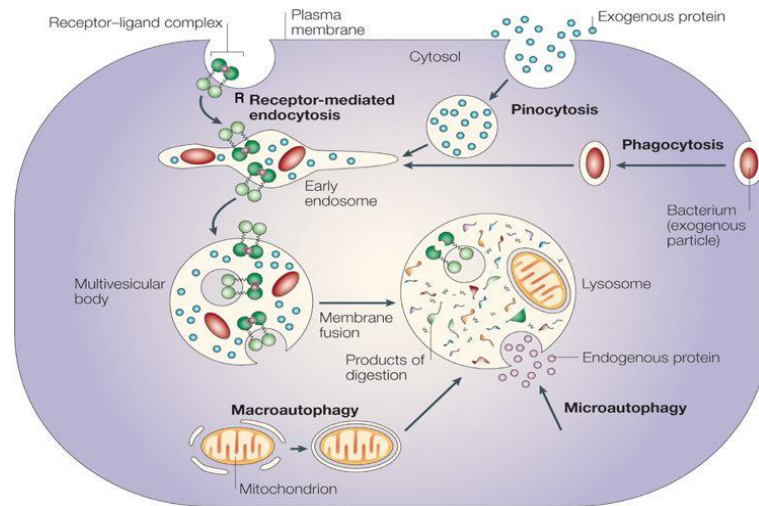
Figure 1.1: Schematic representation of cargo trafficking routes to lysosomes. Three major pathways namely Endocytosis, Phagocytosis and Autophagy deliver cargo to lysosomes. Adapted from (Ciechanover, 2005)

The third route delivering cargo to lysosomes for degradation is autophagy or macroautophagy. Cytoplasmic contents such as worn out organelles, misfolded proteins, and protein aggregates are engulfed in a double membrane structure known as autophagosomes that eventually fuse with late endosomes and lysosomes. Autophagosome formation initiates at ER (Endoplasmic Reticulum) sites enriched in PI3P, recruiting membrane to form isolation membrane/phagophore. As the isolation membrane grows, it incorporates autophagic receptors LC3, GABARAPs and p62 for cargo selection and engulfs the cargo in a double membrane-enclosed compartment known as autophagosome (Luzio et al., 2007). The autophagosomes mature and extensively fuse with the late endocytic compartments forming amphisomes, which finally fuse with lysosomes to form degradative autolysosomal compartments. Once the sequestered material is degraded, the lysosomes are regenerated.

Autophagosome formation is tightly regulated by a conserved set of 18 autophagy-related gene (ATG) products and fusion with lysosomes is known to be regulated by small GTP-binding protein Rab7, tethering factor HOPS complex and Syntaxin-7, Syntaxin-17 SNARE proteins (Klionsky et al., 2016; Zhao and Zhang, 2018). Autophagy is essential for maintaining cellular homeostasis as it regulates the basal turnover of damaged organelles and protein aggregates and is a crucial cell survival mechanism under stress conditions (Zhao and Zhang, 2018).

Recent advancements in the field of lysosomal biology have uncovered that in addition to their traditional role in degradation, these highly dynamic organelles regulate a range of biological processes including plasma membrane repair, antigen presentation, metabolic signaling, cell adhesion, cell migration, gene regulation, and tumor invasion (**Fig 1.2**). Lysosomes are highly dynamic organelles displaying spatially distinct localizations and different characteristics at these localizations, hence regulating a variety of cellular processes and maintaining cellular homeostasis. Lysosomes act as signaling hubs for nutrient sensing machinery dependent upon mTORC1 activity and also regulate Transcription factor-EB (TFEB) mediated transcription of autophagic and lysosomal genes. (Lim and Zoncu, 2016). Lysosomes localized to cell periphery regulate cell adhesion and migration by ensuring the efficient turnover of focal adhesion complexes. Lysosomes in dendritic cells not only digest the bacteria releasing the antigenic peptides to be loaded onto MHC-II molecules but also form tubules to transport peptide-loaded MHC-II molecules to plasma membrane which are presented to CD4+ T-cells for generating immune response (Pu et al., 2016). Cells have devised an elegant mechanism of resealing ruptured plasma membrane by recruiting lysosomes to the site of damage and avoid cell death by apoptosis. Increased calcium ion influx from the extracellular environment due to membrane rupture recruits lysosomes to the site of injury followed by rapid exocytosis (Reddy et al., 2001). Impaired lysosome function is associated with more common diseases such as cancer, neurodegeneration, and obesity. While some pathogens such as *Coxiella*, *Listeria*, *Shigella*, etc. modulate the host endocytic pathway to avoid fusion with lysosomes and escape degradation, there are others like *Salmonella* enterica serovar Typhimurium *(Salmonella* Typhimurium) which reside in lysosomes and exploit the endolysosomal pathway for survival and replication (Tuli and Sharma, 2018).
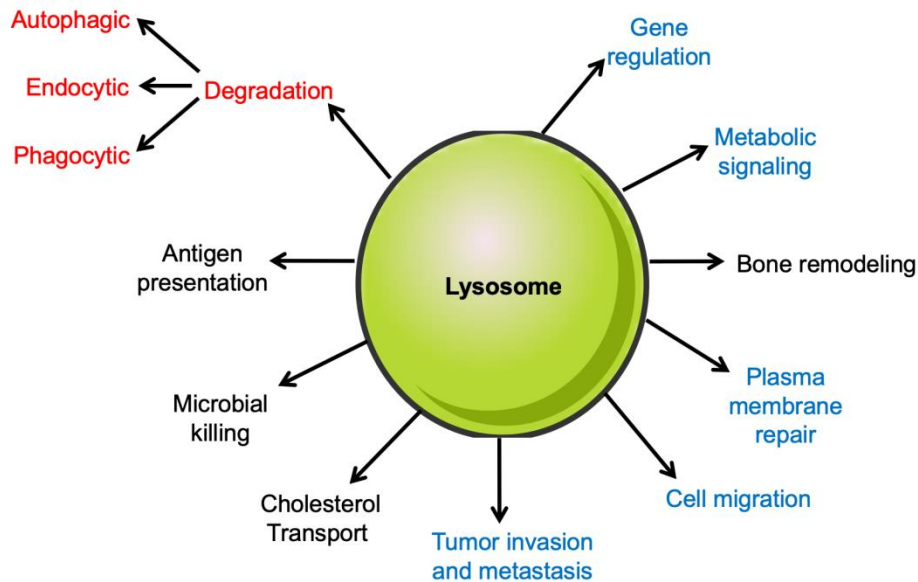
Figure 1.2: Role of lysosomes in a diverse set of cellular functions. Lysosome function is dependent both on its degradative capacity and ability to move on microtubule tracks. Text in red indicates the classical lysosome function of cargo degradation, received by endocytic, autophagic and phagocytic routes. The blue text marks the cellular functions of lysosomes, where the position of the lysosomes to the cell periphery is essential. Cellular functions mentioned in black involve cargo, in parallel to localization of lysosomes to cell periphery.
Made in reference from (Pu et al., 2016)

1.2 Molecular machinery regulating lysosome function

Lysosomes regulate diverse physiological functions by virtue of its fusion with other endocytic compartments and motility on microtubule tracks. The coordinated action of molecular players mediates fusion and spatial distribution of lysosomes.

Exchange of cargo between lysosomes and endosomes/autophagosomes occurs by complete fusion of the two compartments or by transient 'kiss and run' events forming momentary contacts (Luzio et al., 2007). In a general scheme of a vesicle fusion event, the process initiates with the pinching off of cargo loaded vesicle at the donor compartment, followed by its transport on microtubule tracks till it reaches in the proximity of the acceptor compartment. Membrane fusion initiates with the recruitment of tethering factors to the desired site, where they mediate docking of vesicles and SNARE assembly which eventually

leads to the fusion of the two vesicles and subsequent mixing of contents (Vazquez-Martinez and Malagon, 2011). All the steps in the vesicle fusion pathway are regulated by members of the Ras superfamily of small GTP-binding proteins and their downstream interaction partners such as coat proteins,
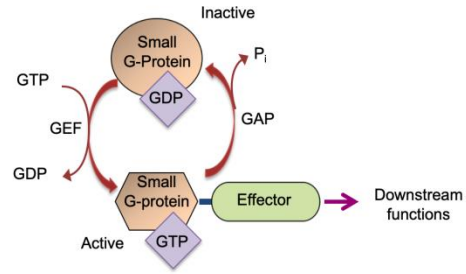
Figure 1.3: General scheme depicting GTP/GDP exchange cycle of small GTP-binding proteins. *Adapted from Marwaha et.al. PINSA, 2019*

kinesin, and dynein motor proteins, tethering factors and SNAREs. Small GTP-binding proteins are molecular switches that shuttle between active GTP bound and inactive GDP bound state. In the active state, small GTP-binding proteins localize to organelle membranes and recruit their downstream effectors implicated in vesicle motility, tethering, and fusion. Regulatory proteins control this switch between active and inactive states, i.e., guanine nucleotide exchange factors (GEFs), catalyze the exchange of GDP for GTP and GTPase-activating proteins (GAPs) accelerate hydrolysis of the bound GTP to GDP (**Fig 1.3**). Vesicle motility is mediated by microtubule-based motor proteins kinesin and dynein which mediate plus end-directed anterograde or minus end-directed retrograde movement respectively. Recruitment of motor proteins to vesicle membranes is either by direct interaction with small GTP-binding proteins or mediated by adaptor proteins (Fu and Holzbaur, 2014). Tethering proteins are either long coiled-coil or multisubunit proteins that link cargo-containing vesicles to acceptor membranes, ensuring accurate vesicle docking and fusion. Tethering factors further proof-read and facilitate the assembly of cognate SNARE proteins which are responsible for catalyzing the final merging of lipid bilayers contributed by vesicles destined for fusion(Chia and Gleeson, 2014) (**Fig 1.4**).
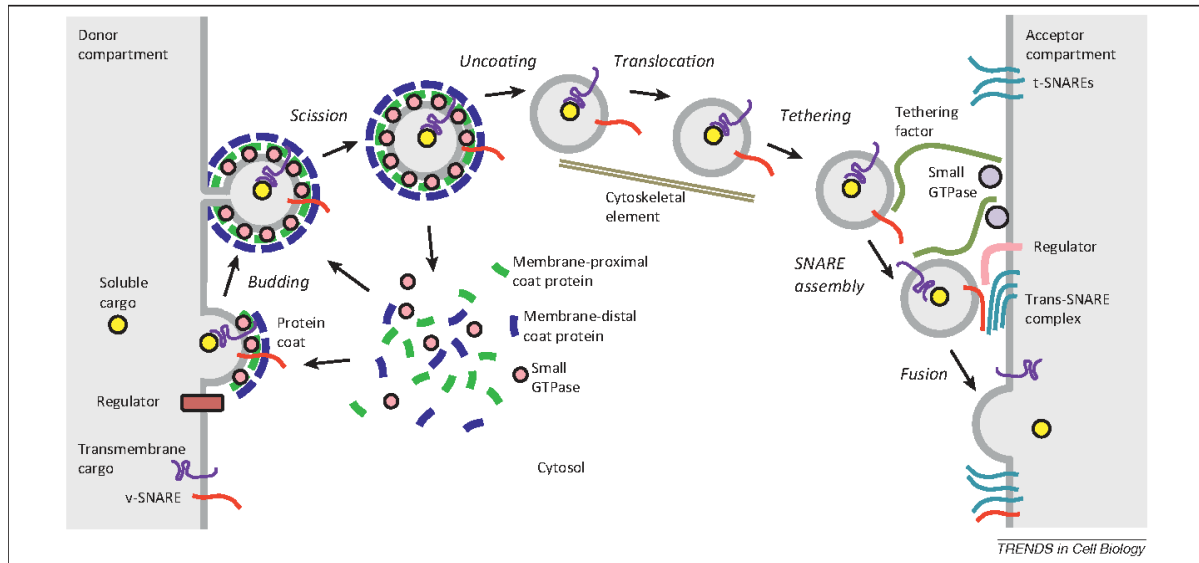
Figure 1.4: Model depicting the steps and classes of regulatory proteins involved in vesicular fusion pathway. (Bonifacino, 2014)

Two small GTP-binding proteins Rab7 on late endosomes and Arl8b on lysosomes are emerging as crucial regulators of endolysosomal biology. Like all other Ras superfamily proteins, Rab7 and Arl8b utilize a simple biochemical strategy of alternating between a GTP-bound (active) and a GDP-bound (inactive) state. In the active state, the G proteins recruit their interaction partners, also known as effectors, and perform downstream functions until GTP hydrolysis returns them to their inactive state. Role of Rab7, Arl8b and their downstream effectors is described below.

1.2.1 Rab7 – Key regulator of LE/lysosome fusion and motility

Rab7 is a well-characterized late endosomal small GTP-binding protein. In mammals two Rab7 proteins, Rab7a and Rab7b are expressed. Rab7a primarily localizes to late endosomes, whereas Rab7b is present on both late endosomes and TGN. Rab7a (hereafter referred as Rab7) binds to several downstream effector proteins and mediates maturation of early endosomes in late endosomes, fusion of late endosomes and autophagosomes with lysosomes in the perinuclear region, motility and positioning of endolysosomes, and biogenesis of lysosomes (Guerra and Bucci, 2016). Mon1-Ccz1 complex facilitates the activation of Rab7 by exchanging GDP for GTP, and its function is conserved from yeast to mammals (Langemeyer et al., 2018). In mammalian cells, Rab7 facilitates fusion of late endosomes with lysosomes and autophagosomes by recruiting its downstream effectors RILP and

8

PLEKHM1 which further bind to multisubunit tethering factor HOPS complex (McEwan et al., 2015a; Wijdeven et al., 2016). Rab7 effector PLEKHM1 also binds to SNARE protein Syntaxin-17 and mediates clearance of autophagic cargo (McEwan and Dikic, 2015). Rab7 along with its effector ORP1L, a cholesterol sensing protein, mediates formation of endoplasmic reticulum-late endosome contact sites, leading to the exclusion of fusion machinery from such sites. It is suggested that ORP1L and Rab7 provide temporal regulation to autophagosome-lysosome fusion (Wijdeven et al., 2016). Yeast cells lack RILP and PLEKHM1, but the fusion function of Ypt7 (the yeast homolog of mammalian Rab7) is conserved as it directly recruits the HOPS complex to vacuole/lysosomes and facilitates cargo degradation (Guerra and Bucci, 2016). Rab7 regulates the motility of late endosomes/lysosomes on microtubule tracks through its effectors RILP and FYCO1 that bind to dynein and kinesin motor proteins respectively (Jordens et al., 2001; Pankiv et al., 2010) (**Fig 1.5**).

Apart from regulating LE/lysosome function, Rab7 by its interaction with retromer subunits Vps35 and Vps26 modulate retrograde trafficking of cargo from endosomes to TGN (Zhang et al., 2009). In neuronal cells, Rab7 and Protudin regulate neurite growth by mediating efficient trafficking of the neutrophin receptor (Bucci et al., 2014). Rab7 is linked to actin cytoskeleton organization and assembly. Notably, loss of function mutation in Rab7 associates with various human disorders such as Charcot-Marie-Tooth type 2B (CMT2B) neuropathy, cancer progression, and accumulation of undigested protein aggregates leading to neurodegeneration.
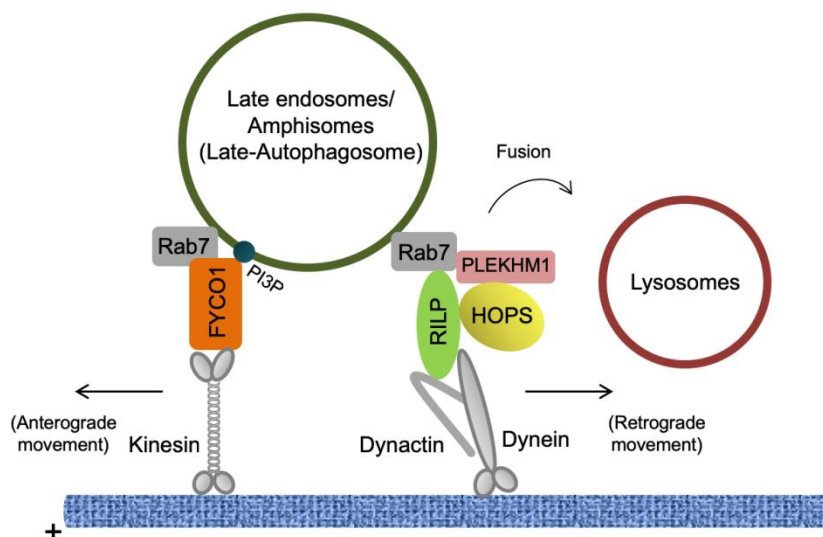
Figure 1.5: Schematic representing the role of Rab7 and its downstream effectors at the late-endosome/autophagosome-lysosome junction. Made by taking reference from (Nakamura and Yoshimori, 2017)

1.2.2 Arl8 – Crucial regulator of lysosome biology (Part of this section is accepted for publication in Proceedings of Indian National Science Academy, 2019)

Arl8 is the only known Arl protein primarily localized to lysosomes, the organelle responsible for degradation of extracellular and intracellular cargo. It is highly conserved from protozoan to metazoans, lost in yeast but reappeared in higher-order organisms. In organisms such as *Drosophila melanogaster*, *Trypanosoma cruzi* and *Caenorhabditis elegans*, a single gene encodes for Arl8, whereas in plants like *Arabidopsis thaliana* and *Nicotiana tabacum*, there are four Arl8-related genes. In mammals, two Arl8 paralogs are present; Arl8a and Arl8b that share 91% sequence identity.

Initial reports on Arl8b suggested its localization on the mitotic spindle with a role in chromosome segregation during mitosis (Okai et al., 2004). Soon these findings were refuted with the data showing lysosomal localization of both Arl8 paralogs and their role in regulating lysosome motility on the microtubule tracks (Bagshaw et al., 2006; Rosa-Ferreira and Munro, 2011). Subsequent studies identified SKIP (Sif-A and kinesin-interacting protein; also known as PLEKHM2) as the downstream effector of Arl8b that mediated kinesin-1 recruitment to promote microtubule-based motility of lysosomes towards the cell periphery (Boucrot et al., 2005; Rosa-Ferreira and Munro, 2011). Accordingly, siRNA-mediated

depletion of both Arl8b and SKIP in mammalian cells resulted in perinuclear clustering of lysosomes. Later studies have revealed that Arl8b-SKIP complex also regulates motility of lysosome-related organelles (lytic granules) in NK cells, and lysosome tubulation in macrophages and dendritic cells (Mrakovic et al., 2012; Tuli et al., 2013). Anterograde movement of p14-MP1 protein complex localized to late-endosomes mediated by Arl8b and kinesin-1 have been reported to modulate focal adhesions, leading to their disassembly and turnover thus helping the cells to migrate (Schiefermeier et al., 2014). In *C. elegans*, where Arl8b effector SKIP is not present, Arl8 directly binds to the kinesin motor protein Unc-104/Kif-1a and transports the pre-synaptic vesicles in neurons (Klassen et al., 2010; Wu et al., 2013). As described in a recent study, Arl8 in its GTP-bound state is recruited to the membranes of synaptic vesicles and promotes the transition of Unc-104 from an auto-inhibited state to active state, thus facilitating the transport of vesicles on microtubule tracks (Niwa et al., 2016).

Lysosome positioning by Arl8b has been implicated in cell migration and cancer cell invasion. Depletion of Arl8b in prostate cancer cells led to the juxtanuclear accumulation of lysosomes and resulted in reduced invasive growth and protease release to degrade the extracellular matrix (Cabukusta and Neefjes, 2018; Dykes et al., 2016a). Arl8b has also been shown to play an essential role in regulating the trafficking of antigen-presenting molecules like CD1d and MHC class II towards lysosomes (Garg et al., 2011; Michelet et al., 2015). Together, these studies provide strong evidence of Arl8's role in regulating lysosome positioning and motility in various cell types and conservation of this function among different organisms.

BORC (BLOC (Biogenesis of lysosome-related organelles complex) One-Related Complex), a multi-subunit protein complex has been recently reported to regulate membrane association of Arl8b (Pu et al., 2015). Knockout of myrlysin, a BORC-specific subunit, led to dissociation of Arl8b from lysosomal membranes and lysosome clustering in the perinuclear region (Pu et al., 2015). In mammalian cell studies, BORC complex did not show any GEF activity towards Arl8b, while in *C. elegans* BORC subunit, SAM-4, was shown to have GEF activity towards Arl8 and BORC-mediated activation of Arl8 was essential for the transport of SVPs (synaptic vesicle precursor) in axons (Niwa et al., 2016). In neuronal cells, the BORC-Arl8-SKIP-Kinesin-1 complex has been shown to regulate lysosome movement

11

specifically in axons and not in dendrites. The axonal lysosomal movement was also shown to be essential for maintaining the growth cone and turnover of autophagosomes in distal axons (Farias et al., 2017). Findings from two recent studies suggest that under nutrient-rich conditions, BORC weakly associates with Ragulator, a scaffold complex that regulates mTOR complex 1 (mTORC1). BORC association with Ragulator recruits mTORC1 to lysosomes, and simultaneously BORC promotes Arl8-kinesin recruitment to lysosomes, positioning them to the cell periphery and leading to mTORC1 activation (Filipek et al., 2017; Pu et al., 2017). Interestingly, BORC and Arl8 recruit two kinds of kinesin motors namely kinesin-1 (also known as KIF5B) and kinesin-3 (also known as KIF1A) for lysosome movement on microtubule tracks (Guardia et al., 2016).

Apart from its role in lysosome positioning, Arl8b is also a crucial factor responsible for mediating fusion of lysosomes with other compartments. The set of downstream effectors of Arl8b that facilitate fusion events are the HOPS (HOmotypic Protein Sorting) complex - a hexameric (consisting of Vps-41 and 39 as accessory and Vps-11, 16, 18 and 33a as core subunits) tethering complex and SKIP/PLEKHM2. First evidence for Arl8's role in cargo trafficking was shown in *C. elegans* where its loss led to an impaired fusion of late endosomes and lysosomes (Nakae et al., 2010). In mammalian cells, Arl8b directly binds to Vps41 subunit of the HOPS complex (Hexameric complex), recruiting it to lysosomal membranes that further facilitate the assembly of the rest of the subunits, except for Vps39 which is brought onto these endosomes through its interaction with SKIP (Garg et al., 2011; Khatter et al., 2015a).

Arl8b and its effectors not only support cellular physiology but are also targeted by the intracellular pathogens, such as *Salmonella* typhimurium and *Mycobacterium tuberculosis* that exploits Arl8b (and its effectors) for its survival and replication in mammalian cells (Michelet et al., 2018; Sindhwani et al., 2017). Arl8b depletion was observed to hamper *Salmonell*a-induced filament (Sif, a structure important for bacterial pathogenesis) formation (Kaniuk et al., 2011). In a recent study from our group, we have reported that HOPS complex is recruited to the vacuolar survival and replicative niche of the pathogen in an Arl8b-dependent manner that helps the bacteria-containing vacuole to gain access to host membrane and nutrition (Sindhwani et al., 2017) (**Fig 1.6**).
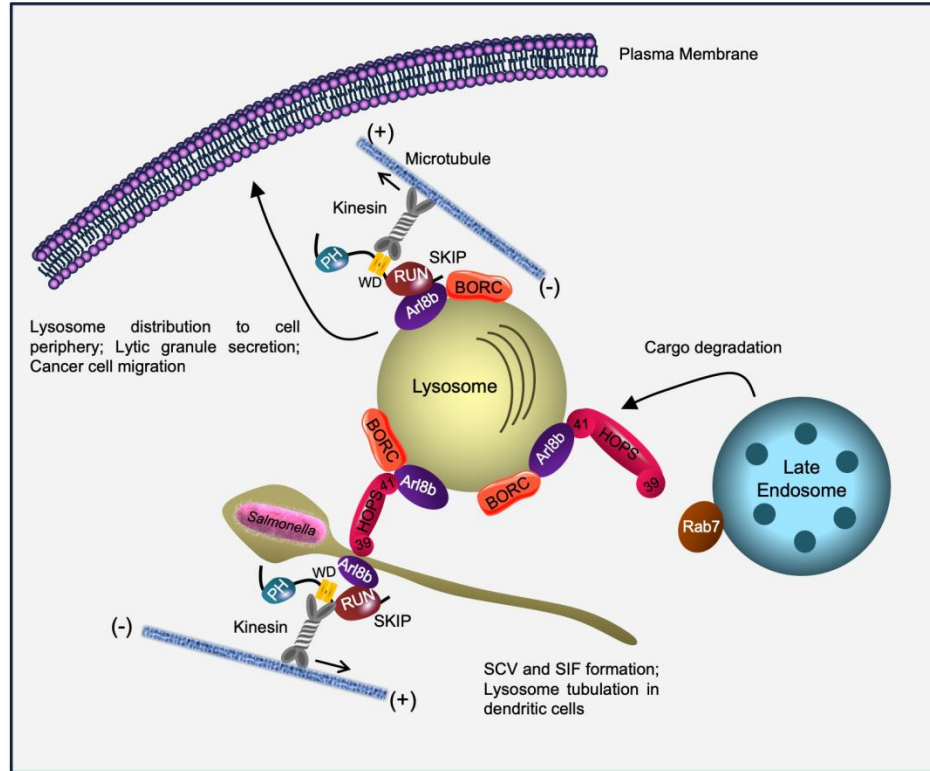
Figure 1.6: Arl8 and its downstream effectors. Arl8b localizes to the lysosomal membranes in the presence of multi-subunit complex BORC. Once on the membranes, in its GTP-bound state, Arl8b binds to its downstream effectors like SKIP, HOPS complex, and PLEKHM1 to regulate lysosome positioning and cargo degradation. The Arl8b-SKIP-HOPS complex machinery is exploited by pathogens like *Salmonella* for establishing infection in cells. (Modified from Marwaha et.al. PINSA, 2019)

Earlier studies have documented that infection with virulent *M. tuberculosis* causes necrosis of the macrophages, a form of cell death. Induction of necrosis leads to puncturing of the plasma membrane, allowing the bacteria to escape from their host macrophage and infect new cells. In contrast, when macrophages are infected with avirulent *M. tuberculosis*, these lesions are rapidly resealed by a repair mechanism (termed as plasma membrane repair) dependent on lysosomes recruitment (Behar et al., 2010; Divangahi et al., 2009). The mechanism of *M. tuberculosis* infection induced plasma membrane repair remains unknown. In a recent study, it has been reported that the presence of Arl8b is crucial factor that regulates the killing of *M. tuberculosis*-infected macrophages as silencing of the Arl8b gene significantly increased the level of necrotic cells upon avirulent *M. tuberculosis* infection (Michelet et al., 2018). Collectively, these studies provide interesting mechanistic insight into how *M. tuberculosis* hijacks the host membrane repair machinery for its survival. Also, in

13

plants, Arl8 is shown to act as a crucial host factor required for Tomato Mosaic virus (ToMV) pathogenesis (Nishikiori et al., 2011). These studies show that Arl8 is an essential factor regulating lysosome biology and further investigation of its diversity in function and effectors will help in understanding the underlying regulatory mechanisms of lysosome function.

1.3 RUN domain-containing proteins – Effectors for small GTP-binding proteins

Small GTP binding proteins of the Ras superfamily are key intracellular signal transduction molecules and crucial regulators of a variety of physiological functions such as proliferation, differentiation, cytoskeleton organization, and membrane trafficking. Members of the Ras superfamily of small GTP-binding proteins in their active GTP bound state recruit downstream effectors which regulate a range of cellular processes. With the advancement of the field, a large set of effectors and the domains in these proteins responsible for interaction with Ras superfamily small GTP-binding proteins are well characterized. Some of the examples include p21-activated kinase (PAK) that binds to Rac-6 via its PBD (p21- Rho-binding domain) or also known as CRIB (Cdc42/Rac interactive binding) domain; Ral guanine nucleotide dissociation stimulator (RalGDS) contains RA (Ras-associating or RalGDS/AF6) domain responsible for binding to small GTP-binding proteins; Ras-binding domain (Raf RBD) mediates interaction between Ras and Raf (Callebaut et al., 2001).

RUN domain-containing proteins are emerging as a class of effectors for some of the Rabs and Rap small GTP-binding proteins which are members of the Ras superfamily. The name RUN domain is derived from RPIP8 (RaP2 interacting protein 8), UNC-14 and NESCA (New molecule containing SH3 at the Carboxyl-terminus). Characterization of the RUN domain began with its identification in RPIP8 protein followed by bioinformatic analysis using PSI-BLAST and HHMer tools to classify other proteins having this domain. RUN domain organizes into six conserved blocks named A to F which are predicted to form the core, and insertions of variable lengths link these blocks. The secondary structure adopted by the core of the RUN domain is predominantly α-helical. Basic residues in block A and D of RUN domain are predicted to be implicated in the interaction with small GTP-binding proteins, similar to the conserved residues in other small GTP-binding domains such as RA

and RBD (Callebaut et al., 2001). Crystal structure analysis of the RUN domain of RPIP8 in conjunction with Rap2 supports the role of basic residues in mediating the interaction with small GTP-binding proteins (Kukimoto-Niino et al., 2006). **Fig 1.7** lists some of the RUN domain-containing proteins and their interacting small GTP-binding proteins.
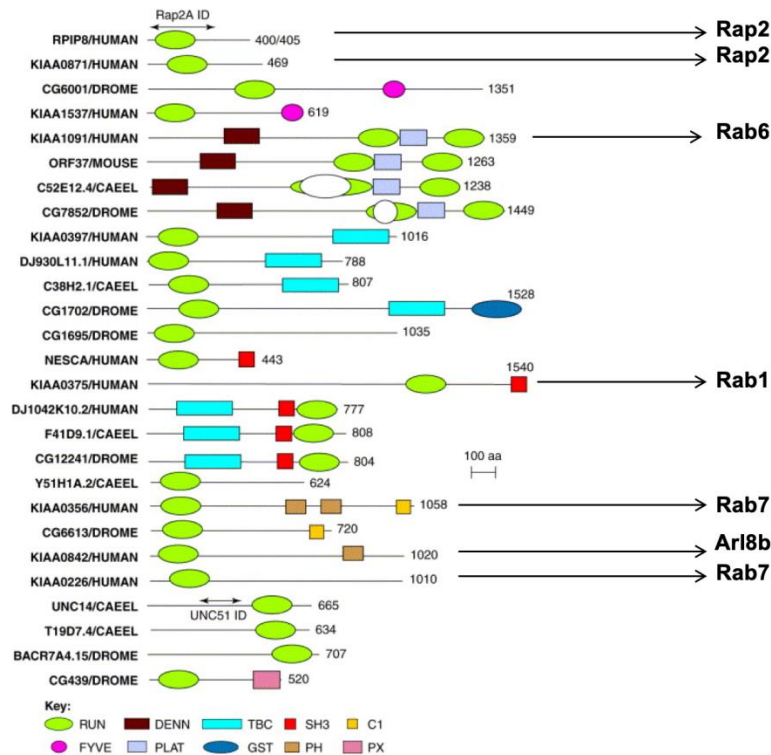
Figure 1.7: List of RUN domain containing proteins. The figure represents the domain architecture of these proteins and known interacting small GTP-binding proteins. Modified from (Callebaut et al., 2001)

 Other than Rabs and Rap small GTP-binding proteins, interestingly RUN domain-containing effectors are now known for at least one member of the Arl family of small G-proteins, Arl8b. As mentioned previously, RUN domain-containing protein SKIP/PLEKHM2 binds to Arl8b to regulate lysosome positioning and cargo trafficking to lysosomes. To further expand our understanding of the regulation of lysosome biology via Arl8b, we explored RUN domain-containing proteins PLEKHM1 and RUFY family protein RUFY1/Rabip4' as potential Arl8b interaction partners. PLEKHM1 and RUFY1/Rabip4' are plausible candidates as previous reports suggest a regulatory role for these proteins in cargo trafficking

to lysosomes and mediating lysosome distribution. PLEKHM1 and RUFY1/Rabip4' are described in detail in the following section.

1.3.1 PLEKHM1 – Multidomain endolysosomal adaptor protein

PLEKHM1, Pleckstrin homology domain-containing family M member-1, is a 1056 amino acid long protein having multiple domains; N-terminal RUN domain, two PH domains, LIR (LC3 interacting region) motif, and a C-terminal C1 domain. The other member of this family is PLEKHM2/SKIP, previously demonstrated as Arl8b effector and described in earlier sections. PLEKHM1 was initially identified as an adaptor protein having oligosaccharide sialyl-Le(x) modification from a human colonic cDNA library and termed as AP162 (Adapter protein, with molecular weight 162) (Hartel-Schenk et al., 2001). One of the first evidence of PLEKHM1's involvement in the vesicular trafficking pathway came when Van Wesenbeeck and colleagues identified PLEKHM1 as one of the genes mutated in Osteopetrosis disease (commonly known as the stone bone disorder). High-density brittle bones characterize osteopetrosis due to dysfunctional osteoclasts (cells responsible for bone remodeling) that fail to form ruffled borders and have hampered bone resorption capacity. PLEKHM1 colocalized with Rab7, a late endosomal small G-protein in HEK293 and osteoclast-like cells and was speculated to play a role in vesicular trafficking in osteoclasts (Van Wesenbeeck et al., 2007). Characterization of R714C mutation in PLEKHM1 isolated from a diseased individual showing impaired vesicular acidification in osteoclasts further speculated the role of this protein in the vesicle maturation pathway (Del Fattore et al., 2008). Since its discovery, PLEKHM1 has been well explored as an effector of Rab7. PLEKHM1 directly binds to GTP bound active form of Rab7 via its C-terminal end, and this interaction was shown to negatively regulate the endocytic pathway. EGFR (Epidermal Growth Factor Receptor) degradation was delayed in lung carcinoma cells over-expressing PLEKHM1 (Tabata et al., 2010). Subsequent studies on PLEKHM1 identify it as a multidomain adaptor protein crucial for the endolysosomal pathway, aiding endocytic and autophagic cargo clearance. PLEKHM1 binds small GTP-binding protein Rab7, tethering factor HOPS complex and autophagy regulators of the Atg8 family simultaneously via its multiple functional domains and mediates the fusion of endosomes and autophagosomes with lysosomes. Lack of PLEKHM1 either by shRNA mediated depletion or genetic loss was

shown to be associated with hampered EGFR degradation and accumulation of autophagic cargo such as protein aggregates in cells, thus supporting the role of PLEKHM1 as a positive regulator of the endolysosome pathway (McEwan et al., 2015a). Other known Rab7 effectors RILP and ORP1L coordinate with PLEKHM1 to regulate positioning and fusion of late endosomes and autophagosomes with lysosomes. PLEKHM1 and RILP binding controls both positioning and fusion of Rab7 positive compartments. PLEKHM1 and RILP promote the dynein-dependent retrograde transport of endolysosomes and facilitate fusion of Rab7+ compartments by recruiting the HOPS complex to vesicle contact sites (McEwan et al., 2015a; Wijdeven et al., 2016). ORP1L is a cholesterol sensing protein that under low cholesterol conditions facilitates the formation of autophagosome-endoplasmic reticulum contact sites and regulates autophagosome fusion by inhibiting the localization of RILP, PLEKHM1 and HOPS complex to these sites (Wijdeven et al., 2016). Some of the recent studies shed light on the specificity of PLEKHM1 towards Atg8 family members GABARAPs and LC3 (Rogov et al., 2017). Using biophysical techniques and structural analysis approach it is seen that previously identified LIR motif of PLEKHM1 is 11 fold more specific to GABARAP than to LC3 which is essential for preferential recruitment of PLEKHM1 to drive autophagosome-lysosome fusion (Nguyen et al., 2016; Rogov et al., 2017). PLEKHM1 regulates positioning of lysosomes in osteoclasts and bone homeostasis by forming a complex with DEF8 and two known dynein accessory proteins NDEL and LIS1 (Fujiwara et al., 2016; Ye et al., 2011).

Intracellular pathogens also target PLEKHM1 which has emerged as a crucial adaptor protein in the autophagic and endocytic pathway for their survival and replication. *Salmonella* enterica is an intracellular pathogen responsible for causing acute gastroenteritis and severe enteric fever in humans. *Salmonella* is known to modulate the endocytic pathway for its benefit extensively. After the invasion in a host cell, *Salmonella* resides in a membrane-enclosed compartment known as *Salmonella*-containing vacuole (SCV) and secretes effectors that bind host factors, thus hijacking the system for its survival and replication. The SCV acquires endocytic proteins as it matures and forms a replicative niche and failure to establish a mature SCV leads to hampered bacterial replication in host cells. Salmonella effector SifA directly binds to PLEKHM1, which further binds to Rab7 and HOPS complex, thus utilizing the host fusion machinery for SCV maintenance. PLEKHM1

17

depletion leads to impaired vacuole formation and Salmonella replication in mammalian cells (McEwan et al., 2015b). Some members of the Picornavirus family are engulfed in autophagosomes and prevent its fusion with lysosomes by releasing proteinases that cleave the SNARE complexes thus inhibiting fusion of vesicles. One such virus, coxsackievirus B3, known to cause gastroenteritis and cardiomyopathies in humans, releases viral proteinase 3C that cleaves PLEKHM1 into a non-functional protein, thus preventing the fusion of virus containing autophagosome with lysosomes during infection and enhanced viral replication (Corona et al., 2018; Mohamud et al., 2018).

1.3.2 RUFY1/Rabip4'

RUN and FYVE domain-containing family of proteins comprises of four members namely RUFY1, RUFY2, RUFY3, and RUFY4. These proteins have a similar domain architecture having an N-terminal RUN domain and a C-terminal FYVE domain and are known to associate with the phospholipids of the early endosomal membranes (Kitagishi and Matsuda, 2013). RUFY family proteins act as docking proteins that bind multiple small GTP binding proteins of the Rab and Rap subfamilies and their role in regulating cellular processes such as vesicular trafficking and cell polarity is being recognized lately. Reports show that RUFY4 acts as the positive regulator of macroautophagy in IL-4 differentiated dendritic cells. RUFY4 binds late endosomal small G-protein Rab7 and facilitates accumulation of phospholipids and SNARE protein SNX-17 and has implications in the autophagic flux and lysosome tethering in cells (Terawaki et al., 2016; Terawaki et al., 2015). RUFY3 is known to interact with Rab5A Q79L and Rap2 via C-terminal end and N-terminal RUN domain respectively (Kukimoto-Niino et al., 2006; Yoshida et al., 2010). RUFY3 and its interaction partners regulate cellular process such as neuronal polarity, maintaining optimum axon growth and cell migration (Mori et al., 2007; Wang et al., 2015; Wei et al., 2014; Xie et al., 2017). RUFY2 is shown to interact with Rab33 and Rab4, small GTP binding proteins of the Rab family by yeast two-hybrid and co-immunoprecipitation assays; however the physiological function of these interactions remains uncharacterized (Fukuda et al., 2011).

RUFY1 is the best-characterized member of the RUFY family of proteins. The RUFY1 gene encodes for two isoforms namely Rabip4 or the shorter isoform having 600 amino acids and Rabip4' (longer isoform) having 708 amino acids. Rabip4 and Rabip4' differ only in the

extra 108 amino acid sequence present in Rabip4' while rest of the sequence is identical and they also share a similar domain architecture having N-terminal RUN domain, three coiled-coil domains and C-terminal FYVE domain. RUFY1 (Rabip4) was identified as an interaction partner of small GTP-binding protein Rab4a, localizing on early endosomes and was shown to be implicated in the regulation of trafficking events at the early endosomes (Cormont et al., 2001). Further studies characterize Rabip4 as a dual effector for Rab4 and Rab14 and as a key regulator of the recycling trafficking events (Yamamoto et al., 2010). Rab14, but not Rab4 is the critical small GTP-binding protein regulating the membrane association of Rabip4 as its depletion led to a completely cytosolic distribution of Rabip4 in mammalian cells. Apart from just binding to Rab14, the N-terminal RUN domain, phospholipid binding FYVE domain, and ETK mediated tyrosine phosphorylation are essential regulators of RUFY1's membrane association (Mari et al., 2001; Yang et al., 2002). Rabip4 together with Rab4 and Rab14 is an essential factor regulating early endosome dynamics and efficient recycling of cargo such as glucose transporter GLUT1 and transferrin receptor. Co-expression of Rabip4 along with either Rab4 or Rab14 leads to the formation of enlarged early endosomal structures and also increases the colocalization of Rab4/Rab14 positive endosomes with Rab5 enriched sorting endosomes and Rab11 positive recycling vesicles (Cormont et al., 2001; Yamamoto et al., 2010). A recent study strengthens the role of both the isoforms of RUFY1 in organizing the sorting endosomes marked by Rab4a and regulating efficient cargo segregation in melanocytes via forming an association with Rab4a, Rabenosyn-5, AP-3 and KIF3 (Nag et al., 2018).

Interestingly, Rabip4' has also been shown to coordinate lysosome positioning in mammalian cells. The role of Rabip4' as a regulator of lysosome positioning in mammalian cells was uncovered in a recent study. Rabip4', a known functional interaction partner for early endosomal Rab4, Rab14 and Rab5 were found to interact with β3 subunit of Adaptor protein-3 (AP-3). Depletion of Rabip4' led to an increased outgrowth of plasma membrane protrusions and accumulation of lysosomes at the peripheral tips. However, Rabip4' and AP-3 colocalized on early endosomes, no mechanism by which the two proteins participate in regulating lysosome positioning is known (Ivan et al., 2012). RUFY1 has been recently reported to be a regulator of ligand-stimulated endocytic trafficking of Epidermal Growth Factor Receptor (EGFR). EGF stimulation of cultured mammalian cells led to the

19

recruitment of RUFY1 onto early endosomes and labeled EGF/EGFR were retained for a longer time in the early endosomes upon siRNA mediated depletion of RUFY1 (Gosney et al., 2018).

Furthermore, reports show that both isoforms of RUFY1 colocalize with the actin cytoskeleton at the cell periphery of migrating fibroblasts and their binding to Rab4 is essential for potentiating cell migration (Vukmirica et al., 2006). A recent study identified RUFY1 as an interaction partner for Podocalyxin-like protein (PODXL), a transmembrane glycoprotein associated with tumor phenotype using mass spectrometry and co-immunoprecipitation assays in gastric cancer (GC) cells. RUFY1 silencing in GC cells impaired PODXL mediated phenotypes and downregulated the underlying signaling pathways (Zhi et al., 2019). RUFY1/Rabip4 is exploited by intracellular pathogen *Porphyromonas gingivalis*, one of the most virulent periodontal pathogens, which positively utilize the fast recycling pathways of the gingival epithelium for infection. The pathogen recruits VAMP2, a SNARE protein and Rab4a onto early endosomes which further associates with the components of the Exocyst complex and also induces the recruitment of RUFY1 onto endosomal membranes mediated by Rab14, creating a functional complex that promotes fusion of endosomes with the plasma membrane leading to bacterial exit and spread to other tissues (Takeuchi et al., 2016).

1.4 Thesis objective

Decades of research has brought much attention to lysosomes, and apart from recognizing its crucial role in the degradation of endocytic, phagocytic and autophagic cargo, they act as important highly dynamic metabolic signaling hub. Lysosomes actively fuse with late-endosomes/autophagosomes to efficiently clear out the cellular waste. Bidirectional movement of lysosomes on microtubule tracks is crucial for regulating cellular processes such as plasma membrane repair, nutrient sensing, metabolic signaling, cell adhesion, and migration. Impaired degradation and motility of lysosomes associates with severe human genetic disorders, neurodegeneration, cancer progression, and obesity. Rab7 and Arl8b have emerged as critical molecular entities regulating late-endosome/lysosome function. Small

GTP-binding proteins Rab7 and Arl8b have overlapping subcellular distribution and function, it remains unclear that if they can coordinate their activity through linker proteins. Previous studies suggest that members of Rab, Arf and Arl small GTP-binding proteins have shared effectors/linker proteins that provide them a platform to congregate and coordinate their signals in the membrane trafficking pathway (Burguete et al., 2008; Shi and Grant, 2013). Intrigued by this, we searched for plausible candidate proteins that can act as a dual interaction partner for Rab7 and Arl8b. Known Rab7 effector PLEKHM1 was picked up as the probable linker protein. PLEKHM1 (Pleckstrin Homology domain containing family M member-1) is a multidomain protein having N-terminal RUN domain, two PH (Pleckstrin Homology) domains and a C-terminal C1 domain. PLEKHM1 binds to Rab7 through its C-terminal PH and C1 domain and functions as an adaptor to recruit the fusion machinery to mediate endocytic and autophagic cargo clearance (McEwan et al., 2015a). Interestingly, the RUN domain of PLEKHM1 shared 40% identity with that of SKIP/PLEKHM2, a previously known RUN domain containing Arl8b effector. Importantly, it is the RUN domain of SKIP that mediates its interaction with Arl8b, and together they are known to regulate lysosome positioning in cells (Rosa-Ferreira and Munro, 2011). As the first part of my thesis, beginning with this background information about PLEKHM1, we were prompted to direct our efforts to address the following questions;

1. To elucidate whether PLEKHM1 can interact with Arl8b using similar binding surface like SKIP.

2. To characterize PLEKHM1 as a dual interaction partner for Rab7 and Arl8b as indicated by the presence of separate binding sites for the two small GTP-binding proteins.

3. To investigate the relevance of PLEKHM1 binding to Arl8b in regulating cargo trafficking to lysosomes.

(This part of the thesis was done in **collaboration** with **Dr.Amit Tuli at CSIR-IMTECH**, Chandigarh and **Subhash B. Arya** from his lab **contributed equally to the project**)

Arl8b is an essential regulator of lysosome positioning and cargo degradation in mammalian cells. Since its discovery, several interaction partners for Arl8b have come forth and are known to regulate lysosome function. RUN domain and FYVE domain containing family of

proteins (RUFYs), consisting of four members, namely RUFY1, RUFY2, RUFY3, and RUFY4, are reported to act as interaction partners for multiple small GTP-binding proteins of the Rab and Rap families and regulate a range of cellular processes such as, endocytic cargo trafficking/recycling, macroautophagy, neurite growth, and cell migration. The family shares common domain architecture with an amino-terminal RUN domain, coiled-coil domains, and carboxy-terminal FYVE domain. Two isoforms of RUFY1, shorter (600 amino acids) and longer (708 amino acids) (Rabip4 and Rabip4', respectively) are known to bind Rab4 and Rab14 via their C-terminal region and localize to the early endosomes. At the early endosomes, RUFY1 regulate transferrin and glucose transporter recycling to the plasma membrane and Rab4a mediated organization of recycling endosomes.

Interestingly, a recent study had identified Rabip4' as a regulator of lysosome subcellular distribution. Depletion of Rabip4s led to the accumulation of lysosomes to the cell periphery. Furthermore, in another study it was shown that RUFY1 depletion leads to longer retention and a subsequent delay in EGFR trafficking to lysosomes. However, the mechanism of Rabip4' -mediated lysosome positioning and receptor trafficking remains unknown. It was intriguing to note that the RUN domain of Rabip4s shares 35% and 38% similarity with that of known Arl8b effectors SKIP/PLEKHM2 (reported previously) and PLEKHM1 (identified in the first part of the thesis). Prompted by the likely role of Rabip4' in mediating lysosome function, we investigated its role as a potential Arl8b interaction partner in the second part of my thesis.

Chapter 2

Materials and Methods

CHAPTER-2

2. Materials and Methods

2.1 Cell Culture and RNAi

HeLa, HEK293T and U2OS (from ATCC) were cultured in DMEM (Lonza) supplemented with 10% FBS (Gibco, Life Technologies) at 37°C with 5% CO_2 in a humidified cell culture chamber. Each cell line was regularly screened for absence of mycoplasma contamination by using MycoAlert™ Mycoplasma Detection Kit (Lonza) and was passaged for no more than 15 passages. For gene silencing, siRNA oligos were purchased from Dharmacon and prepared according to the manufacturer's instructions. Sequences of siRNA oligos used in this study were as follows: control, TGGTTTACATGTCGACTAA; Arl8b, AGGTAACGTCACAATAAAGAT (siRNA #1) and GCTGAAGATGAATATCCCTAA (siRNA #2); PLEKHM1, CCGGTCTCTGCAAGAGGTATTGT (siRNA #1), GGTCTGAAGCTGGTAGTTT (siRNA #2) and GCAAAGTCCTGGCATCCTA (siRNA #3); Vps41, TGACATAGCAGCACGCAAA; and SKIP, CTTCTGAACTGGACCGATT; RUFY1 (siRNA#1), CATCAGATATAGCGACACTT; RUFY1 (siRNA#2), Smart pool

2.2 Generation of Arl8b and PLEKHM1 Knockout Cells by CRISPR/Cas9

Arl8b and PLEKHM1 knockout HeLa cells were generated using the Arl8b sg/RNA (target sequence: GATGGAGCTGACGCTCG) and PLEKHM1 sg/RNA (target sequence: GAAGCTGGTGGGATCCGTGA) CRISPR/Cas9 All-in-One Lentivector Set, respectively (Human; Applied Biological Materials). Briefly, All-in-One plasmid was transfected into HEK293T cells together with lentiviral packaging plasmids for producing viral particles using X-tremeGENE HP DNA Transfection Reagent (Roche). Culture supernatants were harvested 48h post-transfection, centrifuged, and concentrated using Lenti-X concentrator (Clontech). HeLa cells were infected with supernatants containing lentiviral particles in the presence of 8μg/mL polybrene (Sigma). Lentiviral-infected cells were selected by 3μg/mL puromycin (Sigma) for 72h, and then re-seeded in 96-well plate to allow single colony

formation. The identification of the knockout cell clones was confirmed by immunoblot analysis.

2.3 Mammalian Expression Constructs

All the expression plasmids used in this study are listed in **Table I**.

Table II: List of molecular constructs used in this study

Plasmid Name	Description	Source
*Yeast two-hybrid constructs***:**		
pGADT7 vector	GAL4-activation domain yeast two-hybrid vector	Clontech
pGADT7-PLEKHM1 (WT)	Full-length human PLEKHM1 (1-1056 aa) cloned into the pGADT7 vector	This study
pGADT7-NΔ198 PLEKHM1	Human PLEKHM1 (199-1056 aa) cloned into the pGADT7 vector	This study
pGADT7-NΔ300 PLEKHM1	Human PLEKHM1 (301-1056 aa) cloned into the pGADT7 vector	This study
pGADT7-PLEKHM1 (H60A)	Human PLEKHM1 with point mutation at amino acid position 60 changing H with A; cloned into the pGADT7 vector	This study
pGADT7-PLEKHM1 (H63A)	Human PLEKHM1 with point mutation at amino acid position 63 changing H with A; cloned into the pGADT7 vector	This study
pGADT7-PLEKHM1 (RR→A)	Human PLEKHM1 with point mutations at amino acid positions 117 and 119 changing both R with	This study

	A; cloned into the pGADT7 vector	
pGADT7-PLEKHM1 (R123A)	Human PLEKHM1 with point mutation at amino acid position 123 changing R with A; cloned into the pGADT7 vector	This study
pGADT7-PLEKHM1 (HRR→A)	Human PLEKHM1 with point mutations at amino acid positions 60, 117 and 119 changing H with A and both R with A, respectively; cloned into the pGADT7 vector	This study
pGADT7-SKIP (WT)	Full-length human SKIP (1-1019 aa) cloned into the pGADT7 vector	Described previously
pGADT7-NΔ300 SKIP	Human SKIP (301-772 aa) cloned into the pGADT7 vector	This study
pGADT7-SKIP (R92A/R94A)	Human SKIP with point mutations at amino acid positions 92 and 94 changing both R with A; cloned into the pGADT7 vector	This study
pGBKT7 vector	GAL4-DNA binding domain yeast two-hybrid vector	Clontech
pGBKT7-Arl8a	Human Arl8a (lacking first 17 aa) cloned into the pGBKT7 vector	This study
pGBKT7-Arl8b (WT)	Human Arl8b (lacking first 17 aa) cloned into the pGBKT7 vector	This study
pGBKT7-Arl8b (Q75L)	Human Arl8b (lacking first 17 aa) with Q75L point mutation cloned into the pGBKT7 vector	This study
pGBKT7-Arl8b (T34N)	Human Arl8b (lacking first 17 aa) with T34N point mutation cloned into the pGBKT7 vector	This study

pGBDC1-Rab7	Human Rab7 cloned into the pGBDC1 vector	Gift from Dr. Tamotsu Yoshimori
pGBKT7-LC3B	Human LC3B cloned into the pGBKT7 vector	This Study
pGBKT7-Vps11	Full-length human Vps11 cloned into the pGBKT7 vector	(Khatter et al., 2015a)
pGBKT7-Vps16	Full-length human Vps16 cloned into the pGBKT7 vector	(Khatter et al., 2015a)
pGBKT7-Vps18	Full-length human Vps18 cloned into the pGBKT7 vector	(Khatter et al., 2015a)
pGBKT7-Vps33a	Full-length human Vps33a cloned into the pGBKT7 vector	(Khatter et al., 2015a)
pGBKT7-Vps39	Full-length human Vps39 cloned into the pGBKT7 vector	(Khatter et al., 2015a)
pGBKT7-Vps41	Full-length human Vps41 cloned into the pGBKT7 vector	(Khatter et al., 2015a)
Yeast three-hybrid constructs:		
pBridge vector	Yeast three-hybrid vector	Clontech
pBridge-Arl8b	Arl8b (lacking first 17 aa) cloned into the MCS I of the pBridge vector	This study
pBridge-Arl8b/PLEKHM1 (WT)	Arl8b (lacking first 17 aa) cloned into the MCS-I and full-length PLEKHM1 cloned into the MCS-II of the pBridge vector	This study
pBridge-Arl8b/PLEKHM1 (HRR→A)	Arl8b (lacking first 17 aa) cloned into the MCS-I and PLEKHM1 with point mutations at amino acid	This study

	positions 60, 117 and 119 changing H with A and both R with A, respectively, cloned into the MCS-II of the pBridge vector	
Mammalian expression constructs:		
pcDNA3.1(-)	Mammalian expression vector	Invitrogen
pcDNA3.1(-)-FLAG- PLEKHM1 (WT)	N-terminal FLAG-tagged full-length human PLEKHM1 (1-1056 aa) cloned into the pcDNA3.1(-) vector	This study
pcDNA3.1(-)-FLAG-PLEKHM1 (H60A)	N-terminal FLAG-tagged human PLEKHM1 with point mutation at amino acid position 60 changing H with A; cloned into the pcDNA3.1(-) vector	This study
pcDNA3.1(-)-FLAG-PLEKHM1 (H63A)	N-terminal FLAG-tagged human PLEKHM1 with point mutation at amino acid position 63 changing H with A; cloned into the pcDNA3.1(-) vector	This study
pcDNA3.1(-)-FLAG-PLEKHM1 (RR→A)	N-terminal FLAG-tagged human PLEKHM1 with point mutations at amino acid positions 117 and 119 changing both R with A; cloned into the pcDNA3.1(-) vector	This study
pcDNA3.1(-)-FLAG-PLEKHM1 (HRR→A)	N-terminal FLAG-tagged human PLEKHM1 with point mutations at amino acid positions 60, 117 and 119 changing H with A and both R with A, respectively; cloned into the pcDNA3.1(-) vector	This study
pcDNA3.1(-)-FLAG-NΔ198	N-terminal FLAG-tagged human	This study

PLEKHM1	PLEKHM1 (199-1056 aa) cloned into the pcDNA3.1(-) vector	
pcDNA3.1(-)-FLAG-NΔ300 PLEKHM1	N-terminal FLAG-tagged human PLEKHM1 (301-1056 aa) cloned into the pcDNA3.1(-) vector	This study
pcDNA3.1(-)-FLAG-PLEKHM1 (WT) siRNA resistant	N-terminal FLAG-tagged full-length human PLEKHM1 (1-1056 aa) rescue construct against PLEKHM1 siRNA #2 cloned into the pcDNA3.1(-) vector	This study
pcDNA3.1(-)-FLAG-PLEKHM1 (HRR→A) siRNA resistant	N-terminal FLAG-tagged full-length human PLEKHM1 (1-1056 aa) rescue construct against PLEKHM1 siRNA #2 with H60A/R117A/R119A point mutations cloned into the pcDNA3.1(-) vector	This study
pEGFPC1-PLEKHM1 (WT)	N-terminal GFP-tagged full-length human PLEKHM1 (1-1056 aa) cloned into the pEGFP-C1 vector	Gift from Dr. Tamotsu Yoshimori
pEGFPC1-PLEKHM1 (HRR→A)	N-terminal GFP-tagged full-length human PLEKHM1 (1-1056 aa) with point mutations at amino acid positions 60, 117 and 119 changing H with A and both R with A, respectively; cloned into the pEGFP-C1 vector	This study
pEGFPC1-NΔ198 PLEKHM1	N-terminal GFP-tagged human PLEKHM1 (199-1056 aa) cloned into the pEGFP-C1 vector	This study
pEGFPC1-NΔ300 PLEKHM1	N-terminal GFP-tagged human	This study

	PLEKHM1 (301-1056 aa) cloned into the pEGFP-C1 vector	
pEGFPC1-PLEKHM1 ΔC1	N-terminal GFP-tagged human PLEKHM1 (1-895 aa) cloned into the pEGFP-C1 vector	This study
pEGFPC1-PLEKHM1 ΔKML	N-terminal GFP-tagged human PLEKHM1 (lacking 720-722 aa) cloned into the pEGFP-C1 vector	This study
pEGFPC1-PLEKHM1 (WT) siRNA resistant	N-terminal GFP-tagged full-length human PLEKHM1 (1-1056 aa) rescue construct against PLEKHM1 siRNA #2 cloned into the pEGFPC1 vector	This study
pEGFPC1-PLEKHM1 (HRR→A) siRNA resistant	N-terminal GFP-tagged full-length human PLEKHM1 (1-1056 aa) rescue construct against PLEKHM1 siRNA #2 with H60A/R117A/R119A point mutations cloned into the pEGFPC1 vector	This study
pcDNA3.1(-)-FLAG-SKIP	N-terminal FLAG-tagged full-length human SKIP (1-1019 aa) cloned into the pcDNA3.1(-) vector	(Khatter et al., 2015a)
pcDNA3.1(-)-FLAG-SKIP (1-300) only	N-terminal FLAG-tagged human SKIP (1-300 aa) cloned into the pcDNA3.1(-) vector	(Khatter et al., 2015a)
pcDNA3.1(-)-FLAG-SKIP (R92A/R94A)	N-terminal FLAG-tagged human SKIP with point mutations at amino acid positions 92 and 94 changing both R with A; cloned into the pcDNA3.1(-) vector	This study

pcDNA3.1(-)-FLAG-SKIP (WD 2X→A)	N-terminal FLAG-tagged human SKIP with point mutations W207A/D208A/W236A/E237A; cloned into the pcDNA3.1(-) vector	This study
pEGFPC1-SKIP (WT)	N-terminal GFP-tagged full-length human SKIP (1-1019 aa) cloned into the pEGFPC1 vector	This study
pcDNA3.1(-)-Arl8a (WT)-HA	Full-length human Arl8a with C-terminal HA tag cloned into the pcDNA3.1(-) vector	This study
pcDNA3.1(-)-Arl8b (WT)-HA	Full-length human Arl8b with C-terminal HA tag cloned into the pcDNA3.1(-) vector	(Khatter et al., 2015a)
pcDNA3.1(-)-Arl8b (Q75L)-HA	Full-length human Arl8b Q75L with C-terminal HA tag cloned into the pcDNA3.1(-) vector	(Khatter et al., 2015a)
pcDNA3.1(-)-Arl8b (T34N)-HA	Full-length human Arl8b T34N with C-terminal HA tag cloned into the pcDNA3.1(-) vector	(Khatter et al., 2015a)
ptdTomato-N1-Arl8b	Full-length human Arl8b cloned into the ptdTomato-N1 vector	(Khatter et al., 2015a)
ptdTomato-N1-Arl8b rescue	Full-length human Arl8b siRNA rescue (against siRNA #1) construct cloned into the ptdTomato-N1 vector	(Khatter et al., 2015a)
pcDNA3.1(+)-Mouse Arl8b-GFP	Full-length mouse Arl8b with C-terminal GFP tag cloned into the pcDNA3.1(+) vector	(Khatter et al., 2015a)
pEBB-HA-Rab7	Full-length human Rab7 with N-terminal HA tag cloned into the pEBB vector	Gift from Dr. Jason Kinchen

pEGFPC1-Rab7	N-terminal GFP-tagged full-length canine Rab7 cloned into the pEGFPC1 vector	Gift from Dr. Steve Caplan
pEGFPC1-Rab7 Q75L	N-terminal GFP-tagged full-length canine Rab7 Q75L cloned into the pEGFPC1 vector	Gift from Dr. Steve Caplan
pEGFPC1-Rab7 T22N	N-terminal GFP-tagged full-length canine Rab7 T22N cloned into the pEGFPC1 vector	Gift from Dr. Steve Caplan
pcDNA3.1(-)-HA-Vps41	Full-length human Vps41 with N-terminal HA tag cloned into the pcDNA3.1(-) vector	(Khatter et al., 2015a)
pEGFPC1-Vps41	N-terminal GFP-tagged full-length human Vps41 cloned into the pEGFPC1 vector	This study
N-TAP-Vps41-pCDH-CMV-MCS-EF1-Hygro	N-terminal TAP-tagged full-length human Vps41 cloned into the pCDH-CMV-MCS-EF1-Hygro vector	This study
pcDNA3.1(-)-HA-Vps39	Full-length human Vps39 with N-terminal HA tag cloned into the pcDNA3.1(-) vector	(Khatter et al., 2015a)
pEGFPC1-Vps39	N-terminal GFP-tagged mouse Vps39 cloned into the pEGFPC1 vector	Gift from Dr. Robert Piper
pEGFPC1-RILP	N-terminal GFP-tagged RILP cloned into the pEGFPC1 vector	Gift from Dr. Jacques Neefjes
pEGFPC1-KLC2	N-terminal GFP-tagged KLC2 cloned into the pEGFPC1 vector	Gift from Dr. Michael Way
ptf-LC3B	Rat LC3B fused to mRFP and EGFP cloned into pEGFPC1	Gift from Dr. Tamotsu

		Yoshimori
pEGFPC1-Lamp1	N-terminal GFP-tagged Lamp1 cloned into the pEGFPC1 vector	Gift from Dr. Steve Caplan
Rabip4 WT-FLAG pcDNA3.1(-)	Shorter isoform of RUFY (600aa) cloned in mammalian expression vector	This study
Rabip4' WT-FLAG pcDNA3.1(-)	Longer isoform of RUFY1 (708aa) cloned in mammalian expression vector	Genscript
Rabip4' RR→A-FLAG pcDNA3.1(-)	R206 and R208 mutated to A in Rabip4'; Created by SDM	This study
NΔRUN Rabip4'-FLAG pcDNA3.1(-)	1-271aa (RUN domain) deletion; Expresses 272-708aa of Rabip4'	This study
pEGFPN1-Rabip4' WT	Rabip4' WT with C-terminal GFP tag	This study
pEGFPN1-Rabip4' RR→A	Rabip4' RR→A with C-terminal GFP tag	This study
pEGFPN1-NΔRUN Rabip4'	NΔRUN Rabip4' with C-terminal GFP tag	This study
GFP-Rab14	Rab14 WT cloned in pEGFC1	Gift from Isabella Coppens Lab (USA)
Myc-Nischarin	Human Nischarin	Gift from Dr. Suresh Alahari
GFP-PX	PX (1-148) domain of p40PHOX-eGFP-N3	Gift from Dr. John Brumell
GFP-Rab5 Q79L	Dominant active form of Rab5	Gift from Dr. Steve Caplan

Bacterial expression constructs:		
pGEX6P2-PLEKHM1 (1-198)	Human PLEKHM1 (1-198 aa) cloned into the pGEX6P2 vector	This study
pGEX6P2-PLEKHM1 (1-300)	Human PLEKHM1 (1-300 aa) cloned into the pGEX6P2 vector	This study
pET15b(+)-PLEKHM1 (1-300)	Human PLEKHM1 (1-300 aa) with N-terminal His tag cloned into the pET15b(+) vector	This study
pGEX6P2-PLEKHM1 H60A (1-300)	Human PLEKHM1 (1-300 aa) with point mutation at amino acid position 60 changing H with A; cloned into the pGEX6P2 vector	This study
pGEX6P2-PLEKHM1 H63A (1-300)	Human PLEKHM1 (1-300 aa) with point mutation at amino acid position 63 changing H with A; cloned into the pGEX6P2 vector	This study
pGEX6P2-PLEKHM1 RR→A (1-300)	Human PLEKHM1 (1-300 aa) with point mutations at amino acid positions 117 and 119 changing both R with A; cloned into the pGEX6P2 vector	This study
pGEX6P2-PLEKHM1 HRR→A (1-300)	Human PLEKHM1 (1-300 aa) with point mutations at amino acid positions 60, 117 and 119 changing H with A and both R with A, respectively; cloned into the pGEX6P2 vector	This study
pMAL-C2X-SKIP (1-300)	Human SKIP (1-300 aa) with N-terminal MBP tag cloned into the pMAL-C2X vector	This study
pet15b(+)-Arl8b	Full-length human Arl8b with N-	Gift from Dr.

	terminal His tag cloned into the pet15b(+) vector	Michael Brenner
pRSF-His-Rab7	Rab7 with N-terminal His tag cloned into the pRSF vector	Gift from Dr. Anne Spang
pGEX6P2-Rab7	Rab7 cloned into the pGEX6P2 vector	This study
pGEX4T1-Rabip4s RUN only	1-194aa of Rabip4 cloned into peGX4T1 vector	This study

2.4 Antibodies and Chemicals

The following antibodies were used in this study: mouse anti-FLAG M2 clone (F1804, Sigma), rat anti-HA clone 3F10 (11867423001, Roche), rabbit anti-HA (sc-805, Santa Cruz), mouse anti-His (SAB1305538, Sigma), mouse anti-MBP (E8038S, New England Biolabs), mouse anti-α-tubulin (T9026, Sigma), mouse anti-HA (MMS-101P, Covance), rabbit anti-GFP (ab6556, Abcam), mouse anti-GFP (sc-9996, Santa Cruz), rabbit anti-rat (ab6703, Abcam), mouse anti-Arl8 clone F-5 (sc-398679, Santa Cruz), mouse anti-LAMP1 (555798, BD Biosciences), mouse anti-EEA1 (610457, BD Biosciences), rabbit anti-Rab14 (ab28639, Abcam), rabbit anti-EEA1(ab2900, Abcam), rabbit anti-LAMP1 (ab24170, abcam), rabbit anti-Giantin (ab80864, abcam), rabbit anti-Cathepsin D (K50161R, Meridian Life Sciences), mouse anti-Cathepsin B clone 4B11 (414800, Life Technologies), rabbit anti-PLEKHM1 (ab171383, abcam), rabbit anti-SKIP/PLEKHM2 (HPA032304, Sigma), mouse anti-Rab7 clone B-3 (sc-376362, Santa Cruz), mouse anti-RUFY1 (sc-398740, Santa Cruz) and rabbit anti-Rab7 (9367, Cell Signaling Technologies). For detection of HOPS subunit, the following antibodies were used: rabbit anti-Vps11 (ab125083, abcam), rabbit anti-Vps18 (ab178416, abcam), rabbit anti-Vps33a (16896-1-AP, ProteinTech), rabbit anti-Vps41 (ab181078, abcam) and mouse anti-Vps41 (sc-377271, Santa Cruz). For autophagy-related experiments, rabbit anti-LC3B-II (3868) and rabbit anti-p62 (8025) antibodies were purchased from Cell Signaling Technologies. Rabbit anti-PLEKHM1 antibody generated against the N-terminal 497 amino acids of human PLEKHM1 protein was a kind gift from Dr. Paul Odgren (University of Massachusetts Medical School, USA) and has been previously used to detect

endogenous PLEKHM1 by immunofluorescence and Western blotting (Witwicka et al., 2015). Rabbit anti-Arl8 antibody used in this study has been described previously (Garg et al., 2011; Khatter et al., 2015a). All the Alexa fluorophore-conjugated secondary antibodies were purchased from Life Technologies. HRP-conjugated goat anti-mouse and goat anti-rabbit were purchased from Jacksons ImmunoResearch Laboratories. The protein-A gold for immunolabeling was purchased from University Medical Center (Utrecht, the Netherlands). Phalloidin, Alexa Fluor 647-conjuated-Dextran, DQ-BSA, and DAPI were purchased from Invitrogen. EBSS and Bafilomycin A1 were purchased from Sigma. The Magic Red Cathepsin L Assay Kit to monitor activity of the pH-sensitive protease cathepsin L was purchased from ImmunoChemistry Technologies.

2.5 Transfections, Immunofluorescence and Live-Cell Imaging

Cells grown on glass coverslips were transfected with desired constructs using X-tremeGENE-HP DNA transfection reagent (Roche) for 16-18h. Cells were fixed in 4% PFA in PHEM buffer (60mM PIPES, 10mM EGTA, 25mM HEPES and 2mM $MgCl_2$ and final pH 6.8) for 10min at room temperature. Post-fixation, cells were incubated with blocking solution (0.2% saponin + 5% FBS in PHEM buffer) at room temperature for 30min, followed by three washes with 1X PBS. Following this blocking step, cells were incubated with primary antibodies in staining solution (PHEM buffer + 0.2% saponin) for 45min to 1h at room temperature, washed thrice with 1X PBS and further incubated for 30min with alexa fluorophore-conjugated secondary antibodies made in staining solution. Cells were mounted in Fluoromount G (Southern Biotech) and confocal images were acquired using Carl Zeiss 710 Confocal Laser Scanning Microscope. For detecting endogenous staining of PLEKHM1, PLEKHM2/SKIP, Arl8 and Rab7, the primary and secondary antibodies were made in PBS (pH 7.4) containing 0.05% Tween-20 + 0.5% BSA. For Acetate Ringer's solution treatment, cells were incubated with Acetate Ringer's solution (80mM NaCl, 70mM Sodium acetate, 5mM KCl, 2mM $CaCl_2$, 1mM $MgCl_2$, 2mM NaH_2PO_4, 10mM HEPES, and 10mM glucose with final pH 6.9) and processed for confocal imaging as described above.

36

For live-cell imaging, cells were seeded on glass bottom tissue culture treated cell imaging dish (Eppendorf) and transfected with the indicated plasmids. Live-cell imaging was performed using a Zeiss LSM 710 confocal microscope equipped with an environmental chamber set at 37°C and 5% CO_2.

2.6 Structured Illumination Microscopy (SIM)

SIM imaging was carried out at the Advanced Microscopy Core Facility at the University of Nebraska Medical Center, and the samples were processed as previously described(Reinecke et al., 2015). Briefly, cells were fixed and immunostained with appropriate antibodies as described for confocal microscopy. SIM images were collected with a Zeiss ELYRA PS.1 illumination system (Carl Zeiss MicroImaging) using a 63× oil objective lens with a numerical aperture of 1.4 at room temperature. Three orientation angles of the excitation grid were acquired for each Z plane, with Z spacing of 110nm between planes. SIM processing was performed with the SIM module of the Zen black software (Carl Zeiss MicroImaging).

2.7 Image Analysis and Quantification

Pearson's correlation coefficient and Mander's coefficient were determined using JACoP plugin of ImageJ. For measuring particle size of LAMP1- or PLEKHM1-positive compartments, analyse particles function of ImageJ was used after appropriately setting the threshold to detect punctate structures. Lysosome distribution was assessed as a measure of perinuclear index as previously described (Li et al., 2016). Briefly, the fluorescence intensity of LAMP1 staining was measured in whole cell (I_{total}), the nuclear region i.e. area within 5μM from nucleus ($I_{perinuclear}$), and an area >10μm from nucleus ($I_{peripheral}$). The peripheral and perinuclear intensities were calculated and normalized as $I_{>10}=I_{peripheral}/I_{total}$-100 and $I_{<5}=I_{perinuclear}/I_{total}$-100. The perinuclear index was calculated as $I_{<5}$-$I_{>10}$*100.

2.8 Colocalization analysis

For all the colocalization analysis, 25–30 cells per experiment for each treatment were used for three independent experiments. Pearson's correlation coefficient (PC; for Fig. 2 h, see below) and Mander's coefficient (MC) were determined using the JACoP plugin of ImageJ. PC was calculated on the original image where no threshold settings (manual or automatic) were applied. Another method (Costes' approach) to calculate PC was used, as the classical PC is highly sensitive to the intensity values of the two channels and to the background noise parameters that will be different when comparing colocalization of single protein with multiple markers (Costes et al., 2004). In the Costes' method, automated and unbiased threshold is calculated by determining PC at different intensities. The final threshold is set to values that minimize the contribution of noise (i.e., PC under the threshold being negative). Further image randomization (200 times) is done, and the PC is calculated each time between the random image of one channel and the original of the other. Comparison of PCs from nonrandomized and randomized images gives the significance (p-value) of colocalization. The p-value in Fig. 2 h was 100%, suggesting that the colocalization was highly probable. To calculate the MC of endogenous proteins PLE KHM1, Rab7, and Arl8b, threshold values were set by first determining where the estimated background signal is negligible or zero. This was determined by quantification of images from control and gene-specific siRNA-treated cells. At the threshold value, negligible or no punctae in the siRNA-treated cells were highlighted. The same threshold settings were uniformly applied to all images within each experiment. Intensity threshold of 45–55 (value range is from 0 to 255) was selected for endogenous PLE KHM1, which highlighted punctate structures in WT or control siRNA-treated cells. At this threshold value, no punctate signal was highlighted in PLE KHM1-depleted cells. Similarly, a threshold of 35–40 was set for endogenous Rab7 and a threshold of 30 was defined for endogenous Arl8. As little or no background was observed upon immunostaining of EEA1/LAMP1, the threshold settings for these markers was determined where all endosomal punctae were highlighted. The same threshold settings were uniformly applied to all images within each experiment.

2.9 Immunogold-Electron Microscopy

Sample processing and immunogold labeling was performed by the Harvard Medical School EM Facility. For preparation of cryosections, HeLa cells co-transfected with Arl8b-HA and

GFP-PLEKHM1 were fixed with 4% PFA + 0.1% glutaraldehyde (Glut) prepared in 0.1M Sodium Phosphate buffer (pH 7.4). After 2h fixation at room temperature the cell pellet was washed once with PBS and then placed in PBS containing 0.2M glycine for 15min to quench free aldehyde groups. Prior to freezing in liquid nitrogen the cell pellets were cryoprotected by incubating in three drops of 2.3M sucrose in PBS for 15min. Frozen samples were sectioned at -120°C, the sections were transferred to formvar/carbon coated copper grids. Grids were floated on PBS until the immunogold labeling was carried out.

The double immunogold labeling was carried out at room temperature on a piece of parafilm. All the primary antibodies and Protein-A immunogold were diluted in 1% BSA in PBS. Briefly, grids were floated on drops of 1% BSA for 10min to block for unspecific labeling, transferred to 5µl drops of rat anti-HA and incubated for 30min. The grids were then washed in 4 drops of PBS for a total of 15min, transferred to 5µl drops of rabbit anti-rat for 30 min, washed again in 4 drops of PBS for 15min followed by 15nm Protein-A immunogold for 20min (5ul drops). After the 15nm Protein-A immunogold incubation grids were washed in 4 drops of PBS, fixed for 2min with 0.5% Glu followed by 4 drops of PBS containing 0.2M glycine for 15min to quench free aldehyde groups. The labeling process was repeated with rabbit anti-GFP followed by 10nm Protein-A immunogold for 20min in 5ul drops. Finally, the grids were washed in 4 drops of PBS and 6 drops of double distilled water. Contrasting/embedding of the labeled grids was carried out on ice in 0.3% uranyl acetete in 2% methyl cellulose for 10min. Grids were picked up with metal loops and the excess liquid was removed by blotting with a filter paper and were examined in a JEOL 1200EX electron microscope. Images were recorded with an AMT 2k CCD camera.

2.10 Co-immunoprecipitation and Immunoblotting

HEK293T cells transfected with indicated plasmids were lysed in TAP lysis buffer (20mM Tris pH 8.0, 150mM NaCl, 0.5% NP-40, 1mM $MgCl_2$, 1mM Na_3VO_4, 1mM NaF, 1mM PMSF and 1X Protease inhibitor cocktail (Sigma)). The lysates were incubated with indicated antibody conjugated-agarose beads at 4°C rotation for 3h, followed by four washes in TAP wash buffer (20mM Tris pH 8.0, 150mM NaCl, 0.1% NP-40, 1mM $MgCl_2$, 1mM

Na$_3$VO$_4$, 1mM NaF and 1mM PMSF). The samples were then loaded on SDS-PAGE for further analysis. Protein samples separated on SDS-PAGE were transferred onto PVDF membranes (Bio-rad). Membranes were blocked overnight at 4°C in blocking solution (10% skim milk in 0.05% PBS-Tween 20). Indicated primary and secondary antibodies were prepared in 0.05% PBS-Tween20. The membranes were washed for 10min thrice with 0.05% PBS-Tween20 or 0.3% PBS-Tween 20 after 2h incubation with primary antibody and 1h incubation with secondary antibody, respectively. The blots were developed using a chemiluminescence-based method.

2.11 Tandem Affinity Purification (TAP) and Mass Spectrometry

For semi-purification of the HOPS complex from HeLa cells, TAP was carried out using an InterPlay Mammalian TAP system (Stratagene). Briefly, 25 million HeLa cells stably expressing N-terminal TAP-tagged Vps41 were lysed following the manufacture's protocol. TAP is the tandem tag which contains a SBP (45 amino acids long tag) and a CBP (26 amino acids long tag). Whole cell lysate from the cells was first bound to streptavidin beads. Unbound proteins were washed twice with the streptavidin binding buffer and bound proteins were eluted with the streptavidin elution buffer which contains 2mM biotin. The eluate was subsequently bound to calmodulin beads. Unbound proteins were washed twice with calmodulin binding buffer and bound proteins were eluted with the calmodulin elution buffer. The final eluate containing the protein of interest (Vps41) and the proteins that associate with it were subsequently analyzed by tandem mass spectrometry at the Taplin MS Facility (Harvard Medical School).

2.12 GST-pulldown and Dot-blot Assay

GST-fusion proteins were purified as described previously (Khatter et al., 2015a). For pulldown assays, transfected HEK293T cells were lysed in ice-cold TAP lysis buffer and lysates were incubated with GST-tagged proteins bound to glutathione-resin (Gbiosciences) at 4°C for 3h with rotation. Samples were washed four times with TAP wash buffer and

elution was performed by boiling the samples in Laemmli buffer and loaded onto SDS-PAGE for analysis. For dot-blot assay, purified GST and GST-fusion proteins were spotted on nitrocellulose membrane, blocked with 10% skim milk in 0.05% PBS-Tween 20 and washed. The blots were then incubated overnight with purified His-Arl8b and His-Rab7 (in 2% skim milk in 0.05% PBS-Tween 20) at 4°C. The blot was further probed for analysis.

2.13 Yeast two-hybrid and three-hybrid Assay

For yeast two-hybrid assay, plasmids encoding GAL4-AD and GAL4-BD fusion encoding constructs were co-transformed in *Saccharomyces cerevisiae* Gold or AH109 strain (Clontech), streaked on plates lacking leucine and tryptophan and allowed to grow at $30°C$ for three days. The co-transformants were replated on non-selective medium and selective medium to assess interaction. For performing the yeast three-hybrid assay, the *Saccharomyces cerevisiae* Gold strain was made sensitive to methionine by streaking the yeast on an SD-Met plate at least two times before transforming with the desired plasmid.

2.14 DQ Red-BSA Trafficking Assay

Cells were loaded with DQ Red-BSA (Molecular Probes) at a working concentration of 10μg/ml in 1% FBS culture medium for 1h and 6h at $37°C$ and 5% CO_2. In the case of rescue of DQ Red-BSA trafficking, the siRNA-resistant construct of interest was transfected post 50-55h of siRNA treatment of cells, followed by DQ Red-BSA uptake post 10-12h of transfection. The cells were fixed in 4% PFA made in PBS (pH 7.4) and analysed under confocal microscope. Fold change in total fluorescence intensity of DQ-BSA fluorescence from 1h to 6h and the number of DQ Red-BSA spots was quantified using ImageJ software.

2.15 DiI-LDL Trafficking Assay

Cells were transfected with siRNA of interest for 60-65h followed by lysosome pre-labeling with Dextran-Oregon-green (Molecular Probes, Life Technologies). Briefly, the cells were

pulsed with Dextran-Oregon-green (0.25mg/mL) for 1h followed by a chase for 6h of which the first 3h of chase was done in complete media (10% FBS in DMEM) and followed by 3h starvation in 5% charcoal-stripped-FBS (Gibco, Life Technologies) containing DMEM (starvation media). The cells were then pulsed with DiI-LDL 20µg/mL (Molecular Probes, Life Technologies) for 10min in starvation media and chased in complete media (DiI-LDL free medium) for 20min, 40min, 1h, and 1.5h. Cells were fixed with 4% PFA made in PBS (pH 7.4) at the indicated time points and analysed by confocal microscopy. Pearson's correlation coefficient of Dextran-Oregon-green-labeled lysosomes and DiI-LDL was quantified using ImageJ software.

2.16 Autophagy Flux Assay

Autophagic flux was determined by checking for the rescue of LC3B-II degradation by treating U2OS cells with V-ATPase inhibitor Bafilomycin A1 (100nM for 2h) either at steady state or with serum starvation in EBSS for 2h. After treatment, cells were lysed on ice in RIPA buffer supplemented with protease inhibitor. Equal amount of lysates were loaded on SDS-PAGE, transferred to PVDF membrane and probed for LC3B-II and α-tubulin. Densitometry analysis of LC3B-II band intensity normalized to α-tubulin intensity was done using ImageJ software

2.17 Rhodamine-EGF trafficking

HeLa cells treated with Control- or Rabip4s siRNA (#1 and #2) were plated on glass coverslips at 30% confluence. The cells were starved in serum-free DMEM for 4 hours, following which they were pulsed with 500ng/mL Rhodamine-EGF (Life technologies) for 7 minutes at 370C. Further, the cells were chased in complete medium at 370C for the indicated time points, after which they were fixed with 4% paraformaldehyde and immunostained, as described previously. The images were acquired using Zeiss 710Confocal Laser Scanning Microscope, and the EGFR intensity was measured using the ImageJ software. Using the software, boundary of each cell quantified was drawn, and the obtained

parameters (area of cell, mean fluorescence and Integrated density) were used to calculate Corrected Total Cell Florescence (CTCF), by the formula: CTCF = Integrated density - (area x mean fluorescence of background)

2.18 Flowcytometry for assessing lysotracker staining

HeLa cells were treated with Control- and Rabip4s-siRNA (#1 and #2) for 65 hours, followed by incubation in Lysotracker Red DND-99 (Invitrogen) diluted to 100nM from 1mM stock in pre warmed Flurobrite media (Invitrogen) for 2 hours. The conditions used are, excitation at 561nm and PE-Texas red (610/20nm) filter for emission.

2.19 *Salmonella* infection

The strains used in the study are: 1) *Salmonella* typhimurium SL1344; Wildtype; Kind gift from Dr. John Brumell 2) GFP-*Salmonella* typhimurium SL1344; *S.typhimurium* SL1344 transformed with GFP expressing plasmid pFU95. For infection of HeLa cells, late-log *S. typhimurium* cultures were used and prepared using a method optimized for bacterial invasion. Briefly, wild-type bacteria were grown for 16 hr at 37°C with shaking and then subcultured (1:33) in LB (Difco) without antibiotics and grown until late exponential phase (O.D. = 3.0). Bacterial inocula were prepared by pelleting at 10,000 x g for 2 min, diluted 1:100 in Phosphate buffer saline (PBS) (pH 7.2), and added to cells (at the specified MOI) for 10 min at 37°C to allow invasion and synchronized infection. After infection, extracellular bacteria were removed by extensive washing using warm PBS and 50 μg/ml gentamicin was added to the medium at 30 min p.i. for incubation at 37°C. After 2 hr p.i., the concentration of gentamicin in the medium was decreased to 5 μg/ml. HeLa cells were fixed in 2.5% PFA at 37°C for 20mins at the desired time points. Following this infection protocol, cells were processed for microscopy. For infections of RAW264.7 cells, stationary-phase bacterial cultures incubated at 37°C with shaking were diluted (O.D. = 1) and opsonized in PBS supplemented with 20% FBS for 20 min at 37°C. After three washes in PBS, bacteria were resuspended in growth medium without antibiotics, and added to the cells (MOI of

50:1) for 20 min to facilitate phagocytosis. The remaining protocol was similar as in case of infection of HeLa cells.

2.20 Intracellular replication assay for *Salmonella typhimurium*

To enumerate intracellular *Salmonella* growth, gentamicin protection assay was performed. Briefly, cells were infected with designated *Salmonella* strain for different time periods using the protocol described above. At the end of every time point p.i. cells were gently washed with PBS followed by lysis using PBS containing 0.1% Triton X-100 and 1% SDS for 5 min at room temperature. The resulting lysates were serially diluted and plated onto LB agar plates containing streptomycin.

2.21 Statistical Analysis

Data were presented as means $\pm$ standard error of the mean (s.e.m.) unless otherwise specified. *p* values were calculated using Student's *t-test* from three independent biological replicates.

Chapter 3

The Rab7 effector PLEKHM1 binds Arl8b to promote cargo trafficking to lysosomes

The following chapter has been published in Journal of Cell Biology, 2017

vol. 216 no. 4 1051-1070

This chapter contains sections published in the following thesis:

Subhash Babu Arya, 2017, Understanding the role of Arf like small GTP-binding proteins in membrane trafficking, Ph.D. thesis, JNU, New delhi

CHAPTER-3

3.1 Introduction

Lysosomes are a cell's recycling centers that receive, degrade, and recycle the constituents of cargo delivered to them via the endocytic, autophagic, and phagocytic membrane-trafficking pathways (Luzio et al., 2007). Not surprisingly, lysosome function is associated with maintaining cellular homeostasis, impairment of which results in several human diseases including lysosomal storage and neurodegenerative disorders (Jeyakumar et al., 2005; Platt et al., 2012). Recent studies have recognized the unconventional functions of lysosomes in regulating diverse cellular processes such as amino acid sensing, bone remodeling, antigen presentation, plasma membrane repair, cell migration and cancer metastasis (Andrews et al., 2014; Hamalisto and Jaattela, 2016; Korolchuk and Rubinsztein, 2011). These functions have been attributed to the spatial pool of lysosomes present at the cell periphery, which has been recently characterized to be distinct from the juxtanuclear lysosomal pool in relation to their surface protein content and luminal pH (Johnson et al., 2016). Late endosomes (LEs)/lysosomes motility and their fusion with other compartments are regulated by action of two small GTPases, Rab7 and Arl8b, and their multitude of effectors including adaptors, tethering factors and microtubule-based motor-binding proteins (Khatter et al., 2015b; Wang et al., 2011). As with other members of the Rab and Arf-like (Arl) family, Rab7 and Arl8 cycle between inactive (GDP-bound) cytosolic and active (GTP-bound) membrane-bound conformations, recruiting their effectors to lysosomes in their GTP-bound state to mediate downstream functions.

Rab7, the better characterized of the two small GTPases, is primarily enriched on the late endosomal/lysosomal pool present in the perinuclear region of the cell near the MTOC (Wang et al., 2011). Herein Rab7 recruits its effectors, RILP and PLEKHM1, to promote dynein-driven retrograde transport of LEs/lysosomes and their fusion with endocytic, phagocytic and autophagic vesicles, respectively (Jordens et al., 2001; McEwan and Dikic, 2015; McEwan et al., 2015a; Tabata et al., 2010). RILP and PLEKHM1 interact with and recruit the multisubunit tethering factor HOPS complex to Rab7-positive

46

LEs/autophagosome-lysosome contact sites (Lin et al., 2014; McEwan et al., 2015a; van der Kant et al., 2013; Wijdeven et al., 2016). HOPS complex facilitate tethering of LEs/autophagosomes to lysosomes and bind with soluble *N*-ethylmaleimide–sensitive factor attachment protein receptor (SNARE) proteins to mediate membrane fusion (Balderhaar and Ungermann, 2013; Jiang et al., 2014). Another Rab7 effector ORP1L induces formation of endoplasmic reticulum (ER)-LE membrane contact sites that in turn regulate the recruitment of PLEKHM1-HOPS complex to Rab7-positive compartment (Rocha et al., 2009; Wijdeven et al., 2016). FYCO1, another Rab7 effector, plays an opposing role to RILP by recruiting the motor kinesin-1 to promote anterograde movement of LEs/lysosomes (Pankiv et al., 2010).

On the other hand, the recently characterized small GTPase Arl8b is primarily localized to the lysosomal pool enriched at the cell periphery (Bagshaw et al., 2006; Hofmann and Munro, 2006). Johnson et al., (2016) has recently shown that these Arl8b-positive peripheral populations of lysosomes are less acidic and have reduced density of Rab7-RILP proteins. Arl8b mediate anterograde lysosomal motility by recruiting its effector, SKIP (also known as PLEKHM2), which in turn recruits the motor protein kinesin-1 on lysosomes (Rosa-Ferreira and Munro, 2011). Recent studies have established Arl8b-mediated positioning of lysosomes and lysosomes-related organelles as a crucial factor regulating nutrient sensing, cell migration, cancer cell metastasis, natural killer cell-mediated cytotoxicity, antigen presentation and the formation of tubular lysosomes in macrophages (Deshar et al., 2016; Dykes et al., 2016b; Guardia et al., 2016; Kaniuk et al., 2011; Korolchuk et al., 2011; Michelet et al., 2015; Mrakovic et al., 2012; Pu et al., 2015; Schiefermeier et al., 2014; Tuli et al., 2013). Like Rab7, Arl8b regulates both lysosomal motility and cargo trafficking to lysosomes (Garg et al., 2011; Khatter et al., 2015a; Rosa-Ferreira and Munro, 2011). Silencing of Arl8b expression leads to impaired trafficking of endocytic cargo to lysosomes and impaired phago-lysosome fusion. This is partly explained by the direct interaction of Arl8b with one of the HOPS subunits, Vps41, that results in functional assembly of the HOPS complex on the lysosomal membranes (Garg et al., 2011; Khatter et al., 2015a).

While Rab7 and Arl8b have an overlapping subcellular distribution and function in regulating cargo trafficking to lysosomes, it is not known if there is any crosstalk or

coordination between the two GTPases. Previous studies suggest that dual or shared effectors represent a point of convergence of Rab, Arf and Arl signals in membrane traffic (Burguete et al., 2008; Hutagalung and Novick, 2011; Kinchen and Ravichandran, 2010; Naslavsky et al., 2006; Sharma et al., 2009; Shi and Grant, 2013). In line with this, we noted that a recently characterized Rab7 effector, PLEKHM1, shares ~40% similarity over the length of its RUN domain with the known Arl8b effector, SKIP (Rosa-Ferreira and Munro, 2011). Importantly, it is the RUN domain that mediates SKIP binding to Arl8b. This prompted us to investigate if PLEKHM1 can also interact with Arl8b using a similar binding interface as SKIP. PLEKHM1 appeared to be a plausible candidate for a shared effector of Rab7/Arl8b GTPases as expected from the distinct binding sites on PLEKHM1 for the two GTPases, i.e. Arl8b-binding through its N-terminal RUN domain, whereas binding to Rab7 mediated via its C-terminal second PH domain and C1/Zn-Finger (ZnF) domain (**Fig. 3.1 A**) (McEwan et al., 2015a; Tabata et al., 2010).

Here we show that indeed, the Rab7 effector PLEKHM1 binds to Arl8b via its N-terminal RUN domain and acts as a linker between the two GTPases. We further identified conserved basic residues within the N-terminal RUN domain of PLEKHM1 that are required for binding to Arl8b. Using an Arl8b-binding defective mutant of PLEKHM1 or cells lacking Arl8b, we show that 1) Arl8b is required for PLEKHM1 localization to lysosomes, but not LEs; 2) Arl8b mediates recruitment of HOPS complex to Rab7/PLEKHM1-positive vesicle contact sites and consequently their clustering; and 3) Arl8b-binding is crucial for PLEKHM1 to promote lysosomal degradation of endocytic and autophagic cargo.

3.2 Results

3.2.1 PLEKHM1 directly binds to Arl8b via its N-terminal RUN domain-containing region

To investigate whether PLEKHM1 behaves similar to SKIP and interacts with Arl8b via its RUN domain, we performed selective yeast two-hybrid binding with the full-length and a domain deletion mutant of PLEKHM1 lacking the N-terminal RUN domain-containing region (1-300 amino acids, NΔ300 PLEKHM1). We found that full-length PLEKHM1

interacted with the WT (wild-type) and Q75L (constitutively GTP-bound) forms of Arl8b, but not with the T34N (constitutively GDP-bound) form, indicating that PLEKHM1 interacts with Arl8b in its GTP-bound state (**Fig. 3.1 B**). No growth was observed between Arl8b and NΔ300 or a NΔ198 PLEKHM1 mutant (lacking only the RUN domain), demonstrating that interaction of PLEKHM1 with Arl8b was dependent upon the presence of its RUN domain (**Fig. 3.1 B**). In the assay, WT and NΔ300 mutant of SKIP (lacking the RUN domain containing region) were used as controls to confirm the previously reported interaction of Arl8b with SKIP (Rosa-Ferreira and Munro, 2011) (**Fig. 3.1 B**). We also corroborated these findings in cells using co-immunoprecipitation experiments, where PLEKHM1 showed binding to WT and Q75L forms, but not the T34N form of Arl8b (**Fig. 3.1 C**). To further clarify that the RUN domain of PLEKHM1 directly binds to Arl8b, GST and GST-tagged PLEKHM1 (1-300, first 300 amino acids containing the RUN domain) proteins were co-incubated with His-tagged Arl8b in the presence of non-hydrolysable GTP or GDP analogs, as well as with Arl8b-WT and -T34N expressing cell lysates. GST-PLEKHM1 (1-300) displayed a strong binding preference towards Arl8b in presence of GTP but not GDP, suggesting that PLEKHM1 directly binds to Arl8b (**Fig. 3.1 D and E**). We found similar binding of purified Arl8b to GST-PLEKHM1 (1-198), first 198 amino acids containing only the RUN domain (**Fig. 3.2 A**). However, as we consistently observed degradation of GST-PLEKHM1 (1-198) during its purification (see Ponceau S stain in **Fig. 3.2 A**), we used PLEKHM1 (1-300) purified protein in our subsequent binding assays.

Arl8 family has two paralogs in higher vertebrates, Arl8a and Arl8b, both of which are 91% identical at the protein level and have ubiquitous tissue expression (Hofmann and Munro, 2006). A previous study had shown that both paralogs bound to SKIP through its RUN domain (Hofmann and Munro, 2006). Surprisingly, we found a significantly weaker interaction of Arl8a with PLEKHM1 as compared to Arl8b while similar binding to SKIP was observed of both paralogs (**Fig. 3.2 B-E**). Together, these results demonstrate that PLEKHM1 directly binds to Arl8b, and that the N-terminal RUN domain-containing region of PLEKHM1 is both necessary and sufficient for this interaction.
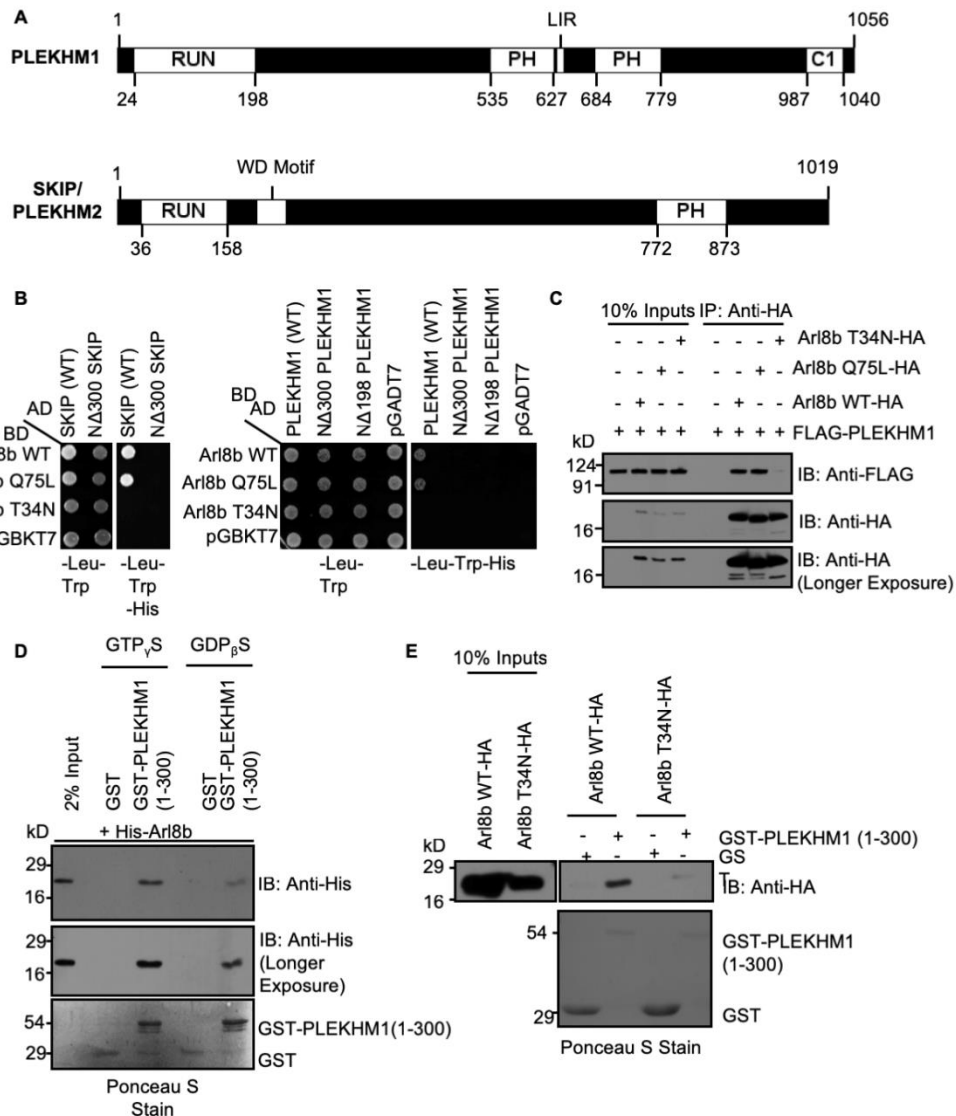
Figure 3.1: PLEKHM1 directly binds to the GTP-bound form of Arl8b via its RUN domain.

A) Schematic representation of the domain architecture of PLEKHM1 and SKIP/PLEKHM2. **B**) Indicated plasmids encoding GAL4-AD and GAL4-BD fusion genes were co-transformed in *Saccharomyces cerevisiae* to examine the interactions. The co-transformants were spotted on non-selective medium (-Leu-Trp) to confirm viability and on selective medium (-Leu-Trp-His) to detect interactions. **C**) FLAG tagged-PLEKHM1 was co-transfected with different forms of C-terminal HA-tagged Arl8b into HEK293T cells and the lysates were immunoprecipitated with anti-HA antibodies-conjugated-agarose beads and the precipitates were immunoblotted with the indicated antibodies. **D**) GST only and GST-PLEKHM1 (1-300 amino acids) proteins were immobilized on glutathione conjugated-agarose beads and incubated with purified His-Arl8b in the presence of GTP$_\gamma$S or GDP$_\beta$S and the interaction of the purified proteins was detected by Western blotting **E**) GST-pulldown assay performed using GST alone and GST-PLEKHM1 (1-300) bound to glutathione-agarose beads and lysates from HEK293T cells expressing either Arl8b WT-HA or Arl8b T34N-HA was incubated with the recombinant GST proteins. The precipitates were immunoblotted with anti-HA antibodies and GST-tagged proteins were visualized using Ponceau S staining.

50
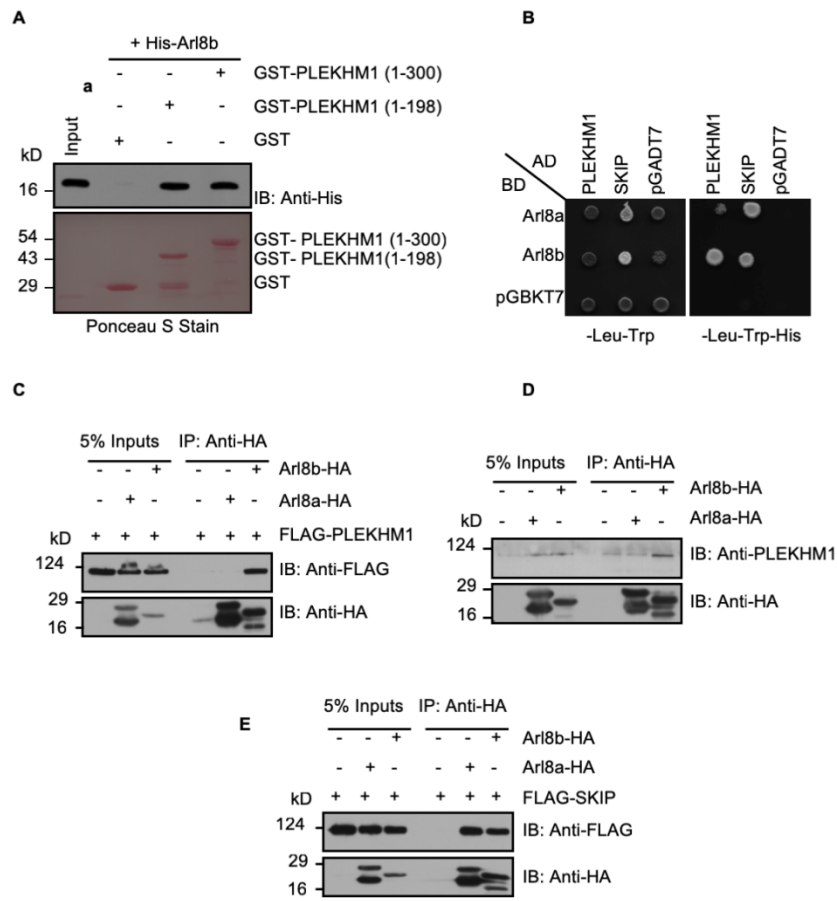
Figure 3.2: PLEKHM1 interacts weakly with Arl8a.

A) Immunoblot showing direct binding of His-Arl8b incubated with GST alone, GST-PLEKHM1 (1-198) and GST-PLEKHM1 (1-300). **B)** Interaction of PLEKHM1 with Arl8a was tested using the yeast two-hybrid assay. Cotransformants expressing the indicated proteins were spotted on non-selective medium (-Leu-Trp) to check viability and on selective medium (-Leu-Trp-His) to assess the interaction. **C-D)** HEK293T cell lysates expressing FLAG-PLEKHM1 (c) or FLAG-SKIP (d) alone and co-expressed with Arl8a-HA or with Arl8b-HA were immunoprecipitaed with anti-HA antibodies-conjugated-agarose beads and immunoblotted with indicated antibodies. **E)** Western blot of HEK293T lysates expressing either Arl8a-HA or Arl8b-HA immunoprecipitated with anti-HA antibodies-conjugated-agarose beads and probed with anti-PLEKHM1 antibody.

3.2.2 RUN domain of PLEKHM1 is required for its association with Arl8b- and LAMP1- but not Rab7–positive endosomes

Given that PLEKHM1 directly interacts with the lysosomal small GTPase Arl8b, we next assessed the significance of Arl8b-binding on PLEKHM1's subcellular localization and its function as an endolysosomal adaptor. To this end, we first verified the specificity of anti-PLEKHM1 antibody whereby; loss of signal upon PLEKHM1-siRNA treatment or in PLEKHM1-knockout (KO) cells was observed by Western blotting and immunofluorescence, confirming the specificity of these antibodies (**Fig. 3.3 A-C**). At physiological expression levels, PLEKHM1 was found to strongly colocalize with late endosomal/lysosomal proteins Rab7 (Pearson's correlation coefficient (R(r)) = 0.62, Mander's coefficient of PLEKHM1 overlap with Rab7 (M1) = 0.514) but also with Arl8b (R(r) = 0.55, M1 = 0.29) and LAMP1 (R(r) = 0.53, M1 = 0.33). Reduced colocalization was observed with EEA1, a marker for early endosomes (R(r) = 0.32, M1 = 0.06) (**Fig. 3.3 D-G**; R(r) quantification shown in **Fig. 3.3 H**). Supporting this, endogenous PLEKHM1 was also recruited to Rab7/Arl8b-labeled punctae in cells transfected with either of the two GTPases (**Fig. 3.4 A and C**). Moreover, as previously shown using an epitope-tagged construct (Tabata et al., 2010), endogenous PLEKHM1 also localized to cytosol upon expression of dominant negative mutant of Rab7 (Rab7 T22N), reinforcing the specificity of this antibody (**Fig. 3.4 B**). In accordance with our previous observations that RUN domain of PLEKHM1 was required for binding to Arl8b, colocalization of Arl8b with NΔ300 PLEKHM1 was significantly reduced as compared to WT, indicating that the colocalization was consistent with binding of the two proteins (**Fig. 3.4 E and F;** quantification shown in **Fig. 3.4 G**). Interestingly, NΔ300 PLEKHM1 continued to localize to punctate structures; however, several of these were LAMP1-negative but Rab7-positive (**Fig. 3.4 K**), suggesting that the RUN domain of PLEKHM1 is required for its association with Arl8b/LAMP1-positive lysosomes but not with Rab7-positive LEs. This is surprising as the conventional function attributed to the small GTPases involved in vesicular trafficking is to recruit their downstream effectors from the cytosol to specific endosomal membranes. Our data indicates that Arl8b does not mediate membrane recruitment of PLEKHM1; rather this role has been attributed to Rab7 (Tabata et al., 2010). Accordingly, PLEKHM1 continued to be endosomal in cells expressing dominant-negative Arl8b (Arl8b T34N) while in cells transfected with

dominant-negative Rab7 (Rab7 T22N), PLEKHM1 was completely cytosolic, and failed to colocalize with Arl8b (**Fig. 3.4 B and C**). These results were also supported by the finding that PLEKHM1 mutants that are unable to bind to Rab7 (i.e. PLEKHM1 ΔC1 and ΔKML) (McEwan et al., 2015a) are cytosolic (**Fig. 3.4 J and K**). Thus, while Rab7 regulates membrane localization of PLEKHM1, it is likely that Arl8b mediates its association with lysosomal membranes.
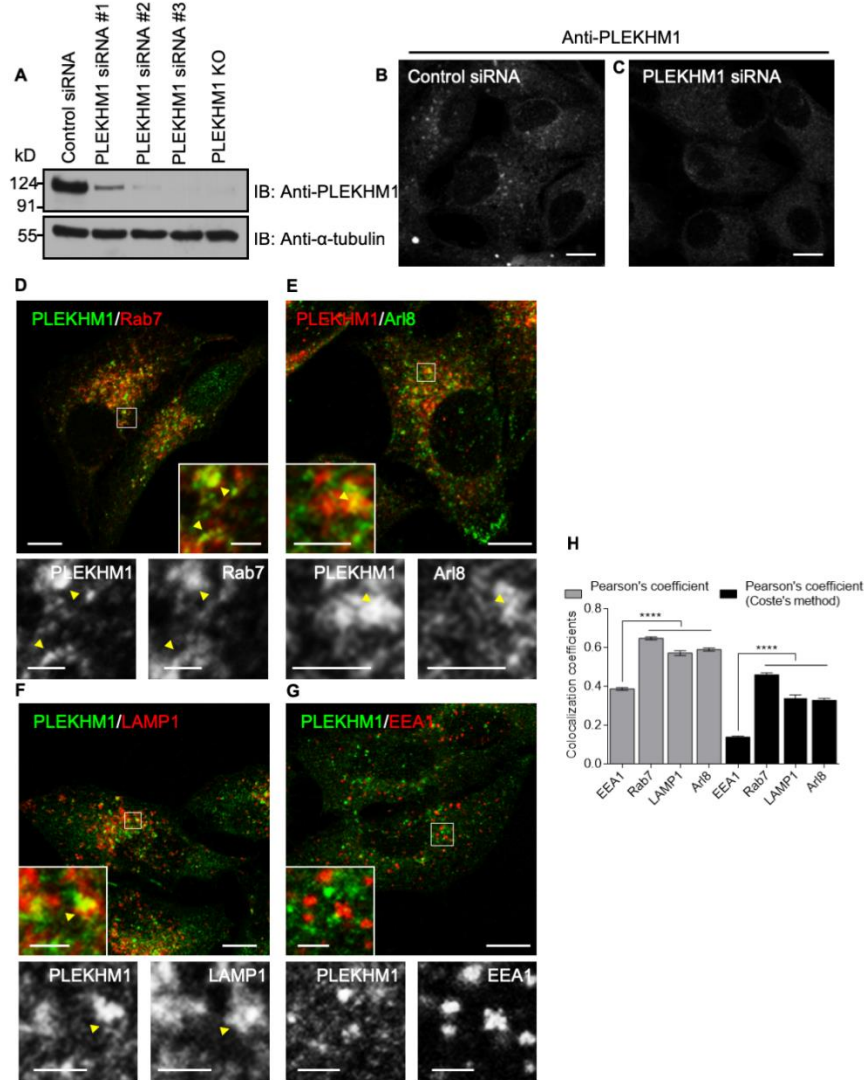
Figure 3.3: PLEKHM1 colocalizes with Rab7 and Arl8b.

A) Lysates from control siRNA treated-, three different PLEKHM1 siRNAs treated- and from PLEKHM1 KO-HeLa cells were probed with anti-PLEKHM1 antibody for assessing the knockdown efficiency and α-tubulin was used as the loading control. **B-C)** Immunofluorescence depicting the specificity of PLEKHM1 antibody in HeLa cells treated with control- and PLEKHM1-siRNA. **D-H)** Confocal micrographs of HeLa cells showing endogenous staining of PLEKHM1 with Rab7, Arl8, LAMP1 and EEA1, and the Pearson's correlation coefficient quantification of endogenous PLEKHM1 with these endocytic markers from three independent experiments is shown (n=25-30 cells per experiment for each treatment; ****p<0.0001). In the insets, arrowheads mark colocalized pixels. Scale bars=10μm.
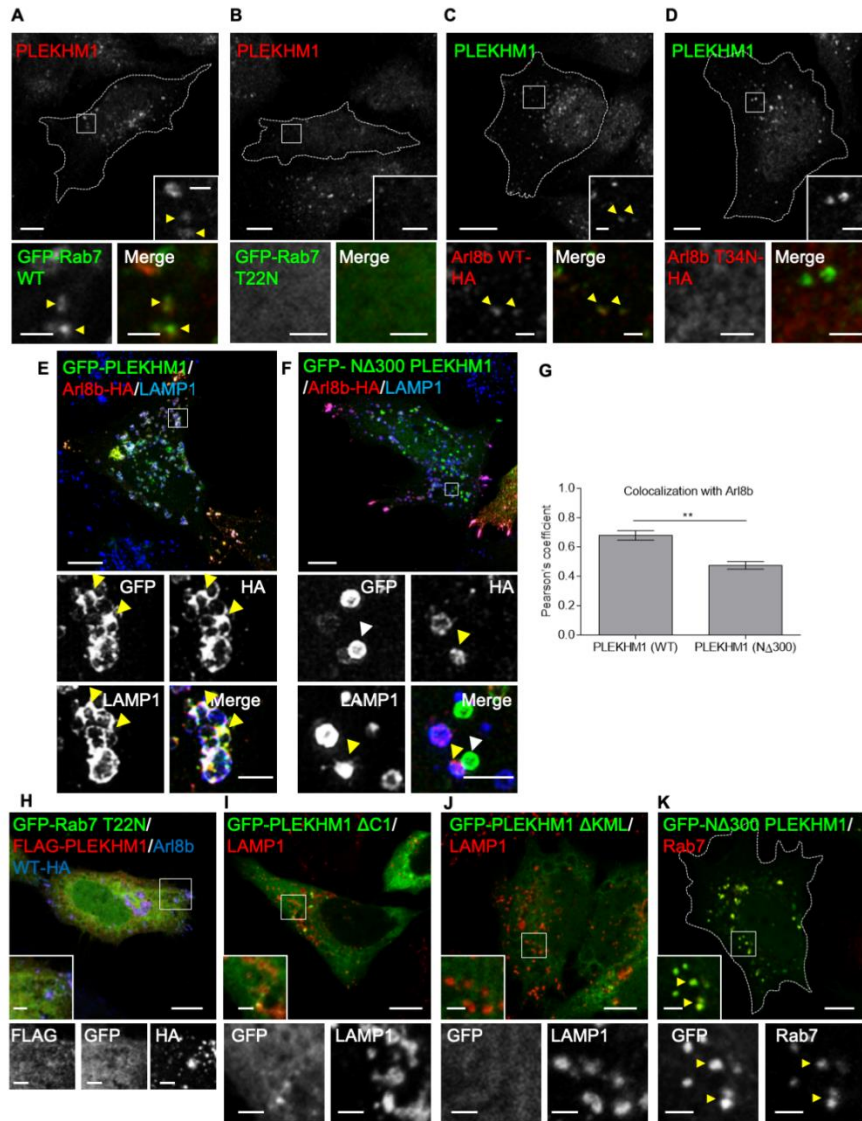
Figure 3.4: PLEKHM1 is recruited to membranes by Rab7 and colocalization with Arl8b depends on RUN domain.

A-D) Confocal micrographs of HeLa cells transfected with either GFP-Rab7 WT, GFP-Rab7 T22N, Arl8bWT-HA or Arl8b T34N-HA and immunostained for endogenous PLEKHM1. Colocalized pixels are marked by arrowheads in the insets. **E-F**) SIM image of HeLa cells co-transfected with Arl8b-HA and GFP-PLEKHM1 or GFP-NΔ300 PLEKHM1 and stained for lysosomes using anti-LAMP1 antibodies. In the insets, yellow arrowheads indicate colocalized pixels and white arrowheads denote NΔ300 PLEKHM1-positive vesicles. **G**) Colocalization of WT and NΔ300 PLEKHM1 with Arl8b was assessed by measuring the Pearson's coefficient. Values plotted are mean ± s.e.m. from three independent experiments (n=75 cells per experiment; **p<0.01). **H-K**) Representative Confocal micrograph of HeLa cells transfected with indiacted plasmids and immunostained. Colocalized pixels are marked by arrowheads in the insets. Scale bars=10μm, Insets (2μm)

54

3.2.3 Arl8b-binding is required for PLEKHM1 to localize to lysosomes and mediate clustering of late endosomes and lysosomes

We observed that co-transfection of PLEKHM1 with Arl8b led to dramatic perinuclear clustering of LAMP1-positive compartments, which was antagonistic to cells transfected with Arl8b alone that promotes lysosome positioning to the cell periphery (**Fig. 3.5 A, B and C**). This effect was restricted only to the late endocytic compartments, as the subcellular distribution of organelles, including early endosomes or Golgi, was not altered (**Fig. 3.5 E and F**). Interestingly, transfection of NΔ300 PLEKHM1 with Arl8b did not induce perinuclear clustering of LAMP1-positive endosomes, rather Arl8b-dependent lysosome positioning to cell periphery was observed in these cells (**Fig. 3.5 B and C**). Using structured illumination microscopy (SIM) and cryo-immunogold-EM, we further observed that Arl8b and PLEKHM1 were present on the limiting membranes of these enlarged and tightly clustered endo-lysosomal compartments along with LAMP1 (**Fig 3.4 E and F**, **Fig. 3.5 G**). Additionally, live-cell imaging experiments (described later in the text) revealed that late endosomal protein-Rab7 is also present on these clustered endosomes along with Arl8b. SIM imaging further showed enrichment of WT PLEKHM1 and Arl8b on the vertices of these perinuclear docked endo-lysosomes (indicated by arrowheads in **Fig. 3.4 E and F**), while NΔ300 PLEKHM1 was present on endosomes distinct from Arl8b/LAMP1-positive endosomes (**Fig. 3.4 F**), and are likely to be Rab7-positive LEs (as depicted in **Fig. 3.4 K**). This localization pattern indicates function of PLEKHM1 and Arl8b in the vesicle fusion pathway, and is in accordance with the attributed function of PLEKHM1 in mediating autophagosome-lysosome fusion (McEwan et al., 2015a). In lieu of a recent study by Johnson et al., (2016) our observations suggest that PLEKHM1-mediated repositioning of Arl8b-positive lysosomes from cell periphery to perinuclear region could also alter the pH and degradative capacity of these compartments.
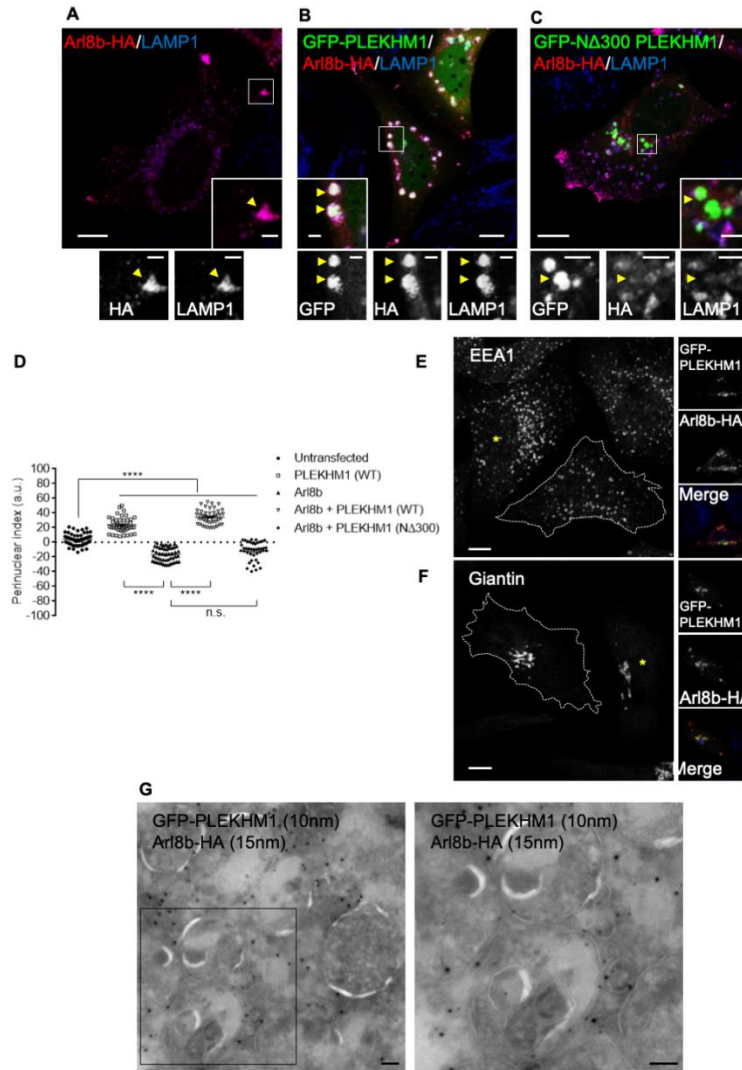
**Figure 3.5: PLEKHM1 colocalizes with Rab7 and Arl8b and promotes perinuclear clustering of lysosomes.**

A-C) Confocal micrographs of HeLa cells transfected with Arl8b-HA alone or co-transfected with GFP-PLEKHM1 or -NΔ300 PLEKHM1, respectively, and stained for LAMP1. In the insets, arrowheads mark colocalized pixels. **D)** Perinuclear index of LAMP1$^+$ compartments in HeLa cells transfected with indicated plasmids. Values plotted are mean ± s.e.m. from three independent experiments (n=25-30 cells per experiment for each treatment; ****p<0.0001; n.s., not significant). **E-F**) Representative confocal micrograph of HeLa cells co-transfected with Arl8b-HA and GFP-PLEKHM1 and stained for early endosomal marker, EEA1 or golgi marker, Giantin (* marks untransfected cells). Scale bar=10μm, Insets (2μm**) G)** Representative immunogold EM image of HeLa cells co-transfected with GFP-PLEKHM1 and Arl8b-HA and labeled with 10nm and 15nm gold particles, respectively. Boxed region is magnified on the right. Scale bar=100nm.

Since deletion of 300 amino acid residues from PLEKHM1 might disrupt its binding to other interaction partners besides Arl8b, we sought to identify the residues within the RUN domain of PLEKHM1 that might regulate Arl8b-binding. RUN domains are present in several effectors of the Ras superfamily of small GTPases (Callebaut et al., 2001). Multiple sequence alignment of the conserved core of the RUN domain family members (organized in six blocks from A-F) has revealed polar amino acids (in blocks A and D) that may regulate interaction with the small GTPases (Callebaut et al., 2001). Sequence alignment of the first 300 residues of PLEKHM1 and SKIP/PLEKHM2 illustrate the positions of these conserved polar residues within these proteins (Data not shown). To this end, we created single (H60A, H63A and R123A), double (R117A/R119A; "RR→A") or triple (H60A/R117A/R119A; "HRR→A") point mutants substituting the conserved basic residues in the RUN domain-containing region of PLEKHM1 with alanine, and assessed interaction with Arl8b. Our yeast two-hybrid and dot-blot assays demonstrated that of the five conserved basic residues within the RUN domain, four (H60, R117, R119, and R123) were important for Arl8b-binding (**Fig. 3.6 A and B**). For the dot-blot assay, His-tagged Rab7 was used as a control, since it does not bind within the first 300 residues of PLEKHM1 (Tabata et al., 2010). Consistent with their lack of interaction with Arl8b, RUN domain mutants of PLEKHM1 had reduced overlap (~1.5-fold decrease) with LAMP1 as compared to the WT protein (**Fig. 3.6 C-E**). Notably, several of the PLEKHM1 (WT/mutant) endosomes that were positive for LAMP1 are likely to be LEs, as LAMP1 localizes to both LEs and lysosomes (Falcon-Perez et al., 2005; Geuze et al., 1988). As compared to Arl8b, no differences were observed in the binding and colocalization of RUN domain mutants of PLEKHM1 with Rab7 (**Fig. 3.6 A, E and F**). Importantly, PLEKHM1 (HRR→A), similar to NΔ300 and NΔ198 PLEKHM1, had an impaired ability to cluster/tether LAMP1-positive compartments (compare the enlarged insets in **Fig. 3.7 A and B**; quantification of average size of LAMP1-positive vesicles shown in **Fig. 3.7 C**). On the other hand, PLEKHM1 (H63A) mutant that continues to bind Arl8b was able to cluster LEs/lysosomes similar to WT PLEKHM1 (**Fig. 3.7 C**).
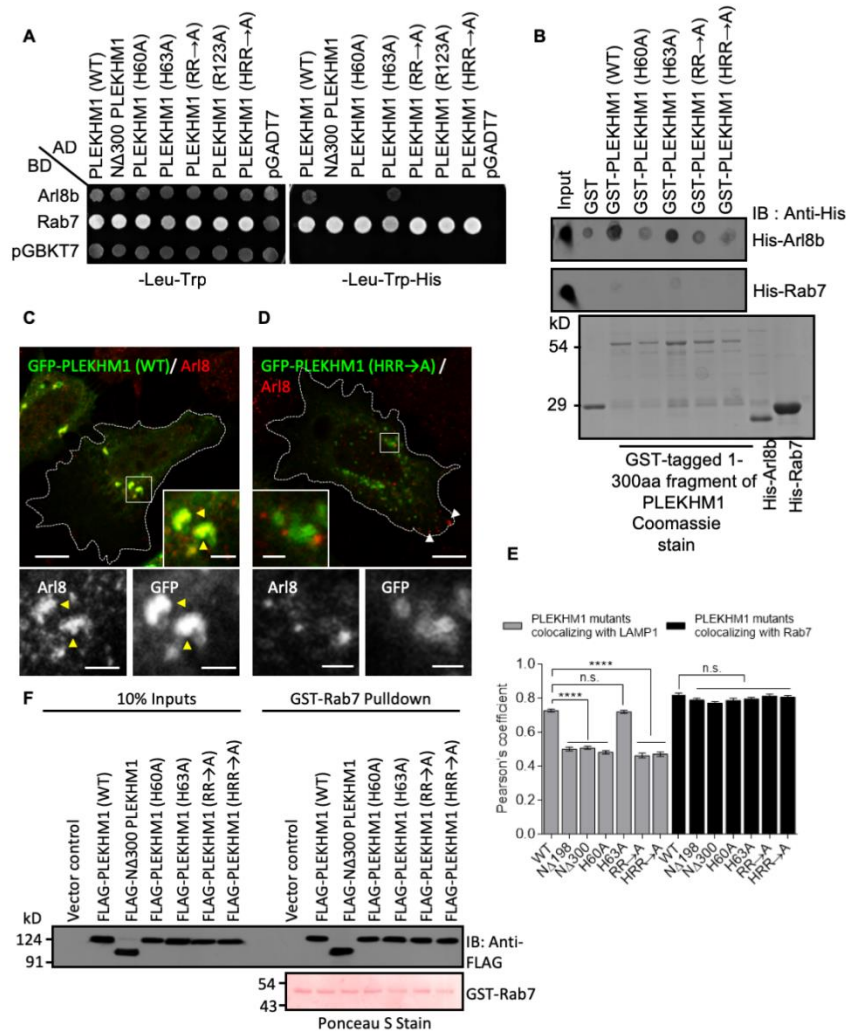
Figure 3.6: Conserved basic residues within the RUN domain of PLEKHM1 are important for its interaction with Arl8b.

A) Binding of RUN domain point mutants of PLEKHM1 with Arl8b and Rab7 was tested using yeast two-hybrid assay. **B)** For dot-blot assay, GST alone or GST-PLEKHM1 (1-300) or indicated point mutant(s) were spotted on nitrocellulose membrane and incubated with His-Arl8b or His-Rab7. The interaction was analysed by immunoblotting with anti-His antibody. The purified proteins were visualized by Coomassie staining. **C-D)** Confocal images showing HeLa cells transfected with GFP-PLEKHM1 or GFP-PLEKHM1 (HRR→A) and immunostained for endogenous Arl8. In the insets, yellow arrowheads mark colocalized pixels and white arrowheads mark peripheral Arl8b+-lysosomes. Scale bars=10μm, Insets (2μm) **E)** Pearson's correlation coefficient quantification of WT or indicated mutant of PLEKHM1 colocalization with LAMP1 and Rab7 is shown. Values plotted are mean ± s.e.m. from three independent experiments (n=30 cells per experiment; ****p<0.0001; n.s., not significant). **F)** Representative immunoblot of a GST pulldown assay using HEK293T cell lysates expressing FLAG-PLEKHM1 (WT) or -Arl8b binding defective mutants of PLEKHM1 incubated with GST-Rab7 bound to glutathione-coated beads. Purified GST-Rab7 protein was visualized by Ponceau S staining.
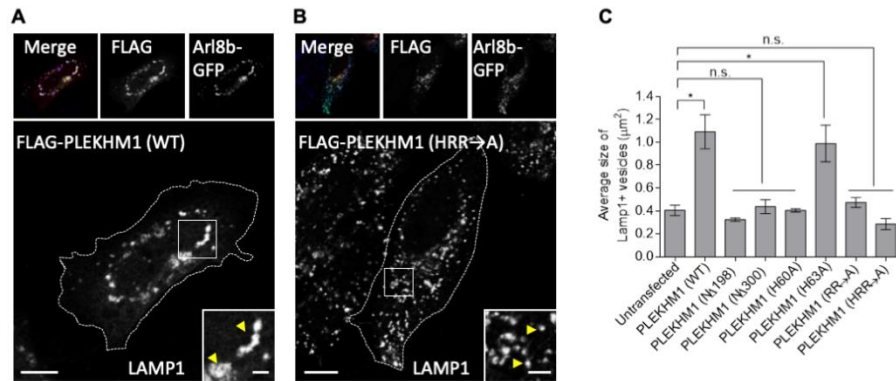
Figure 3.7: Arl8b binding defective mutants are unable to cause endoslysosomal tetehring.

A-B) Confocal panels showing LAMP1 staining in HeLa cells co-transfected with Arl8b-GFP and FLAG-PLEKHM1 (WT) or HRR→A mutant. In the insets, LAMP1 staining is shown. **C)** Average size of LAMP1$^+$ compartments in HeLa cells co-transfected with indicated PLEKHM1 plasmid and Arl8b-GFP. Values plotted are mean ± s.e.m. from three independent experiments (n=25 cells analysed per experiment for each treatment; *p<0.05; n.s., not significant). Scale bars=10μm, Insets (2μm).

Next, we depleted Arl8b from HeLa cells to directly assess its role in regulating lysosomal localization of PLEKHM1 and in PLEKHM1-mediated clustering/tethering of LEs and lysosomes. The efficiency of Arl8b depletion (using two different oligos) was >90% as assessed by immunoblotting using an anti-Arl8 antibody (**Fig. 3.8 A**). As previously observed with Arl8b-binding defective mutants of PLEKHM1, Arl8b-depletion also led to significantly reduced localization of PLEKHM1 to dextran loaded-lysosomes. This localization defect was rescued by expression of siRNA-resistant Arl8b construct, suggesting that binding to Arl8b is essential for lysosomal localization of PLEKHM1 (**Fig. 3.8 B-E; quantification shown in Fig. 3.8 I**). For these experiments, overnight incubation of dextran was done to ensure that it accumulates within the terminal lysosomes, which was verified by quantifying dextran colocalization with LAMP1 in control- and Arl8b-depleted cells (**Fig. 3.8 J and K;** quantification shown in **Fig. 3.8 L**). Next, we assessed whether Arl8b-depletion affects PLEKHM1 colocalization with Rab7. As shown in **Fig. 3.8 F-H**, PLEKHM1-labeled endosomes continued to be Rab7-positive upon Arl8b-depletion; rather a modest but significant increase in colocalization with Rab7 was observed in Arl8b-depleted cells (**Fig. 3.8 F-H** quantification shown in **Fig. 3.8 I**). Furthermore, as previously observed upon expression of Arl8b-binding defective mutants of PLEKHM1, average size of PLEKHM1-positive endosomes was reduced by ~2-fold upon Arl8b-depletion and this effect was rescued

by the expression of siRNA-resistant Arl8b construct (**Fig. 3.9 A-D**; quantification shown in **Fig. 3.9 E**). Taken together, our results suggest that Arl8b-binding is required for PLEKHM1 localization to lysosomes, but not Rab7-positive LEs, and for PLEKHM1's ability to mediate clustering of LEs and lysosomes.
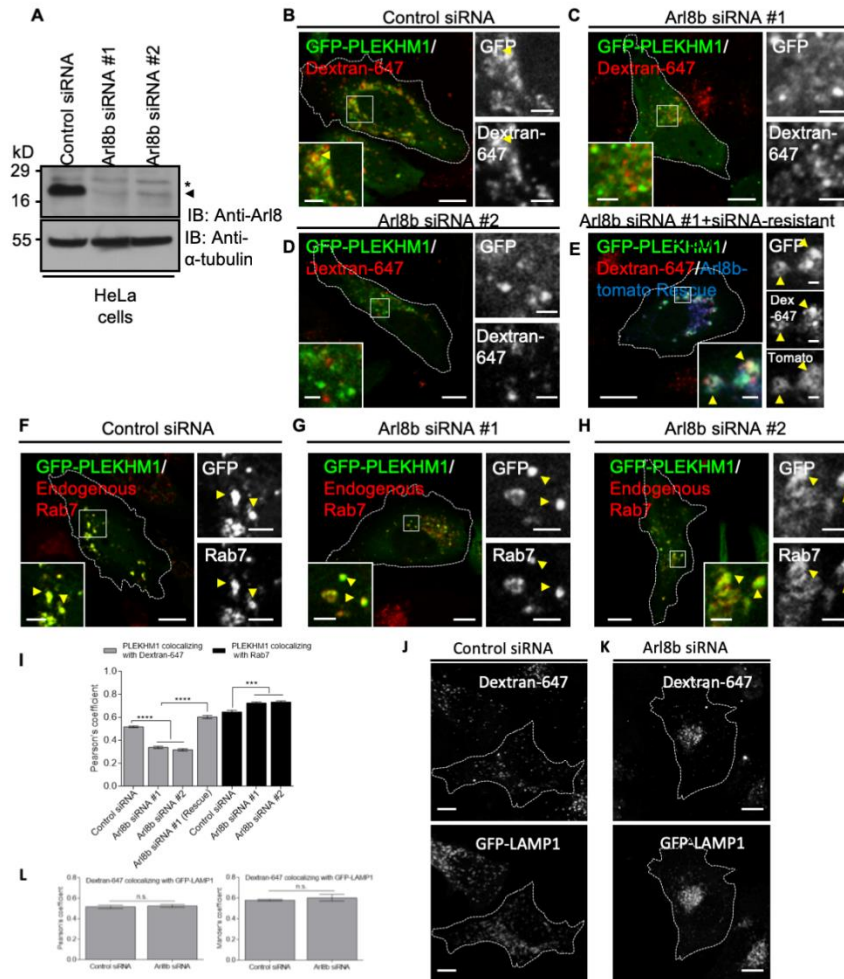
**Figure 3.8: Arl8b is required for PLEKHM1 association with lysosomes**

a) Control- and Arl8b-siRNA (#1 and #2) treated HeLa cell lysates were probed with anti-Arl8 antibody for assessing the knockdown efficiency and α-tubulin was used as the loading control. Asterisk and arrowhead denotes Arl8a and Arl8b protein bands, respectively. **B-E)** Confocal micrographs depicting the localization of GFP-PLEKHM1 with Dextran-647-loaded lysosomes in indicated siRNA treatments and Arl8b siRNA-rescued HeLa cells. In the insets, arrowheads mark colocalized pixels. **F-H)** Representative confocal micrographs of HeLa cells treated with control- or Arl8b-siRNAs and transfected with GFP-PLEKHM1 followed by immunostaining for endogenous Rab7. In the insets, arrowheads mark colocalized pixels. **I)** Pearson's correlation coefficient was calculated as a measure of colocalization of PLEKHM1 with Dextran-647-loaded lysosomes or with Rab7 in control siRNA- and Arl8b siRNA-treated HeLa cells. Values plotted are mean ± s.e.m. from three independent experiments (n=30 cells analysed per experiment for each treatment; ***p<0.001; n.s., not significant). **J-L)** Control- or Arl8b- siRNA treated HeLa cells were incubated overnight with Dextran-647 followed by transfection of GFP-LAMP1 and their colocalization was analysed by confocal microscopy. Colocalization was also quantified by measuring Pearson's and Mander's correlation coefficients. Values plotted are mean ± s.e.m. from three independent experiments (n=30 cells analysed per experiment for each treatment; n.s., not significant).

60
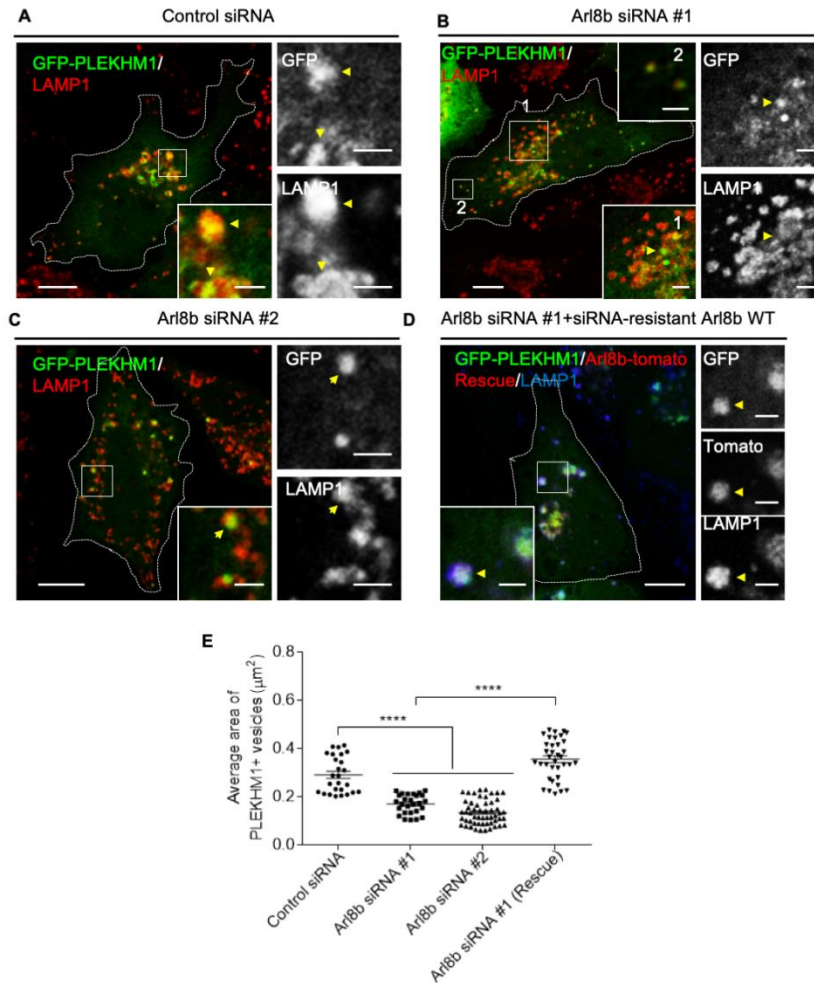
Figure 3.9: Arl8b is required for PLEKHM1 mediated late endosome and lysosome clustering. A-D) Confocal micrographs of HeLa cells expressing GFP-PLEKHM1 and stained for LAMP1 in indicated siRNA treatments and Arl8b siRNA-rescued HeLa cells. In the insets, arrowheads mark colocalized pixels. **E)** Average size of PLEKHM1$^+$ compartments in indicated siRNA treatments and Arl8b siRNA-rescued HeLa cells. Values plotted are mean ± s.e.m. from four independent experiments (n=15 cells analysed per experiment for each treatment; ****p<0.0001). Scale bars=10μm.

3.2.4 PLEKHM1 acts as a linker between the small GTPases Arl8b and Rab7

Previously Tabata et al., (2010) had described PLEKHM1 as a Rab7 effector that binds Rab7 via its C-terminal C1/ZnF domain (also known as the Rubicon Homology domain). Recent experiments, however, showed that both C1/ZnF and the second PH domain were required for efficient binding to Rab7 (McEwan et al., 2015a). Also, Rab7 regulates recruitment of PLEKHM1 from cytosol to endosomal membranes (Tabata et al., 2010). Our results here indicate that the N-terminal RUN domain of PLEKHM1 is required for binding to Arl8b, which in turn promotes PLEKHM1 lysosomal localization and facilitates its function in clustering of the late endocytic compartments. Based on these evidences, we hypothesized a model whereby PLEKHM1 acts as a linker between the two GTPases, with Rab7 primarily localized on LEs and Arl8b on lysosomes, to mediate clustering of these compartments. To test this hypothesis, we visualized interaction of Rab7 and Arl8b by using biochemical approaches, and by live-cell imaging and super resolution microscopy experiments. In live-cell imaging experiments, we observed numerous transient kiss-and-run events between epitope-tagged Rab7 and Arl8b, which was consistent with a weak co-immunoprecipitation of Arl8b with Rab7 (and vice-versa) detected in cells with physiological expression of PLEKHM1 (**Fig. 3.10 A, D (lane 4) and F (lane 5)**). Overexpression of WT, but not the (HRR→A) mutant of PLEKHM1 enhanced the interaction between the two GTPases, while no interaction was observed in PLEKHM1-siRNA treated cells (**Fig. 3.10 D (lanes 5 and 6) and F (lane 6)**). This was also observed in live-cell imaging, wherein Rab7 and Arl8b remained highly colocalized over time on the tightly clustered, less motile endolysosomes (**Fig. 3.10 B**). Notably, in cells expressing PLEKHM1 mutants that do not bind Arl8b but bind Rab7, dramatically reduced interaction and colocalization between the two GTPases was observed (**Fig. 3.10 C**). Consistent with this, colocalization of endogenous Rab7 and Arl8b was also strikingly reduced in cells expressing Arl8b-binding defective mutants of PLEKHM1 (**Fig. 3.10 E**). One possible explanation for this dominant-negative behavior is that the ectopically expressed mutant proteins compete with endogenous PLEKHM1 for binding to Rab7, thereby disrupting the membrane localization of the endogenous protein.
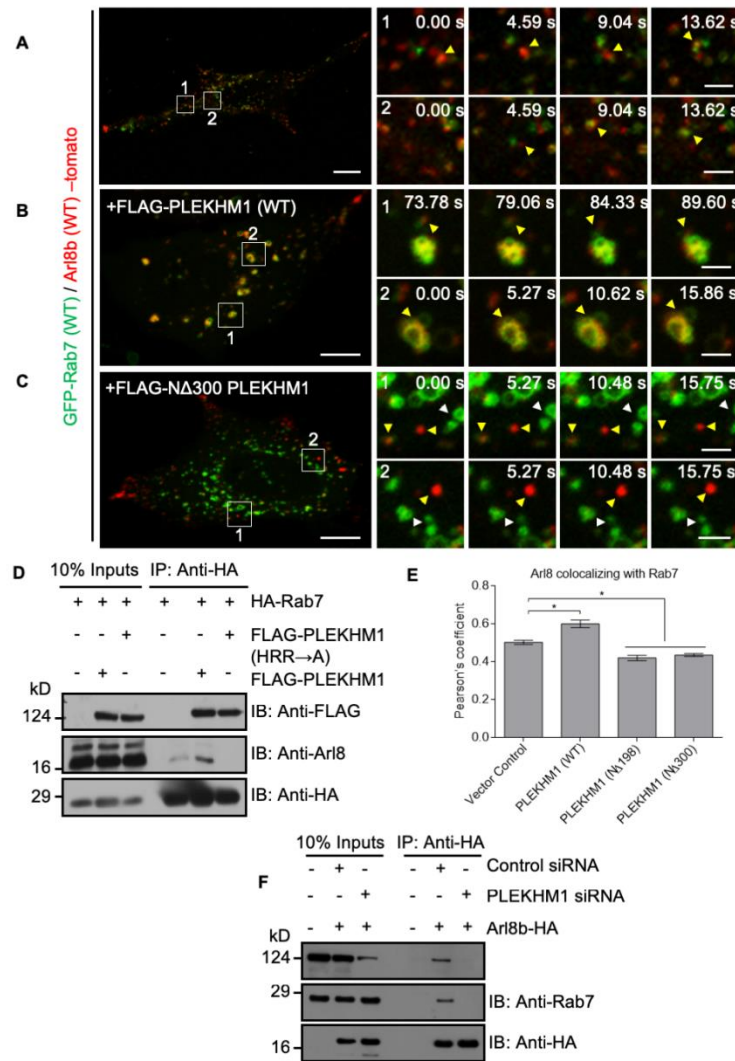
Figure 3.10: PLEKHM1 acts as a multivalent adaptor that promotes physical interaction between Rab7 and Arl8b.

A-C) Live-cell imaging was performed on cells expressing GFP-Rab7 and Arl8b-tomato along with either FLAG-PLEKHM1 or FLAG- NΔ300 PLEKHM1. The yellow arrowhead depicts kiss-and-run events in (a) and clustered enlarged endolysosomes in (b), respectively. Rab7- and Arl8b-positive punctate structures that do not fuse in (c) are marked by white and yellow arrowheads. **D)** HEK293T cell lysates expressing HA-Rab7 alone or co-expressed with either FLAG-PLEKHM1 (WT) or FLAG-PLEKHM1 (HRR→A) were immunoprecipitated with anti-HA antibodies-conjugated-agarose beads and immunoblotted using the indicated antibodies. **E)** Pearson's correlation coefficient was measured for endogenous Arl8 and Rab7 immunostained in HeLa cells transfected with indicated plasmids. Values plotted are mean ± s.e.m. from three independent experiments (n=30 cells analysed per experiment for each treatment; *p<0.05). **F)** Arl8b-HA was transfected in control- or PLEKHM1-siRNA treated HEK293T cells. The lysates were immunoprecipitated with anti-HA antibodies-conjugated-agarose beads and immunoblotted using the indicated antibodies.
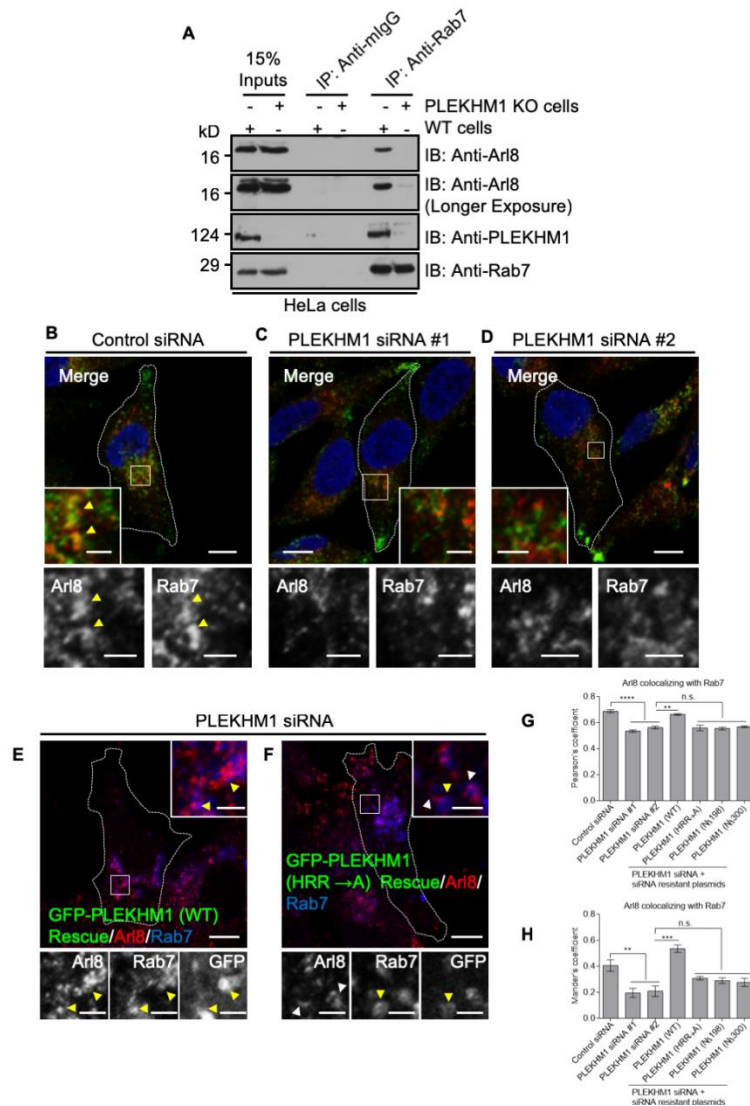
**Figure 3.11: PLEKHM1 acts as linker for Rab7 and Arl8b at endogenous level.**

A) Lysates of WT- and PLEKHM1 KO-HeLa cells were immunoprecipitated with anti-Rab7 antibody-conjugated-agarose beads and immunoblotted with indicated antibodies. **B-D)** Confocal images of HeLa cells treated with either control siRNA or PLEKHM1 siRNAs and immunostained with anti-Arl8 and anti-Rab7 antibodies. In the insets, arrowheads mark colocalized pixels and nucleus was stained using DAPI. **E-F)** Representative confocal micrographs of PLEKHM1 siRNA treated HeLa cells expressing siRNA resistant GFP-PLEKHM1 (WT) or GFP-PLEKHM1 (HRR→A) and immunostained for endogenous Arl8 and Rab7. In the insets, yellow arrowheads mark colocalized pixels. **G-H)** Pearson's and Mander's correlation coefficients were calculated for Arl8 and Rab7 colocalization in indicated siRNA treatments of HeLa cells. Values plotted are mean ± s.e.m. from three independent experiments (n=30 cells analysed per experiment for each treatment; **p<0.01; ***p<0.001; ****p<0.0001; n.s., not significant). Scale bars=10μm.

64

Since the above-mentioned experiments were performed under conditions where one of the two GTPases was ectopically expressed, we tested if at physiological expression levels Rab7 interacts with Arl8b. Indeed, as shown in **Fig. 3.11 A**, Arl8b was co-immunoprecipitated with Rab7 under physiological conditions, and this interaction was abrogated in a PLEKHM1-KO cell line. Notably, we also detected endogenous PLEKHM1 in complex with Rab7 and Arl8b. In accordance with our biochemical experiments, colocalization of endogenous Arl8b and Rab7 was significantly reduced upon PLEKHM1-depletion, which was rescued by siRNA-resistant PLEKHM1 (WT), but not by the Arl8b-binding defective mutants (**Fig. 3.11 B-F;** quantification shown in **Fig. 3.11 G and H**). Taken together, these results illustrate that PLEKHM1 acts as a multivalent adaptor that promotes physical interaction between two key regulators of the LE/lysosomal pathway, Rab7 and Arl8b.

3.2.5 Arl8b is required for PLEKHM1 interaction with the multisubunit tethering factor HOPS complex

PLEKHM1 interacts with the multisubunit tethering factor HOPS complex and recruit it to vesicle contact sites of LEs/autophagosomes and lysosomes, promoting tethering and fusion of these compartments (McEwan et al., 2015a). This was previously shown by co-immunoprecipitation and GST-pulldown experiments where the GST-RUN domain of PLEKHM1 was shown to interact with the HOPS subunits Vps41 and Vps39. Moreover, direct binding of the Vps39 C-terminal domain to full-length PLEKHM1 was also reported using purified proteins (McEwan et al., 2015a). While we observed interaction of Vps39 with PLEKHM1 by yeast two-hybrid, no interaction was detected with Vps41. A weaker but detectable interaction was also observed with Vps18 subunit of the HOPS complex (**Fig. 3.12 A**). Evidently, similar to the WT protein, PLEKHM1 (HRR→A) mutant continued to colocalize and interact with Vps39 (**Fig. 3.12 B and C**). As shown previously, (HRR→A) mutant of PLEKHM1 was defective in Arl8b-binding and LE/lysosome clustering, therefore we hypothesized that Arl8b was required for PLEKHM1 to recruit other subunits of the HOPS complex. In support of this hypothesis, Vps41, a known Arl8b effector, localizes to and recruits other subunits of the HOPS complex to lysosomes in an Arl8b-dependent

manner (Garg et al., 2011; Khatter et al., 2015a). Indeed, unlike WT, PLEKHM1 (HRR→A) mutant failed to co-immunoprecipitate multiple HOPS subunits except Vps39 (**Fig. 3.12 D**)
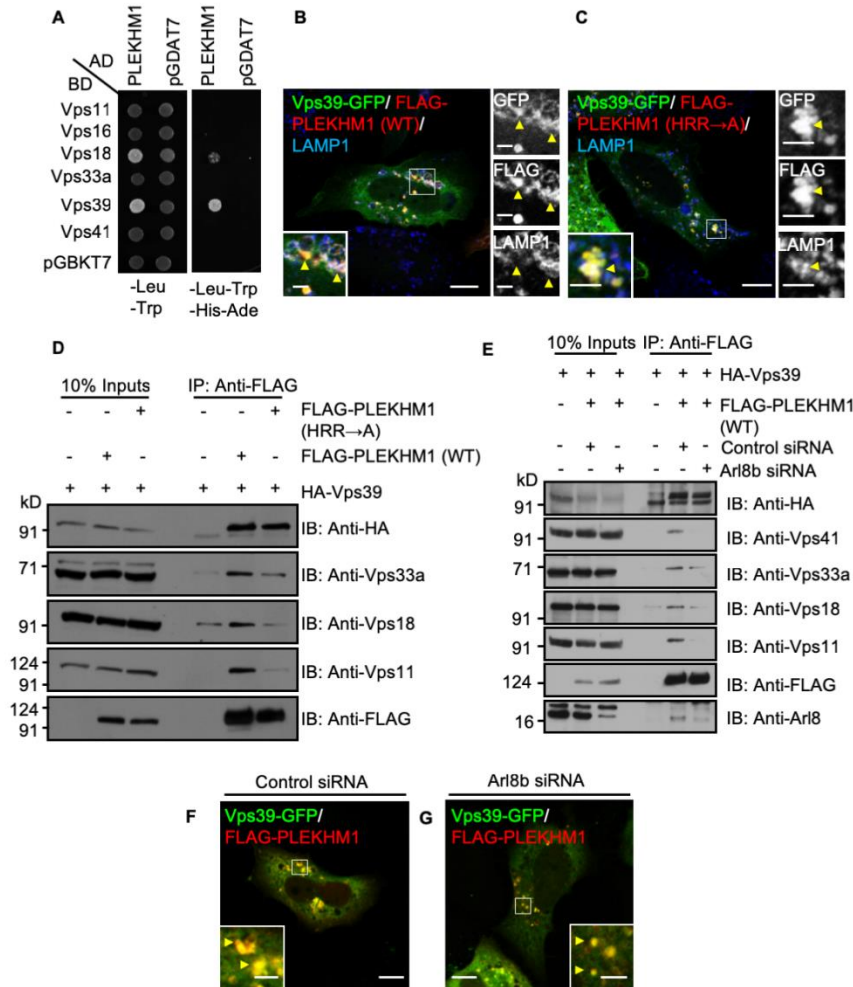
Figure 3.12: PLEKHM1 directly interacts with Vps39 but requires Arl8b for its interaction with other subunits of the HOPS complex.

A) Interaction of individual HOPS complex subunits with PLEKHM1 was tested using the yeast two-hybrid assay. The co-transformants were spotted on non-selective medium (-Leu-Trp) to check for viability and on selective medium (-Leu-Trp-His-Ade) to detect interaction. **B-C)** Confocal micrographs of HeLa cells co-expressing Vps39-GFP with FLAG-PLEKHM1 or -PLEKHM1 (HRR→A) and immunostained with anti-LAMP1 antibodies. Colocalized pixels are marked by arrowheads in the insets. **D)** Lysates from HEK293T cells co-expressing HA-Vps39 along with FLAG-PLEKHM1 or FLAG-PLEKHM1 (HRR→A) were immunoprecipitated using anti-FLAG antibodies-conjugated-agarose beads and immunoblotted with the indicated antibodies against the different HOPS subunits. **E)** HEK293T cells treated with control- or Arl8b-siRNA and co-expressing HA-Vps39 and FLAG-PLEKHM1 were immunoprecipitated with anti-FLAG antibodies-conjugated-agarose beads and immunoblotted with indicated antibodies. **F-G)** Confocal images of HeLa cells treated with either control- or Arl8b-siRNA and co-transfected with Vps39-GFP and FLAG-PLEKHM1. Colocalized pixels are marked by arrowheads in the insets.

Further, silencing of Arl8b profoundly reduced the fraction of HOPS subunits (except Vps39) co-immunoprecipitated with PLEKHM1 (**Fig. 3.12 E** and **Fig. 3.13 A**). Consistent with these results, colocalization of endogenous HOPS subunits, Vps41 and Vps18, with PLEKHM1 was also reduced upon Arl8b-depletion and this effect was rescued upon siRNA-resistant Arl8b expression (**Fig. 3.13 B-I**; quantification shown in **Fig. 3.13 J and K**). As expected by its direct binding, Vps39 was recruited to PLEKHM1-positive endosomes in both control and Arl8b-depleted cells (**Fig. 3.12 F and G**). Previous studies have shown that RUN domain of PLEKHM1 binds to epitope-tagged Vps41 from transfected cell lysates (McEwan et al., 2015a). We reasoned that direct binding of Arl8b with the RUN domain of PLEKHM1 explains these observations. Indeed, we found reduced binding of endogenous HOPS subunits, Vps41 and Vps18, with GST-PLEKHM1 (1-300) protein fragment from Arl8b-KO cell lysates when compared to WT cell lysates (**Fig. 3.14 A**). Binding to HOPS subunits was reconstituted by addition of increasing amounts of purified His-tagged Arl8b protein to the cell lysates, validating that Arl8b mediates interaction of HOPS complex with PLEKHM1 (**Fig. 3.14 A**). We also performed tandem affinity purification using TAP-tagged Vps41 as bait to semi-purify HOPS complex from HeLa cell lysates. Mass spectrometry analysis confirmed enrichment of HOPS subunits in these eluates (Data not shown). Binding of the semi-purified HOPS complex was observed with GST-PLEKHM1 (1-300) protein fragment in the presence of Arl8b upon addition of excess of GTP but not GDP (**Fig. 3.14 B**). These results clearly demonstrate Arl8b as an essential factor required for HOPS complex interaction with PLEKHM1. Conversely, Arl8b interaction with multiple HOPS subunits was not dependent on PLEKHM1 expression; although it is likely that PLEKHM1 regulates recruitment of Vps39 to Arl8b-positive lysosomes (**Fig. 3.14 D**). In further support of Arl8b function in recruitment of HOPS complex, co-immunoprecipitation of multiple HOPS subunits with Rab7-PLEKHM1 complex also required presence of Arl8b. Accordingly, little or no interaction of HOPS subunits was observed with Rab7 and PLEKHM1 in Arl8b-silenced cells as compared to control (**Fig. 3.14 C**). As expected, no effect on PLEKHM1 interaction with Rab7 was observed upon Arl8b-depletion (**Fig. 3.14 C**, top panel).
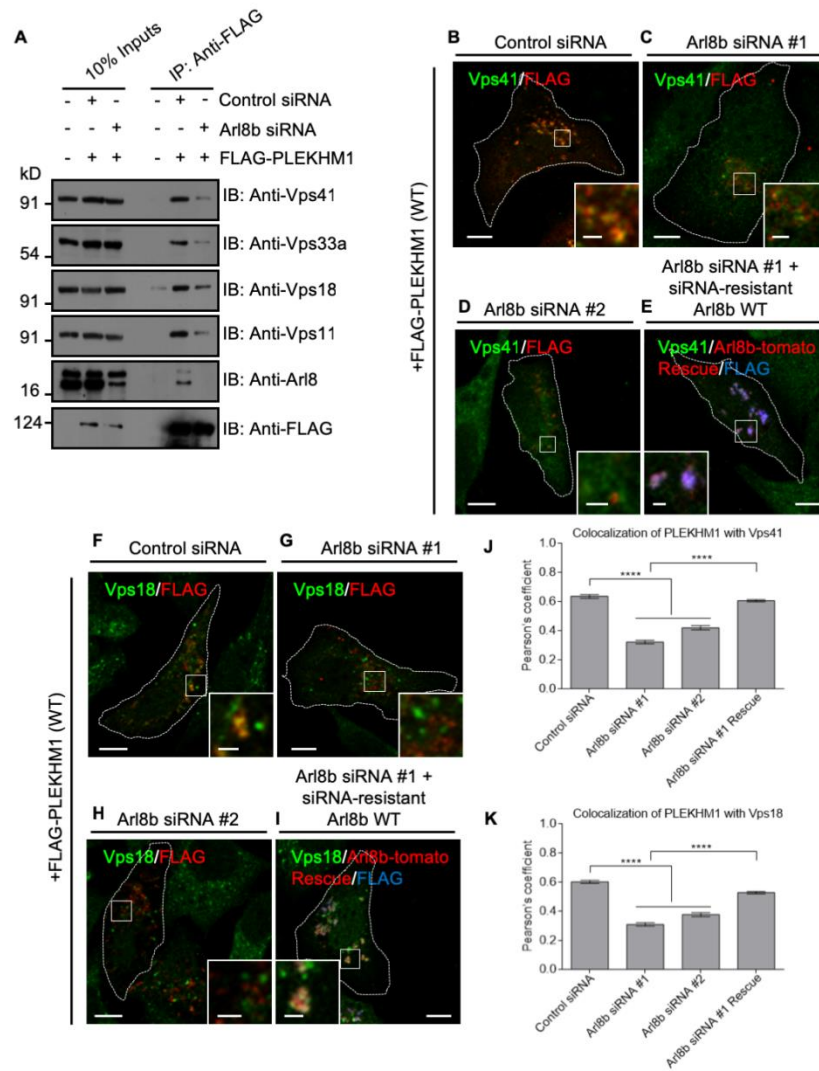
Figure 3.13: Arl8b recruits HOPS complex to Rab7-PLEKHM1-positive endosomes.

A) Lysates from HEK293T cells treated with control- or Arl8b-siRNA and expressing FLAG-PLEKHM1 were immunoprecipitated with anti-FLAG antibody conjugated-agarose beads and immunoblotted with indicated antibodies. **B-I)** Representative confocal micrographs of HeLa cells treated with either control- or Arl8b-siRNA and expressing FLAG-PLEKHM1 (WT) alone or co-expressed with siRNA resistant Arl8b-tomato and stained for endogenous Vps41 or Vps18. **J-K)** Colocalization of FLAG-PLEKHM1 with endogenous Vps41 or Vps18 was quantified by measuring Pearson's correlation coefficient in indicated siRNA treated HeLa cells. Values plotted are mean ± s.e.m. from three independent experiments (n=30 cells analysed per experiment for each treatment; ****p<0.0001). Scale bars=10μm.
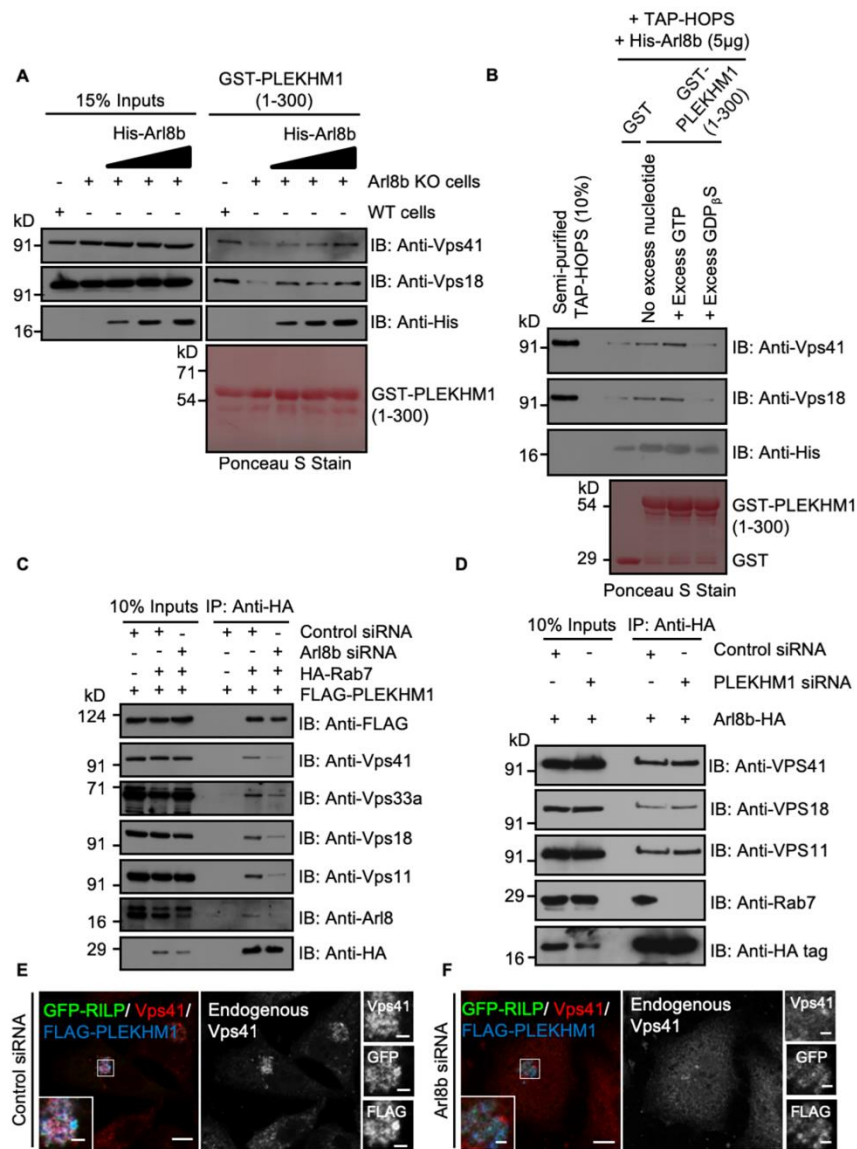
Figure 3.14: Arl8b mediates interaction between PLEKHM1 and HOPS complex.

A) Western blot of GST-pulldown assay using GST-PLEKHM1 (1-300) as bait incubated with lysates from either WT- or Arl8b KO-HeLa cells with increasing concentration of His-Arl8b protein and probed with indicated antibodies. **B)** GST-pulldown assay using semi-purified TAP-HOPS complex isolated from HeLa cells incubated with either GST or GST-PLEKHM1 (1-300), His-Arl8b and excess GTP or GDP. **C)** Lysates of HEK293T cells treated with either control- or Arl8b-siRNA followed by co-transfection with FLAG-PLEKHM1 and HA-Rab7 were subjected to immunoprecipitation with anti-HA antibody-conjugated-agarose beads and immunoblotted with indicated antibodies. **D)** Western blot of control- or PLEKHM1-siRNA treated HEK293T cell lysates expressing Arl8b-HA and immunoprecipitated with anti-HA antibody and immunoblotted with indicated antibodies. **E-F)** Representative confocal micrographs of HeLa cells treated with either control- or Arl8b-siRNA and co-transfected with GFP-RILP and FLAG-PLEKHM1 and immunostained for endogenous Vps41. Different channels are shown in the inset. Scale bars=10μm.

Previously, Rab7 effector-RILP has been shown to directly bind and recruit Vps41 to Rab7/PLEKHM1-positive endosomes (Lin et al., 2014; van der Kant et al., 2013; Wijdeven et al., 2016). We found that while PLEKHM1 continued to colocalize with RILP, recruitment of endogenous Vps41 to these perinuclear LEs/lysosomes was strikingly reduced in Arl8b-silenced cells (**Fig. 3.14 E and F**). These results are in agreement with our previous observations that Rab7 and RILP are unable to recruit Vps41 on lysosomes upon Arl8b depletion (Khatter et al., 2015a). Future structural studies are needed to clarify whether membrane binding of Vps41 mediated by Arl8b is essential for a structural conformation of Vps41 that enables it to efficiently bind RILP. Taken together, these results suggest that Arl8b mediates recruitment of the HOPS complex to PLEKHM1-positive endosomes, which is required for tethering and fusion of LEs and lysosomes.

3.2.6 Arl8b regulates PLEKHM1 function in degradation of endocytosed cargo

To this point, our findings suggest that PLEKHM1 acts as a linker to promote endolysosome formation by binding to the small GTPases Rab7 and Arl8b via distinct domains. Moreover, Arl8b recruits vesicle tethering/fusion machinery, the HOPS complex, to PLEKHM1-containing endosomes. To first confirm whether PLEKHM1 mediates delivery of cargo towards lysosomes, control- and PLEKHM1-siRNA transfected cells were incubated with DQ-BSA, an endocytic cargo that becomes fluorescent upon proteolytic cleavage in lysosomes (**Fig. 3.15 A**). The intensity of fluorescent DQ-BSA punctae in PLEKHM1-siRNA transfected cells was reduced by ~2-fold as compared to control-siRNA treated cells, suggesting that PLEKHM1 depletion impairs endo-lysosome fusion (**Fig.3.15 B-E; quantification shown in Fig. 3.15 F**). As a positive control for this assay, we treated cells with siRNA against Vps41, which has been previously shown to regulate endo-lysosome fusion (**Fig. 3.15 E and F**). To establish if Arl8b-binding was required for PLEKHM1 to function during endocytic cargo degradation, rescue of DQ-BSA degradation was quantified in PLEKHM1-siRNA treated cells transfected with siRNA-resistant WT or PLEKHM1 (HRR→A) mutant (**Fig. 3.15 G-J**; quantification shown in **Fig. 3.15 K**). While PLEKHM1 (WT) was able to rescue the defect in cargo degradation as indicated by an increase in DQ-BSA punctae, PLEKHM1 (HRR→A) mutant failed to rescue this effect (**Fig. 3.15 K**), suggesting that Arl8b-binding is required for PLEKHM1 function in degradation of

endocytic cargo. Similarly, trafficking of another endocytic cargo, DiI-LDL to lysosomes was impaired upon PLEKHM1-depletion (**Fig. 3.16 A-F**; quantification shown in **Fig. 3.16 G**)
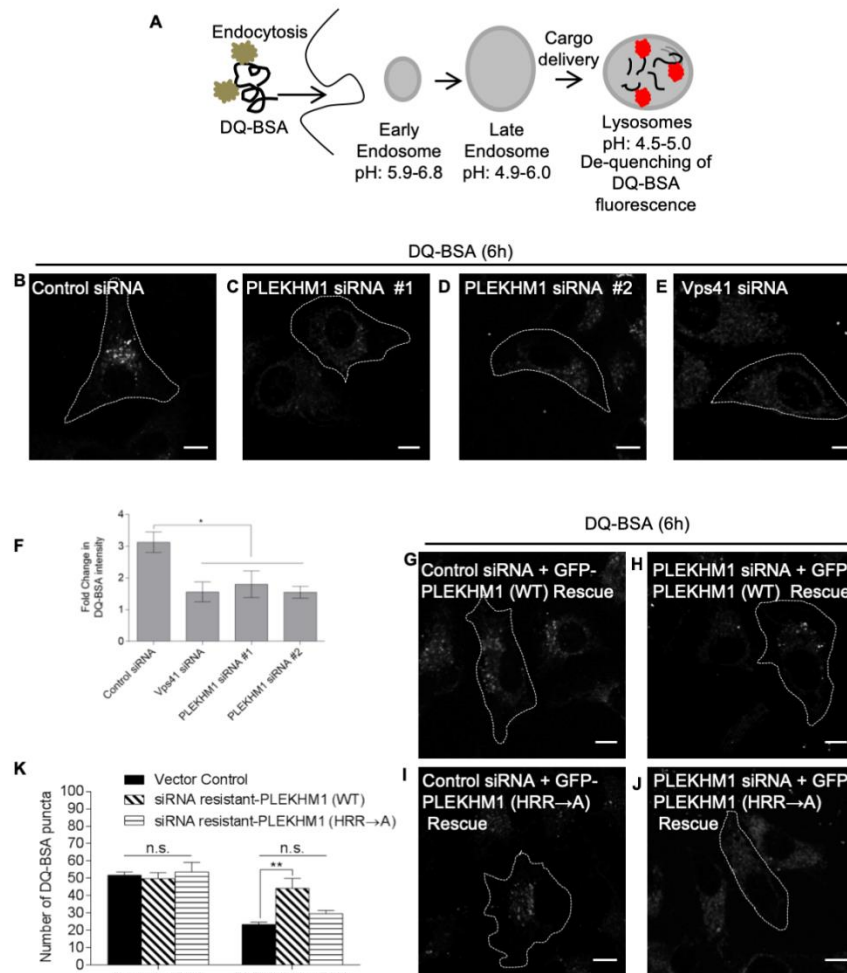
Figure 3.15: Binding to Arl8b is necessary for PLEKHM1 function in regulating endocytic cargo trafficking to lysosomes.

A) Schematic illustrating the uptake and further processing of DQ-BSA, an endocytic cargo in the cells. **B-E)** Confocal images of HeLa cells treated with indicated siRNAs and subjected to DQ-BSA uptake for 6h. The cells were then fixed and analysed for DQ-BSA fluorescence. **F)** Fold change in the fluorescence intensity of DQ-BSA from 1h to 6h was quantified using ImageJ software. Values plotted are mean ± s.e.m. from three independent experiments (n=50 cells analysed per experiment for each treatment; *p<0.05). **G-J)** Confocal micrographs of HeLa cells treated with indicated siRNAs and transfected with either siRNA-resistant PLEKHM1 (WT) or siRNA resistant PLEKHM1 (HRR→A) construct and subjected to DQ-BSA uptake for 6h. **K)** Quantification of DQ-BSA trafficking in HeLa cells treated with indicated siRNAs and transfected with either siRNA-resistant PLEKHM1 (WT) or siRNA resistant PLEKHM1 (HRR→A) construct. Values plotted are mean ± s.e.m. from three independent experiments (n=50 cells analysed per experiment for each treatment; **p<0.01; n.s., not significant). Scale bars=10μm.
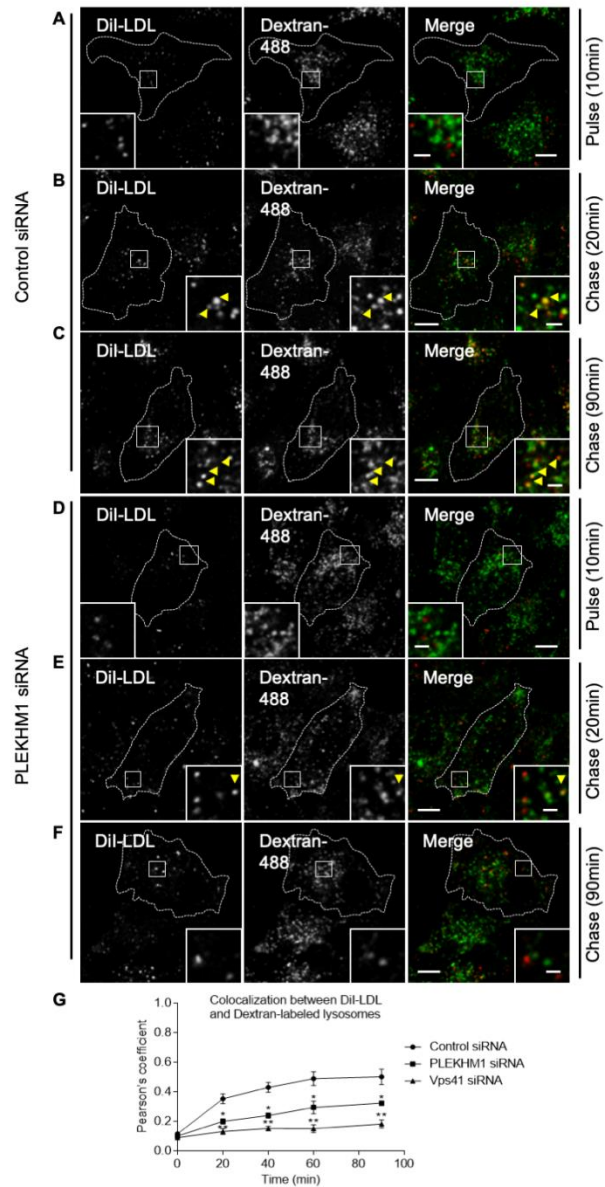
Figure 3.16: PLEKHM1 depletion delays DiI-LDL trafficking to lysosomes.

A-F) Shown are the representative confocal micrographs of LDL trafficking in control- and PLEKHM1-depleted cells. Arrowheads indicate colocalized pixels. **G)** Colocalization between DiI-LDL and Dextran-labeled lysosomes for indicated time points in control-, PLEKHM1-, or Vps41-siRNA treated HeLa cells was quantified by measuring Pearson's correlation coefficient using ImageJ software (n=30 cells analysed per time point for each treatment in three independent experiments; *p<0.05; **p<0.01). Scale bars=10μm.

To clarify if the delay in lysosomal degradation of cargo in PLEKHM1-depleted cells was due to impaired activity of lysosomal proteases, we compared the levels of mature cathepsin B and D in control- and PLEKHM1-siRNA treated cells. As shown in **Fig. 3.17 A**, no differences in the levels of mature cathepsin(s) in control- and PLEKHM1-siRNA treated cell lysates were observed. Colocalization of cathepsin D with LAMP1 was also found to be unchanged upon PLEKHM1-siRNA (**Fig. 3.17 B**). We also measured cathepsin activity by incubating control- and PLEKHM1-siRNA treated cells with the membrane permeable probe 'Magic red cathepsin L substrate' that emits fluorescence upon cleavage by cathepsin L. As shown in **Fig. 3.17 C**, fluorescence intensity of the cleaved cathepsin substrate was almost similar between control and PLEKHM1-depleted cells, suggesting that PLEKHM1 regulates endocytic cargo delivery to lysosomes but not lysosomal protease activity.
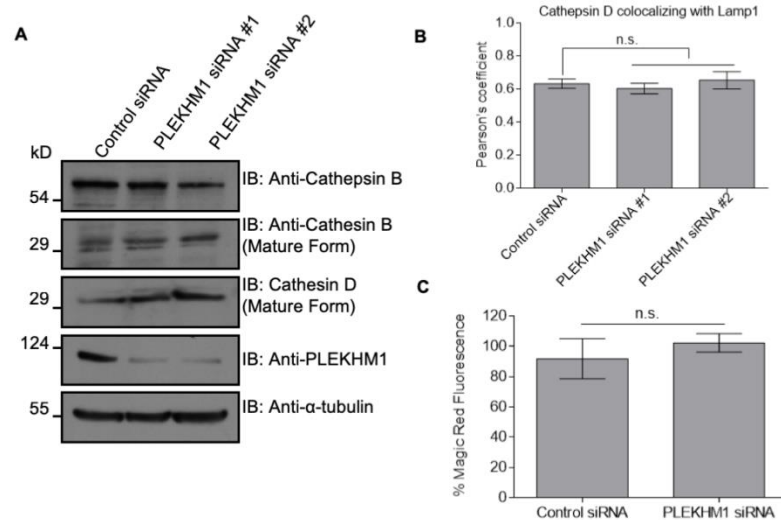
Figure 3.17: PLEKHM1 depletion does not alter acid hydrolases in lysosomes.

A) Western blot of mature Cathepsin-B and -D levels in control- or PLEKHM1-siRNA treated HeLa cells. **B)** Pearson's correlation coefficient was measured for Cathepsin D and LAMP1 colocalization in control- or PLEKHM1-siRNA treated HeLa cells for three independent experiments (n=30 cells per experiment for each treatment; n.s., not significant). **C)** Quantification of the intensity of the Magic Red Cathepsin L signal using flow cytometry. HeLa cells treated with control- or PLEKHM1-siRNA were incubated for 1h in growth medium supplemented with Magic Red Cathepsin L substrate and fluorescence intensity was measured by flow cytometry.

3.2.7 Arl8b regulates PLEKHM1 function in autolysosome formation

PLEKHM1 harbors an LC3/GABARAP-interaction (LIR) motif located between the two PH domains that enable it to promote clustering and fusion of LC3-positive autophagosomes with LEs/lysosomes (McEwan et al., 2015a). We hypothesized that Arl8b-binding required for PLEKHM1 should be important for its function in promoting autolysosome formation. To test this, we used the tandem-fluorescence (RFP-GFP) LC3B (tfLC3B) construct, in which the acid-sensitive GFP signal is quenched at the low pH of autolysosomes but no change is observed in the acid-insensitive RFP signal (Kimura et al., 2007; Klionsky et al., 2016). While we noted an increase in autolysosome formation in PLEKHM1 (WT)-transfected cells, this effect was completely abrogated in cells expressing PLEKHM1 (HRR→A) mutant (**Fig. 3.18 A-C**). Given that PLEKHM1 directly binds to LC3B/GABARAP proteins, we confirmed that this outcome was not due to lack of the PLEKHM1 (HRR→A) mutant's ability to bind LC3B (**Fig. 3.18 D**). Finally, we rescued LC3B-II accumulation observed upon PLEKHM1 depletion with either siRNA-resistant PLEKHM1 (WT) or the PLEKHM1 (HRR→A) mutant. As shown in **Fig. 3.18 E-F** under both non-starved and starved conditions, there was almost a ~3-fold increase in LC3B-II levels in PLEKHM1-siRNA-transfected cells compared to control siRNA transfection, with no further increase observed upon treatment with Baf A1. Strikingly, unlike the siRNA-resistant PLEKHM1 (WT), the Arl8b-binding defective mutant of PLEKHM1 was unable to rescue LC3B-II accumulation in PLEKHM1-siRNA treated cells (**Fig. 3.18 E and F**). A similar result was obtained when we analysed levels of the autophagy substrate p62 in these cell lysates (**Fig. 3.18 E**, second panel). Taken together, our data implicates PLEKHM1 interaction with Arl8b as a crucial factor regulating assembly of the vesicle fusion machinery at the membrane contacts sites of endosomes/autophagosomes and lysosomes, which leads to degradation of lysosomal cargo.
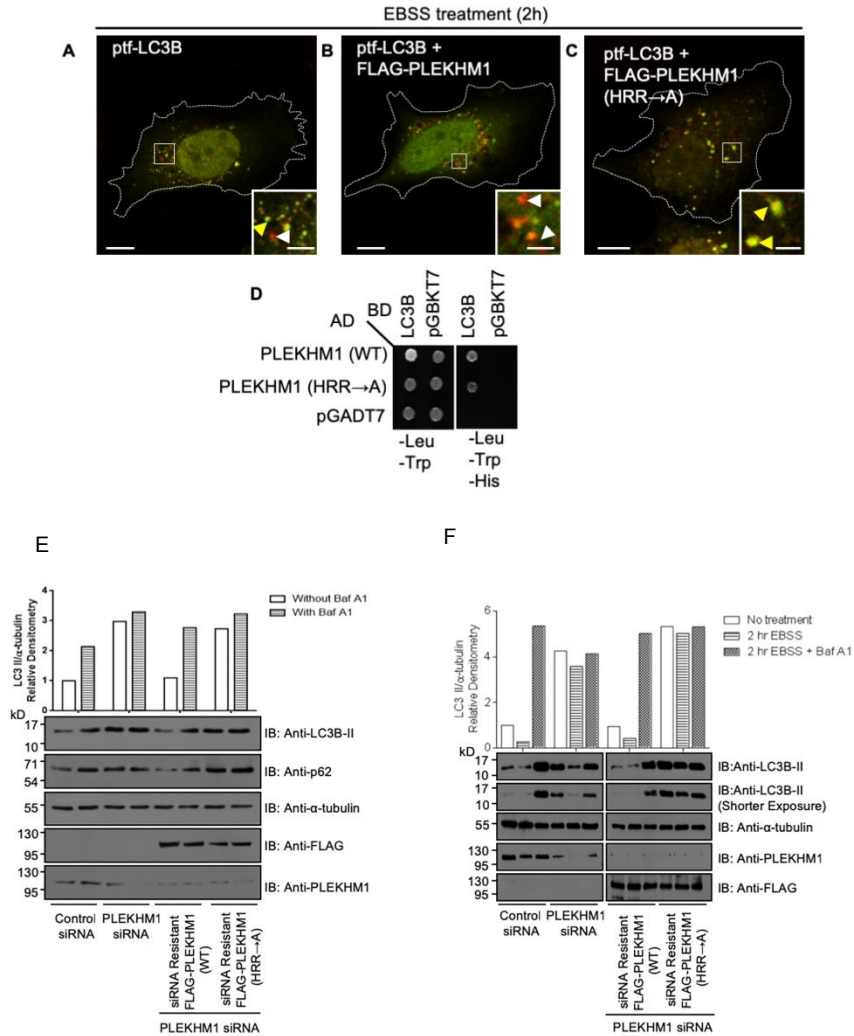
Figure 3.18: PLEKHM1 binds Arl8b to mediate autophagosome-lysosome fusion.

A-C) Confocal micrographs of HeLa cells expressing ptf-LC3B alone, co-transfected with FLAG-PLEKHM1 (WT) or FLAG-PLEKHM1 (HRR→A) and starved for 2h in EBSS. Red only punctate structures in magnified insets represent autolysosomes marked by white arrowheads and yellow punctate structures represent autophagosomes marked by yellow arrowheads. **D)** Yeast two-hybrid assay was performed to test interaction of PLEKHM1 (WT) and PLEKHM1 (HRR→A) with LC3B. Cotransformants were plated on non-selective medium (-Leu-Trp) to check viability and on selective medium (-Leu-Trp-His) to detect the interaction. **E)** U2OS cells treated with indicated siRNAs were given Baf A1 treatment in normal growth medium. Lysates were immunoblotted with the indicated antibodies. The levels of LC3B-II normalized to α-tubulin were quantified using densitometric analysis as shown. **F)** U2OS cells treated with indicated siRNAs were further subjected to the following treatments: normal growth medium or starvation in EBSS media for 2h with or without Baf A1. The lysates were immunoblotted for the indicated antibodies. Scale bars=10μm.

75

3.3 Discussion

The small GTPases, Rab7 and Arl8b, are central players that orchestrate microtubule-dependent transport of LEs/lysosomes and their fusion with endosomes, autophagosomes and phagosomes. Mechanistically, GTP-bound Rab7 and Arl8b recruit their downstream effectors, including motor-binding proteins, tethering factors, and adaptor proteins, to late endosomal/lysosomal membranes (Khatter et al., 2015a; Khatter et al., 2015b; Wang et al., 2011). While these GTPases act antagonistically to mediate directional transport of lysosomes on microtubule tracks, both function analogously to regulate cargo delivery to lysosomes (Garg et al., 2011; Johnson et al., 2016; Khatter et al., 2015a; McEwan et al., 2015a; Rosa-Ferreira and Munro, 2011). Despite an overlapping subcellular localization, and similar roles in membrane trafficking, it was not known whether there is crosstalk between Rab7 and Arl8b to coordinate their functions. Here, we have identified a role for the late endosomal/lysosomal protein, PLEKHM1, as a linker between Rab7 and Arl8b that under physiological conditions bind to both GTPases, and promote endo-lysosome and autophagosome-lysosome fusion. While Rab7 is required for membrane recruitment of PLEKHM1, our study shows that Arl8b-binding regulates localization of PLEKHM1 to lysosomes (dextran/LAMP1-positive). Moreover, disrupting Arl8b-binding or lack of Arl8b expression impairs PLEKHM1's ability to promote clustering of the late endosomal/lysosomal compartments. Our findings suggest that PLEKHM1 requires coordinated activation of both Rab7 and Arl8b GTPases to function as an adaptor in the endolysosomal pathway.

McEwan et al., (2015a) had previously reported direct binding of PLEKHM1 to subunits Vps39 and Vps41 of the multisubunit tethering factor, HOPS complex. Further PLEKHM1-mediated recruitment of HOPS complex and the associated SNARE protein (syntaxin17) to vesicle contact sites were found to be crucial for lysosome fusion with LEs and autophagosomes (McEwan et al., 2015a). Surprisingly, while PLEKHM1 directly bound to Vps39, we did not find interaction with the Vps41 subunit of the HOPS complex. Intriguingly, Vps39-binding was not sufficient for PLEKHM1 to recruit other subunits of the HOPS complex and to promote tethering of the endo-lysosomal compartment. Since Arl8b regulates HOPS assembly to lysosomes by its direct binding to Vps41 (Khatter et al., 2015a),

we hypothesized that Arl8b facilitates association between PLEKHM1 and HOPS complex to promote LE/autophagosome-lysosome fusion. In agreement with this, little or no interaction of HOPS subunits was observed with PLEKHM1 in the absence of Arl8b, which was reconstituted upon addition of Arl8b. Based on these findings, we propose a model where simultaneous binding of PLEKHM1 to Rab7 and Arl8b, and Arl8b-mediated recruitment of HOPS complex promotes endo-lysosome and autophagosome-lysosome fusion. Accordingly, a PLEKHM1 mutant that does not interact with Arl8b failed to rescue defects in endocytic cargo degradation and autolysosome formation observed upon PLEKHM1-depletion.

In summary, PLEKHM1 is a dual Rab/Arl effector that binds to the late endosomal and lysosomal small GTPases Rab7 and Arl8b and orchestrates assembly of the vesicle fusion machinery leading to lysosomal degradation of cargo internalized via endocytic and autophagic pathways.
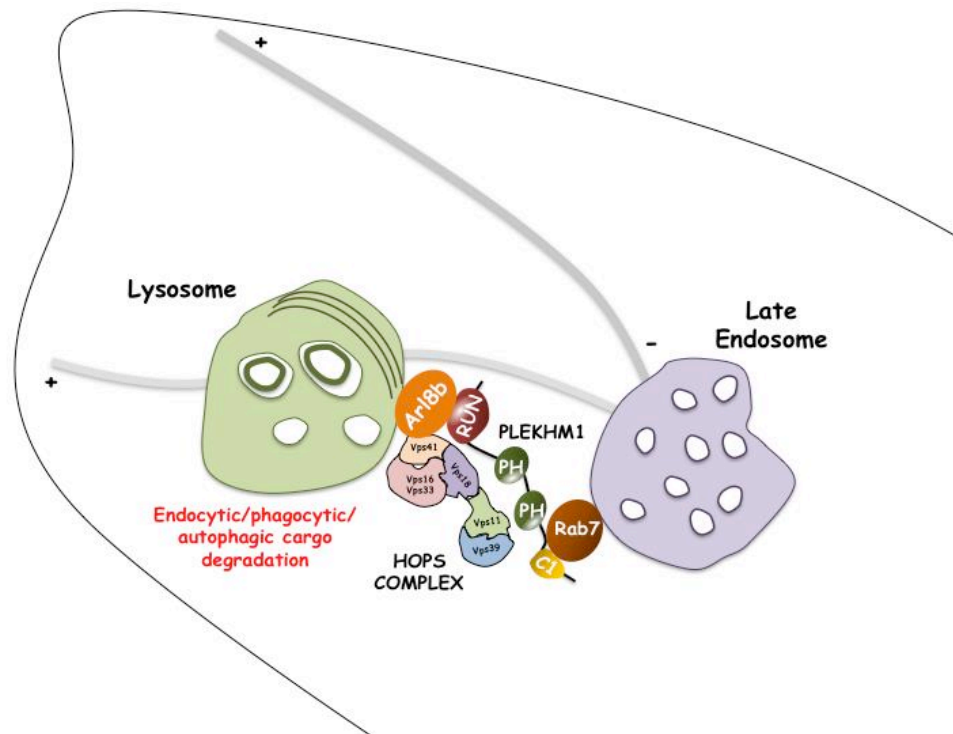
Figure 3.19: Schematic representation showing fusion machinery at the lysosome-late endosome junction.
PLEKHM1 is bound to Rab7 on late endosomes via its C-terminal end and N-terminal RUN domain is engaged with lysosomal Arl8b. Arl8b present on lysosomal membranes binds to Vps41 subunit of the HOPS complex and initiates the assembly of the complex and PLEKHM1 provides a scaffold/multi-domain platform bridging the two endosomal compartments.

Chapter 4

RUN domain–containing proteins PLE KHM1 and SKIP compete for binding to Arl8b and regulate lysosome positioning

This chapter contains sections published in the following thesis:

Subhash Babu Arya, 2017, Understanding the role of Arf like small GTP-binding proteins in membrane trafficking, Ph.D. thesis, JNU, New delhi

CHAPTER-4

4.1 Introduction

Lysosomes majorly display two distinct populations in cells: a relatively immobile pool near the nucleus and a highly motile pool present at the periphery of cells. Several reports suggest that these distinctly distributed lysosomes have specific characteristics such as luminal pH and contribute to different biological functions (Cabukusta and Neefjes, 2018). Perinuclear lysosomes have a lower pH, making them suitable for degradation of extracellular and intracellular cargo. While peripheral lysosomes are relatively less acidic as demonstrated by pH differentiating fluorescent dye-based assays (Johnson et al., 2016). The peripheral lysosomes are implicated in mediating plasma membrane repair, nutrient sensing via mTORC1 activation, cell adhesion and migration (Pu et al., 2016). Spatially distinct lysosome populations are maintained by bidirectional movement of the compartment on microtubule tracks. Lysosomal small G-protein, Arl8b has emerged as a crucial regulator of lysosome positioning in mammalian cells. Arl8b promotes peripheral positioning of lysosomes by recruiting SKIP/PLEKHM2 to lysosomal membranes which in turn binds the kinesin-1 motor protein to assist anterograde motility (Rosa-Ferreira and Munro, 2011). We observed that over-expression of PLEKHM1 led to clustering of Arl8b and LAMP1 positive structures in the perinuclear region of the cell. In contrast, SKIP over-expression resulted in the peripheral accumulation of Arl8b-LAMP1 positive compartments. Our results show that similar to SKIP/PLEKHM2, PLEKHM1 binds Arl8b via its RUN domain. Intrigued by the opposite lysosome distribution phenotype observed in case of PLEKHM1 and SKIP/PLEKHM2 over-expression and interaction of the two proteins with Arl8b via a similar domain, we tested if there is any competition between the two. Here in this part of the study, we show that indeed PLEKHM1 and SKIP compete for binding to Arl8b and regulate opposing lysosome distribution in mammalian cells.

4.2 Results

4.2.1 RUN domain-containing proteins PLEKHM1 and SKIP mediate opposing lysosome distribution. Arl8b and regulate lysosome distribution

79

Lysosomes residing in the cell periphery have attracted considerable attention for their role in nutrient sensing, cell migration, ECM degradation and metastasis, bone remodeling, and plasma membrane repair (Andrews et al., 2014; Hamalisto and Jaattela, 2016; Korolchuk and Rubinsztein, 2011). In accordance with its function in promoting anterograde motility of lysosomes, Arl8b is predominantly localized to the peripheral pool of lysosomes, as visualized both endogenously (**Fig. 4.1 A**) or when overexpressed in cells (Data not shown). Interestingly, upon transfection of PLEKHM1, Arl8b-positive lysosomes were repositioned to the perinuclear region, instead of the cell periphery (**Fig. 4.1 B**). In contrast, transfection of SKIP, led to an opposite phenotype of Arl8b-positive lysosome accumulation at the cell periphery (**Fig. 4.1 C**). Corresponding to the opposing roles of PLEKHM1 and SKIP on lysosomal distribution, we observed that under physiological conditions PLEKHM1 and SKIP were localized to perinuclear and peripheral Arl8b-positive endosomes, respectively (**Fig. 4.1 D and E**). Perinuclear index quantification of only the colocalized pixels (using cut mask images) showed this opposite distribution of the two Arl8b effectors on lysosomes (**Fig. 4.1 F**). Next, we analyzed distribution of the Arl8b/LAMP1-positive endosomes in PLEKHM1- and SKIP-depleted cells. As previously reported (Rosa-Ferreira and Munro, 2011), siRNA-mediated knockdown of SKIP resulted in the clustering of Arl8b/LAMP1-positive compartment in the perinuclear region (**Fig. 4.2 B and C**; quantification shown in **Fig. 4.2 F**). PLEKHM1 depletion, on the other hand, led to a striking accumulation of Arl8b/LAMP1-positive endosomes at the cell periphery (**Fig. 4.2 D-E**). Lysosomal distribution was restored by transfection of the siRNA-resistant constructs (SKIP and PLEKHM1) in respective siRNA-treated cells (**Fig. 4.2 F**).

It has been previously shown that a reduction in cytoplasmic pH drives anterograde motility of lysosomes in Arl8b- and SKIP-dependent manner (Rosa-Ferreira and Munro, 2011). We also found a similar dramatic decrease in the acid-induced peripheral pool of lysosomes upon depletion of either SKIP or Arl8b (**Fig. 4.2 G-H**; quantification shown in **Fig. 4.2 K**). In contrast, a significant increase in the acid-induced peripheral pool of lysosomes was observed in PLEKHM1-depleted cells (**Fig. 4.2 I and J**). These results clearly demonstrate that PLEKHM1 and SKIP have opposing effects on lysosomal distribution, which is expected from their localizations to different lysosomal population. Although we cannot rule out that the lysosomal levels of the retrograde motor protein,

dynein, are reduced upon PLEKHM1 depletion, we found that overexpression of RILP, an adaptor that recruits the dynein-dynactin complex to lysosomes, completely reversed the peripheral lysosomal accumulation observed in PLEKHM1-siRNA treated cells (**Fig. 4.3 A and B**). These data indicate that most likely dynein-dynactin complex is recruited to lysosomes upon PLEKHM1-depletion.
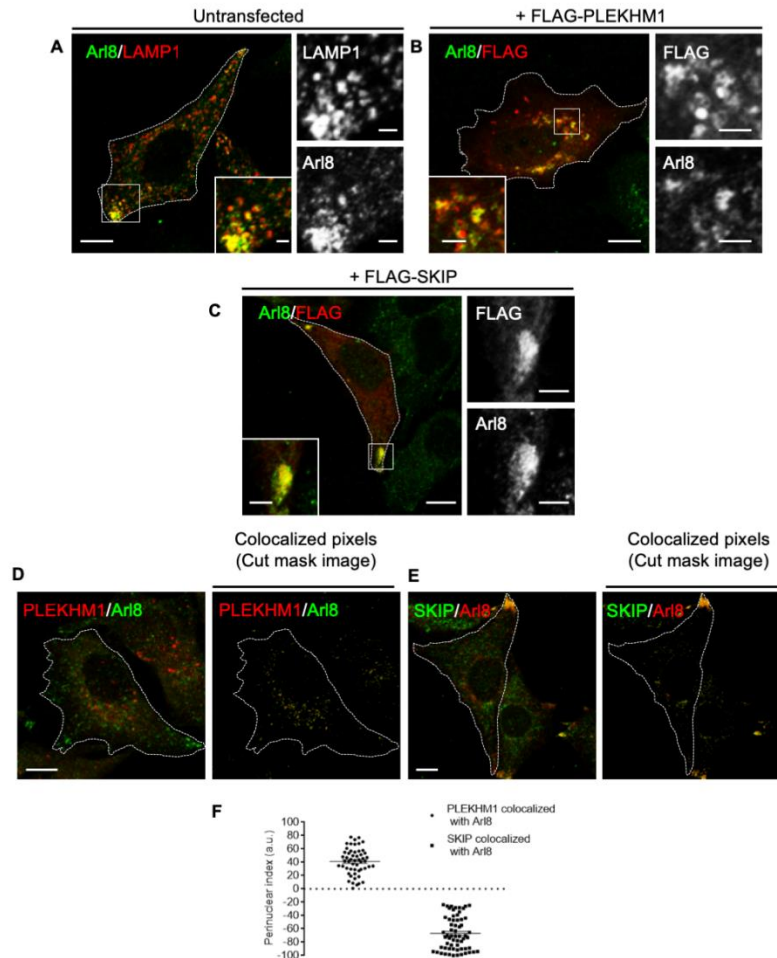
Figure 4.1: PLEKHM1 and SKIP colocalize with Arl8b in the perinuclear region and cell periphery respectively.

A-C) Representative confocal images of HeLa cells transfected with vector, FLAG-PLEKHM1 or FLAG-SKIP and immunostained for endogenous Arl8 and LAMP1. Note the distribution of Arl8/LAMP1-positive lysosomes under different conditions as shown in the insets. **D-E)** Confocal images of HeLa cells immunostained for endogenous Arl8 and PLEKHM1 or SKIP. Only cut-mask image of the colocalized pixels eliminating background and individual pixels are shown on the right. **F)** Perinuclear index of colocalized Arl8/PLEKHM1 or Arl8/SKIP pixels were calculated for three independent experiments (n=30 cells per experiment for each treatment). Scale bars=10μm, Insets (2μm).
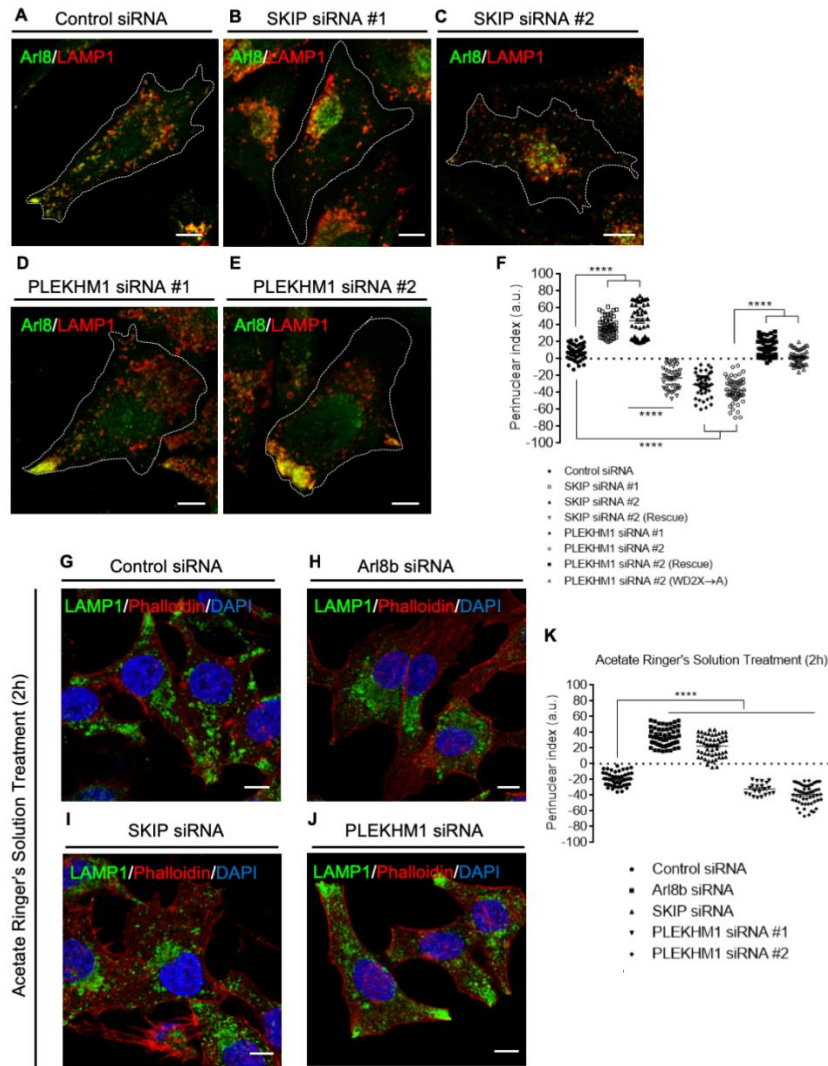
Figure 4.2: PLEKHM1 and SKIP depletion leads to opposing lysosome distribution in cells.

A-E) Representative confocal images of HeLa cells treated with indicated siRNAs and stained for Arl8 and LAMP1. **F)** Perinuclear index of LAMP1$^+$-compartments in HeLa cells transfected with indicated siRNAs and siRNA-resistant constructs. Values plotted are mean ± s.e.m. from three independent experiments (n=15-20 cells per experiment for each treatment; ****p<0.0001). **G-J)** Confocal micrographs of HeLa cells treated with indicated siRNAs followed by 2h incubation in Acetate Ringer's solution (pH 6.9) and immunostained for LAMP1 to mark lysosomes. To mark the boundary of the cells, actin staining was performed using phalloidin, and the nucleus was stained using DAPI. Scale bars=10μm. **K)** Quantification of perinuclear index in HeLa cells treated with indicated siRNAs followed by 2h incubation in Acetate Ringer's solution (pH 6.9). Values plotted are mean ± s.e.m. from three independent experiments (n=25-30 cells per experiment for each treatment; ****p<0.0001).
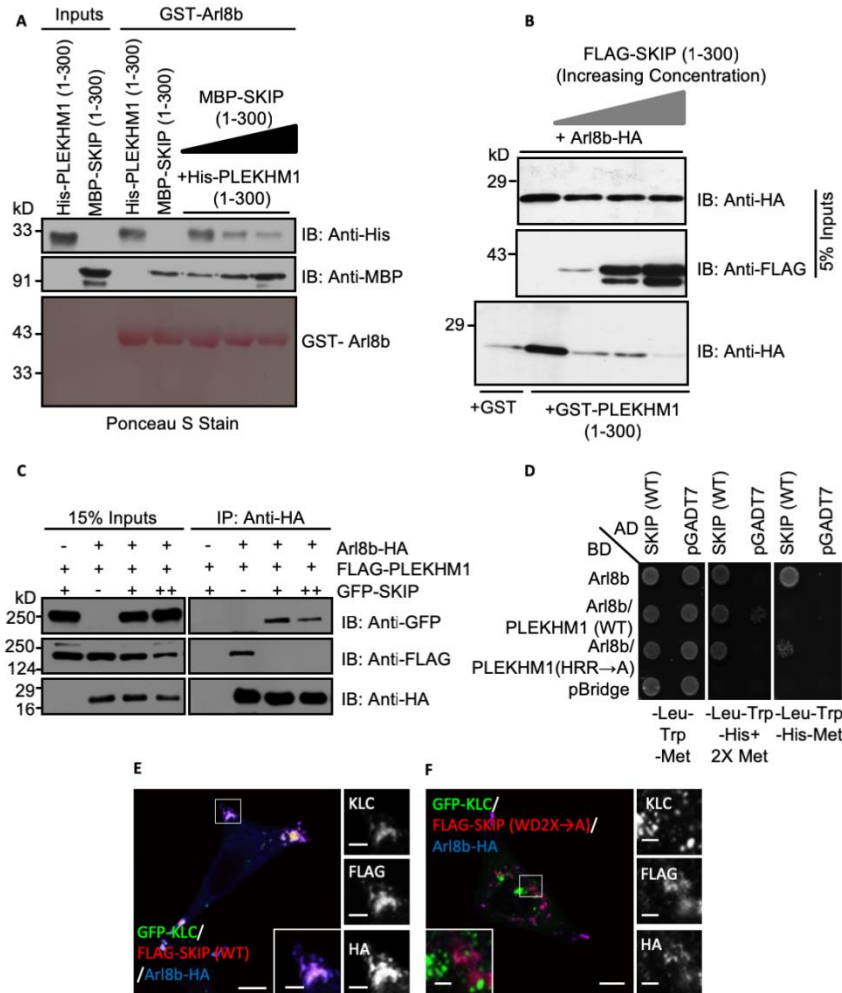
82
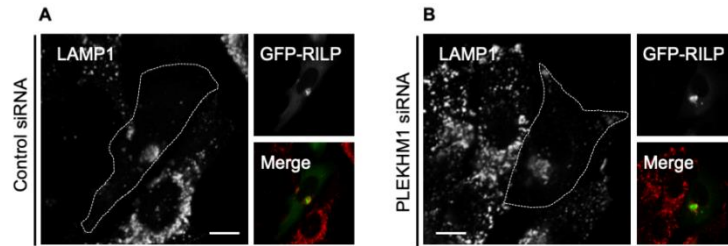
Figure 4.3: Lysosomes redistribute to cell center in RILP dependent manner in PLEKHM1 depleted cells.

A-B) Representative confocal image of HeLa cells treated with control- or PLEKHM1-siRNA and transfected with GFP-RILP and immunostained with anti-LAMP1 antibodies. Scale bar=10μm

4.2.2 PLEKHM1 and SKIP compete for binding to Arl8b

Our results led us to hypothesize that the RUN domain-containing proteins, SKIP and PLEKHM1, compete for binding to Arl8b, which in turn regulates lysosomes positioning. In support of this hypothesis, we found that arginine residues within the block D of the conserved core of SKIP RUN domain (R92 and R94; residues shown in **Fig. 4.4 B**) were required for binding to Arl8b (**Fig. 4.4 C**). To test whether SKIP competes with PLEKHM1 for binding to Arl8b, we performed a purified protein-protein interaction assay where increasing amounts of MBP-tagged SKIP (1-300) was able to compete out His-tagged PLEKHM1 (1-300) for binding to GST-Arl8b (**Fig. 4.5 A**). Additionally, as shown in **Fig. 4.5 B** and **C,** transfection with SKIP (1-300) or full-length resulted in loss of PLEKHM1 binding to Arl8b in a dose-dependent manner, determined by GST-pulldown and co-immunoprecipitation approaches, respectively. We also employed a yeast three-hybrid assay to test the interaction of Arl8b and SKIP in the presence of either PLEKHM1 (WT) or PLEKHM1 (HRR→A) mutant. In this assay PLEKHM1 (WT) and PLEKHM1 (HRR→A) expression were under the control of the Met25 promoter, which is repressed in the presence of methionine in the growth media. As depicted in **Fig. 4.5 D**, under methionine-deficient conditions, Arl8b interaction with SKIP was abrogated in the presence of PLEKHM1 (WT) but not upon expression of the PLEKHM1 (HRR→A) mutant, suggesting that SKIP and PLEKHM1 compete with each other for Arl8b-binding. To verify that the altered lysosomal distribution in PLEKHM1-siRNA treated cells could result from an increased binding of Arl8b to SKIP, we created a dominant-negative mutant of SKIP (WD2X→A) that has been

previously shown to bind Arl8b but not recruit the motor protein kinesin-1 on lysosomal membranes (Rosa-Ferreira and Munro, 2011). We confirmed these findings by visualizing recruitment of kinesin light chain (KLC2) in cells expressing WT or (WD2X→A) SKIP mutant along with Arl8b (**Fig. 4.5 E and F**). Notably, (WD2X→A) SKIP mutant partially reversed the peripheral lysosomal distribution observed in PLEKHM1-siRNA treated cells, suggesting that increased association of SKIP with Arl8b drives lysosomes to the cell periphery upon PLEKHM1 depletion (**Fig. 4.5 F**). Taken together, our findings suggest that the RUN domain-containing proteins PLEKHM1 and SKIP compete for Arl8b-binding that in turn regulates the subcellular distribution of lysosomes.

Figure 4.4: Conserved basic residues within the RUN domain of SKIP are required for its interaction with Arl8b.

A-B) Representative confocal images of HeLa cells expressing Arl8b-GFP along with FLAG-SKIP (WT) or FLAG-SKIP (R92A/R94A) mutant, and stained with anti-LAMP1 antibodies. **C**) Interaction of SKIP (WT), NΔ300 SKIP and SKIP (R92A/R94A) mutant with Arl8b was tested in a yeast two-hybrid assay.

**Figure 4.5: PLEKHM1 and SKIP compete for binding to Arl8b via their respective RUN domains.**

A) Immnuoblot of competition assay done using GST-Arl8b as bait, incubated with His-PLEKHM1 (1-300) and increasing concentration of MBP-SKIP (1-300). **B**) Lysates from HEK293T cells co-transfected with Arl8b-HA and vector or increasing amounts of FLAG-SKIP (1-300) were incubated with GST or GST-PLEKHM1 (1-300) and analysed by Western blotting using the indicated antibodies. **C**) Immunoblot of co-immunoprecipitation assay using HEK293T cells lysates co-expressing Arl8b-HA and FLAG-PLEKHM1 with increasing amounts of GFP-SKIP. **D**) A yeast three-hybrid assay was performed to examine competition between SKIP and PLEKHM1 for binding to Arl8b. The S. cerevisiae was co-transformed with the indicated Gal4-fusion constructs. The co-transformants were plated on non-selective medium (-Leu-Trp-Met) to check for viability and on selection plates -Leu-Trp-His+2X Met and -Leu-Trp-His-Met to test the interaction and competition, respectively. **E-F**) Confocal micrographs of HeLa cells transfected with Arl8-HA, GFP-KLC2 with FLAG-SKIP (WT) or FLAG-SKIP (WD2X→A) mutant. Scale bars=10μm, Insets (2μm).

4.3 Discussion

A key function of Arl8b is to promote anterograde motility of lysosomes on microtubule tracks towards the cell periphery (Bagshaw et al., 2006; Dykes et al., 2016b; Rosa-Ferreira and Munro, 2011). Mechanistically, it is now understood that Arl8b recruits SKIP, which in turn recruits the plus-end motor protein kinesin-1 to lysosomal membranes, facilitating the movement of lysosomes to the cell periphery (Rosa-Ferreira and Munro, 2011). Interestingly, we found that lysosomes were clustered at the tips of cellular protrusions in PLEKHM1-depleted cells, an effect opposite to SKIP depletion that was more pronounced upon lowering the pH of the extracellular milieu. Indeed, several lines of evidence suggest that the two RUN domain-containing proteins compete for binding to Arl8b that might explain their antagonistic effect on lysosome distribution: 1) PLEKHM1 shares a significant homology with SKIP over the length of its RUN domain, and both RUN domains require the conserved basic residues for binding to Arl8b; 2) Arl8b-binding to RUN domain-containing region of PLEKHM1 was disrupted with increasing amounts of a corresponding purified region of SKIP; 3) Arl8b-binding to SKIP was disrupted by PLEKHM1, but not by expression of the PLEKHM1 (HRR→A) mutant that does not bind Arl8b; and 4) peripheral accumulation of lysosomes in PLEKHM1-siRNA treated cells was partially rescued by expression of the SKIP (WD2X→A) mutant that does not bind kinesin-1 but can displace endogenous SKIP by binding to Arl8b. We propose a model whereby Arl8b regulates both lysosome motility and fusion with endosomes/autophagosomes by recruiting its effectors SKIP and PLEKHM1/HOPS complex respectively (**Fig. 4.6**).

We speculate that Arl8b association with one or the other RUN domain effectors might be regulated by factors that are known to control lysosome positioning, including cytosolic pH, growth factor stimulation, activity of lysosomal calcium channel TRPML1, plasma membrane injury, amino acid starvation and mTOR activation (Andrews et al., 2014; Heuser, 1989; Korolchuk et al., 2011; Li et al., 2016; Pu et al., 2016). This will be an important avenue for future research, as recent studies have identified Arl8b function in regulating cell migration and extracellular matrix remodeling to promote tumor invasion and metastasis (Dykes et al., 2016b; Hamalisto and Jaattela, 2016; Pu et al., 2015; Schiefermeier et al., 2014). Binding sites of PLEKHM1 and PLEKHM2 in Arl8b remains to be explored.

Rigorous biophysical experiments will help in delineating whether PLEKHM1 and PLEKHM2 bind to the same site in Arl8b or have different binding preferences. Another important avenue will be to elucidate the role of Arl8b-PLEKHM1 interaction in osteoclasts, which are bone-resorbing macrophages that secrete lysosomal proteases in the extracellular milieu to mediate bone resorption (Bo et al., 2016; Del Fattore et al., 2008; Van Wesenbeeck et al., 2007). Loss-of-function mutations in *PLEKHM1* gene results in "osteopetrosis", a disease characterized by accumulation of structurally disorganized bone and defective bone resorption (Bo et al., 2016; Del Fattore et al., 2008; Fujiwara et al., 2016; Sobacchi et al., 2013; Van Wesenbeeck et al., 2007; Witwicka et al., 2015). An important question therefore is, whether Arl8b is required for bone remodeling function of osteoclasts and how PLEKHM1/SKIP binding to Arl8b regulates lysosome secretion.
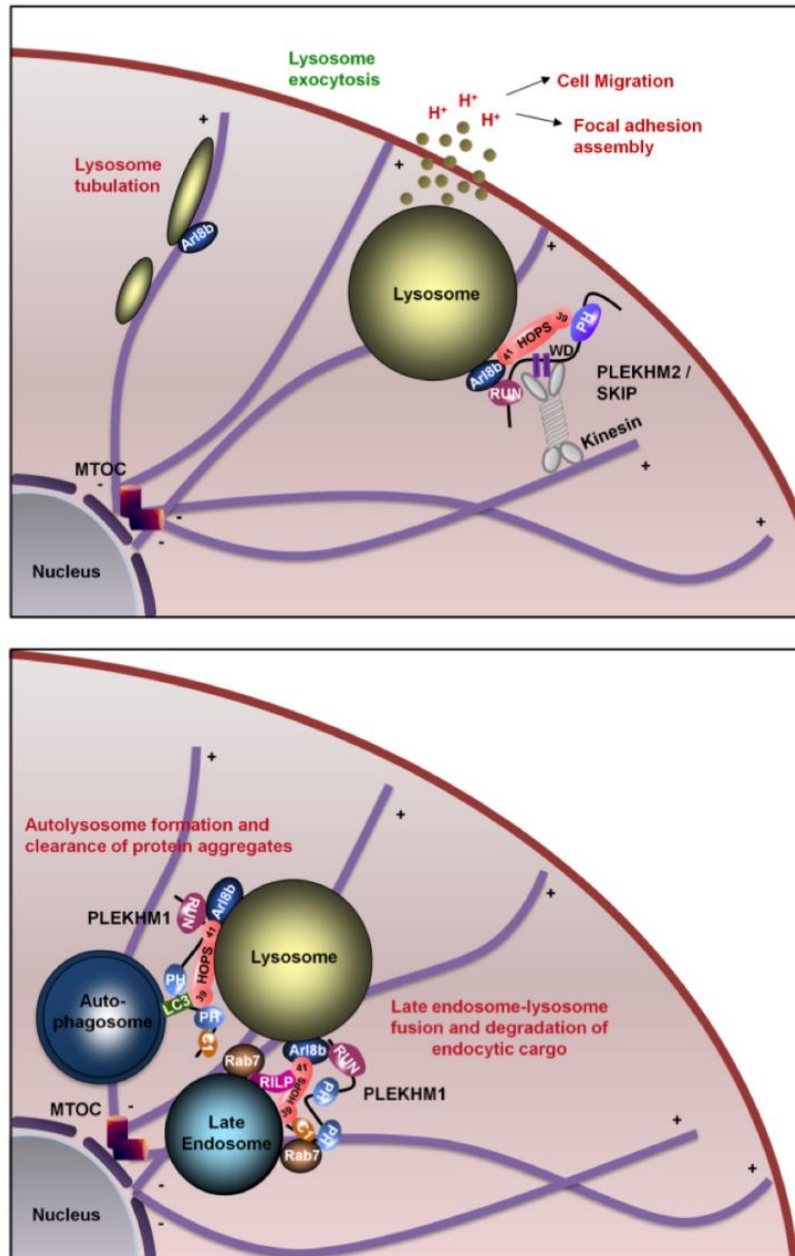
Figure 4.6: Diagrammatic representation of proposed model of lysosome distribution and function regulation by small GTPase Arl8b and its effectors PLEKHM1 and SKIP. SKIP interacts with Arl8b via its RUN domain, further recruiting kinesin motor that drives anterograde lysosomes motility which is implicated in regulating cellular processes like cell migration/invasion and focal adhesion assembly. Here we report PLEKHM1 as a dual effector of Rab7 and Arl8b that simultaneously binds these GTPases, bringing about clustering and fusion of late endosomes and lysosomes. PLEKHM1 also binds to LC3 and promotes autolysosome formation.

Chapter 5

Rabip4' interacts with Arl8b and regulates endolysosomal morphology and

cargo trafficking

CHAPTER 5

5.1 Introduction

Lysosomes are the terminal degradative and recycling units of cells. With recent advancements in the field of lysosomal biology, unconventional roles for lysosomes are being recognized bringing much attention to this organelle. Apart from its role in degradation, lysosomes play a vital role in regulating cellular processes such as metabolic signaling, plasma membrane repair, antigen presentation, tumor invasion, cell adhesion and migration (Lim and Zoncu, 2016; Pu et al., 2016). The ability of lysosomes to regulate the functions mentioned above depends upon its subcellular spatial distribution and movement on microtubule tracks. Lysosomes are emerging as crucial regulators of cellular homeostasis, as any dysfunction leads to lysosomal storage disorders, neurodegeneration, and cancer (Cabukusta and Neefjes, 2018; Pu et al., 2016).

Arl8b is a small GTP-binding protein (G) that predominantly resides on lysosomes and regulates both its anterograde motility and fusion with late endosomes by recruiting its downstream effectors- SKIP, PLEKHM1 and HOPS complex. Arl8b interacts with two RUN domain-containing proteins SKIP/PLEKHM2 and PLEKHM1 (Khatter et al., 2015b; Marwaha et al., 2017). Arl8b regulates anterograde lysosome motility by binding its downstream effector SKIP/PLEKHM2 which in turn recruits to kinesin-1 to lysosomes (Rosa-Ferreira and Munro, 2011). Our lab recently showed that PLEKHM1 serves as a linker between Arl8b and late endosomal small GTP binding-protein Rab7, facilitating the recruitment of multisubunit tethering factor HOPS complex to vesicle contact sites and regulates degradation of endocytic and autophagic cargo. We also noted that PLEKHM1 and SKIP, both of which bind to Arl8b via their respective RUN domains compete for binding to Arl8b and position lysosomes in opposing manner (Marwaha et al., 2017). Interestingly, these recent findings suggest the likely role of RUN-domain containing proteins as potential Arl8b interaction partners.

Previous studies have shed light on RUN and FYVE domain-containing (RUFY) protein family that comprises of four members RUFY1, RUFY2, RUFY3, and RUFY4. RUFY family members share a similar domain architecture consisting of an amino-terminal RUN

domain, coiled-coil domains, and a carboxyl-terminal FYVE domain. They have been reported to associate with phosphatidylinositol 3-phosphate in endosomal membranes. RUFYs have been suggested to act as docking proteins for multiple GTPases in previous studies, and their functions in the regulation of membrane trafficking and polarity have just begun to be understood (Kitagishi and Matsuda, 2013). RUFY1, the best-characterized member of the RUFY family of proteins, was discovered as an effector of small GTPase Rab4 and Rab14. A single RUFY1 expresses two isoforms namely Rabip4' (708 amino acids long) and Rabip4 (600 amino acid long) (**Fig 5.1 A**). Binding of RUFY1/Rabip4s to small G-protein Rab14, N-terminal RUN domain, phospholipid binding by C-terminal FYVE domain and tyrosine phosphorylation at residues between the coiled-coil domains by ETK kinase are essential factors for RUFY1/Rabip4s membrane association (Yamamoto et al., 2010; Yang et al., 2002). RUFY1/Rabip4s have been implicated in efficient Rab4a mediated organization of sorting endosomes, recycling of transferrin, transport of GLUT1/4 storage vesicles to plasma membrane and migration of NIH 3T3 fibroblasts (Cormont et al., 2001; Nag et al., 2018; Vukmirica et al., 2006; Yamamoto et al., 2010).

Interestingly, a recent study uncovered the role of Rabip4' as a coordinator of lysosome positioning in mammalian cells. It was reported that Rabip4' and AP-3 (Adaptor protein-3) bind and colocalize on early endosomes and siRNA mediated depletion of either protein led to the redistribution of lysosomes to the cell periphery (Ivan et al., 2012). Furthermore, in another study, it was shown that Rabip4s depletion leads to longer retention and a subsequent delay in EGFR trafficking to lysosomes (Gosney et al., 2018). However, the mechanism of Rabip4'-mediated lysosome positioning and receptor trafficking remains unknown. It was Intriguing to note that RUN domain of Rabip4' shares 38% and 35% identity with known Arl8b-interaction partners PLEKHM1 and PLEKHM2/SKIP, respectively. Rab4, Rab14 and Rab5 bind to carboxy-terminal of Rabip4' and no association of any small GTP-binding protein with Rabip4' RUN-domain is known up until now. These observations motivated us to probe if Rabip4' can interact with lysosomal small GTP-binding protein Arl8b to regulate lysosomal functions.

Here in this study, we show that Rabip4' interacts with Arl8b via its N-Terminal RUN domain and conserved basic residues within the RUN domain are essential for this interaction. Arl8b primarily localizes to LAMP1-positive compartments, but a subset of

Arl8b pool colocalized with Rabip4' on early endosomal compartments. Using Arl8b binding defective mutants of Rabip4' and siRNA mediated Arl8b depletion we show that Arl8b is essential for the membrane association of Rabip4s at the endogenous level. Depletion of Rabip4s led to the formation of enlarged LAMP1-positive compartments as compared to control cells. siRNA resistant wild-type Rabip4' but not Arl8b binding defective mutants of Rabip4' was able to restore the typical endolysosomal morphology in case of cells depleted of Rabip4s. Further, Rabip4' regulates LAMP1 membrane acquisition onto SCVs (*Salmonella*-containing vacuoles) and its depletion led to defective *Salmonella* replication in mammalian cells**.**

5.2 Results

5.2.1 Rabip4' interacts with lysosomal small GTPase Arl8b via its N-terminal RUN domain

To investigate the role of Rabip4s, we first tested the interaction of Rabip4 and Rabip4' with Arl8b in GST-pulldown assay. We observed that GST tagged Arl8b was able to pulldown both the shorter, Rabip4 and longer Rabip4' isoform from transfected HEK293T cell lysates. Stronger binding of Rabip4' as compared to Rabip4 was indicated by densitometry analysis (**Fig 5.1 D-E**). Further, using an anti-Rabip4s antibody that recognizes both the longer and shorter isoforms, we observed expression of only the longer isoform in the HeLa cell line. A non-specific band was seen in the immunoblot (marked by *) that was nonetheless running at the size of the shorter isoform, however, it remained unaffected by siRNA treatment that was effective against both the RUFY1 isoforms (**Fig 5.1 B**). To rule out the possibility of the siRNA not being effective against the shorter form, we over-expressed FLAG-tagged Rabip4 in HeLa cells and immunoblotting showed that the expression of shorter isoform effectively reduced by siRNA treatment. We conclude that primarily the longer isoform is expressed in HeLa cells and detected by the antibody we had. Also previous studies have shown that longer isoform is expressed at higher levels as compared to shorter isoform in HeLa cells (Ivan et al., 2012).
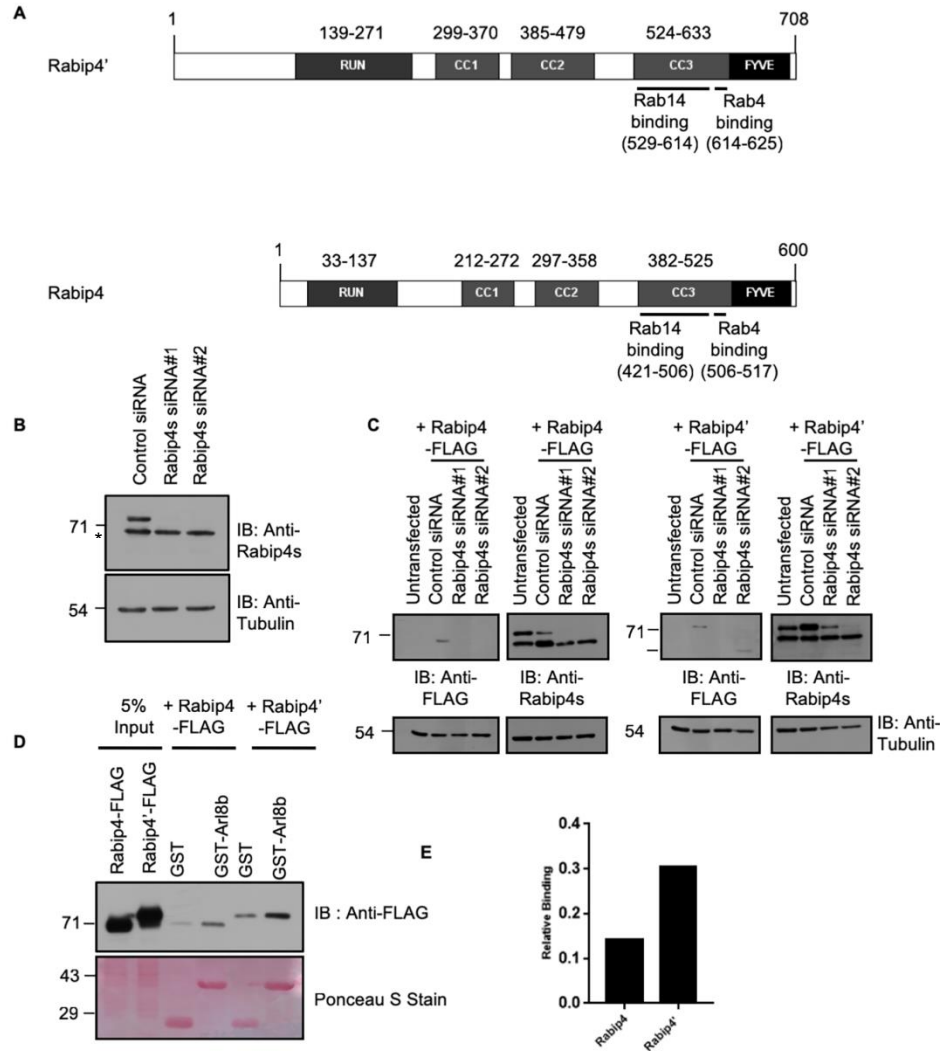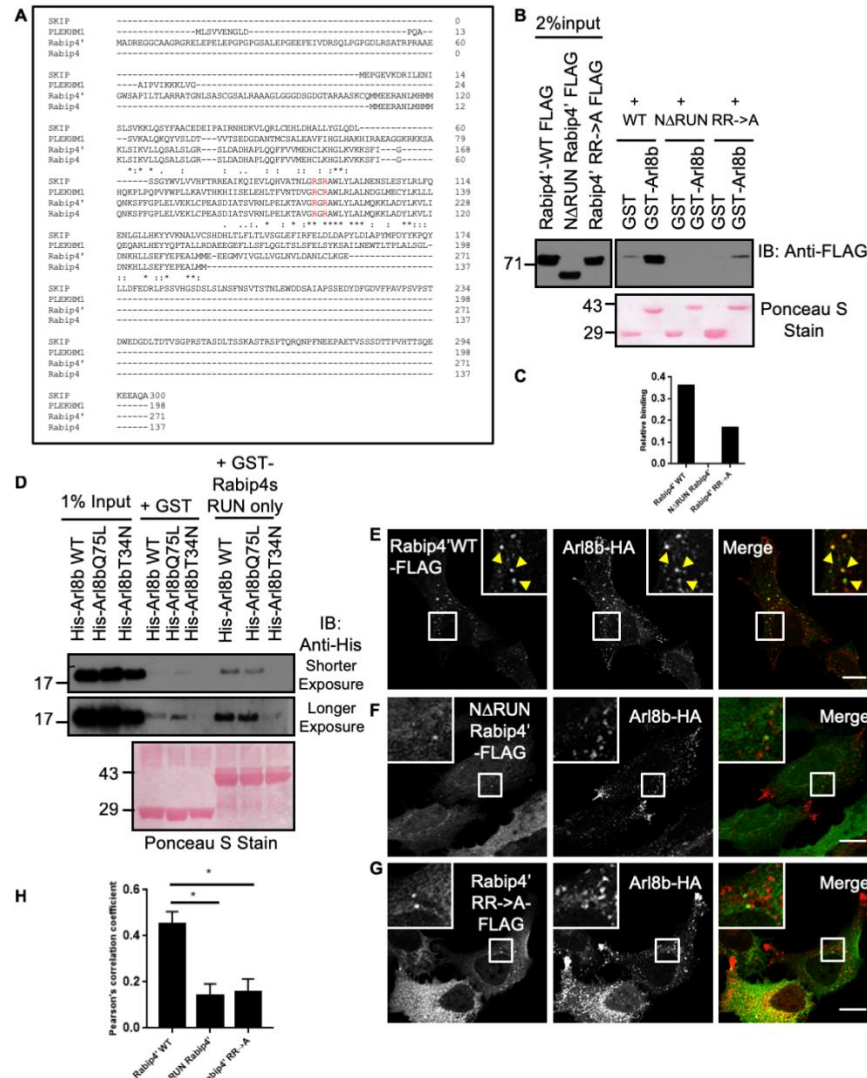
Figure 5.1: Rabip4' interacts with Arl8b

A) Schematic representing the domain architecture of Rabip4' and Rabip4. **B)** HeLa cell lysates from Control-siRNA, Rabip4s siRNA#1 and Rabip4s siRNA#2 treatments were immunoblotted with anti-Rabip4s to assess the specificity of the antibody and knockdown efficiency and anti-tubulin was used as the loading control. **C)** Western blot showing the knockdown efficiency of the Rabip4s siRNA#1 and #2 in depleting the shorter isoform Rabip4 and Rabip4'. HeLa cell lysates were treated with indiacted siRNA, followed by over-expression of FLAG tagged Rabip4 and Rabip4' and subjected to immunoblotting with anti-FLAG and anti-Rabip4s to assess the knockdown and anti-tubulin was used as loading control. **D)** Immunoblot of GST pulldown assay using GST-Arl8b as bait, incubated with lysates from HEK293T cells transiently expressing either Rabip4-FLAG or Rabip4'-FLAG and immunoblotted with indicated antibodies. Ponceau S staining was done to visualize the purified proteins. **E)** Densitometry analysis of GST pulldown assay represented in D) from two independent experiments. Graph is plotted as relative binding of Rabip4 and Rabip4' using GST-Arl8b as bait.

Previous studies have shed light on the importance of RUN domain in PLEKHM1 and PLEKHM2 for their interaction with Arl8b (Marwaha et al., 2017; Rosa-Ferreira and Munro, 2011). In line with this, we generated RUN domain deletion mutant of Rabip4' (272-708 amino acids, hereafter referred as NΔRUN) and tested its interaction with Arl8b using GST pulldown approach (**Fig 5.2 B**). GST-Arl8b used as bait was able to pulldown Rabip4' WT-FLAG but not NΔRUN Rabip4'-FLAG from respectively transfected HEK293T cell lysates. Bioinformatics analyses depicted that, similar to PLEKHM1 and PLEKHM2, Rabip4s have conserved basic amino acid residues in the RUN domain, which are implicated in the interaction with small GTP-binding protein Arl8b (**Fig 5.2 A**). Since deletion of RUN domain involves the loss of a large stretch of amino acids, we employed site-directed mutagenesis to mutate the arginine residues (R206 and R208) to alanine in Rabip4' (RR→A). Similar to loss of interaction of NΔRUN Rabip4', diminished interaction of Rabip4' RR→A mutant was also observed with Arl8b as compared to the WT protein in GST-pulldown assay, where GST tagged Arl8b was used as bait (**Fig 5.2 B** and densitometry analysis in **C**). To further clarify that the RUN domain of Rabip4' directly binds to Arl8b, GST and GST-tagged RUN only Rabip4s proteins were co-incubated with His tagged Arl8b-WT, Arl8b-Q75L, and -T34N. GST-RUN only Rabip4s displayed a strong binding preference towards Arl8b-WT and Arl8b Q75L but not Arl8b-T34N, suggesting that the RUN domain of Rabip4' directly binds to Arl8b in a GTP-GDP dependent manner (**Fig 5.2 D**).

Since we observed *in-vitro* binding of Rabip4' with Arl8b via its N-terminal RUN domain, we next analyzed whether RUN domain modulates the subcellular distribution of Rabip4'. Immunofluorescence data suggested that Arl8b binding-defective mutants of Rabip4' (collective name for NΔRUN and RR→A Rabip4' mutants) and were largely cytosolic upon expression in HeLa cells, in contrast to wild-type Rabip4' that was found to be punctate. These mutants remain cytosolic and localize to very few membrane-bound structures even upon co-expression of Arl8b, indicating that binding of Rabip4' to Arl8b via RUN domain is essential for their membrane localization (**Fig 5.2 E-G** and quantification in **H**). Earlier reports have suggested that binding sites for the small GTPases Rab4 and Rab14 lie in the C-terminal region of Rabip4s (Yamamoto et al., 2010). Previous reports and our siRNA-mediated Rab14 depletion experiments show that Rab14 is a critical membrane recruiting

factor for Rabip4s at endogenous levels (**Fig 5.3 A and B**). In accordance, Arl8b binding defective mutants of Rabip4' continued to colocalize to early endosomal compartments marked by the GFP-Rab14 and co-expression of these mutants with GFP-Rab14 led to partial restoration of their membrane localization (**Fig 5.3 C-E**).

Figure 5.2: The N-terminal RUN domain of Rabip4' is required for its interaction with Arl8b.

A) Sequence alignment of RUN domains of indicated proteins. **B**) GST and GST-Arl8b protein immobilized on glutathione (GSH) beads was incubated with HEK293T cell lysates expressing FLAG tagged Rabip4'-WT, NΔRUN Rabip4'or Rabip4' RR→A and immublotted with anti-FLAG. Ponceau S staining was done to visualize purified proteins. **C**) Densitometry analysis plot from two independent experiments showing relative binding of Rabip4' WT and mutants with Arl8b in GST pulldown assay represented in B). **D**) Representative western blot of purified protein interaction assay done using GST-Rabip4s RUN only as bait incubated with His tagged Arl8b-WT, Arl8b-Q75L and Arl8b-T34N and immublotted with anti-His antibody . **E-G**) Representative confocal micrographs of HeLa cells co-transfected with indicated plasmids. Colocalized pixels are shown in insets marked by arrowheads. Scale bar=10μm. **H**) Quantification of colocalization of WT, ΔRUN and RR→A Rabip4' with Arl8b analysed by measuring the Pearson's coefficient (Using Coste's Randomization) (n=3, 30cells per experiment for each treatment). Values plotted as mean±sem. * indicates p<0.05

Co-localization analysis of Rabip4' WT and the Arl8b binding-defective mutants show that there is a drop in the colocalization coefficient for NΔRUN Rabip4' and Rabip4' RR→A with GFP tagged Rab14 (**Fig 5.3 F**). We speculate that this is due to partial loss of membrane association of the Arl8b binding-defective mutants of Rabip4', which can contribute to a slight drop in colocalization with Rab14. Together these results indicate that Rabip4' has separate interaction sites for small GTP-binding proteins Rab14 and Arl8b, which are located in the C-terminal region and the RUN domain respectively. Also, interaction of Rabip4' with Arl8b via its RUN domain might play a role in its membrane association.
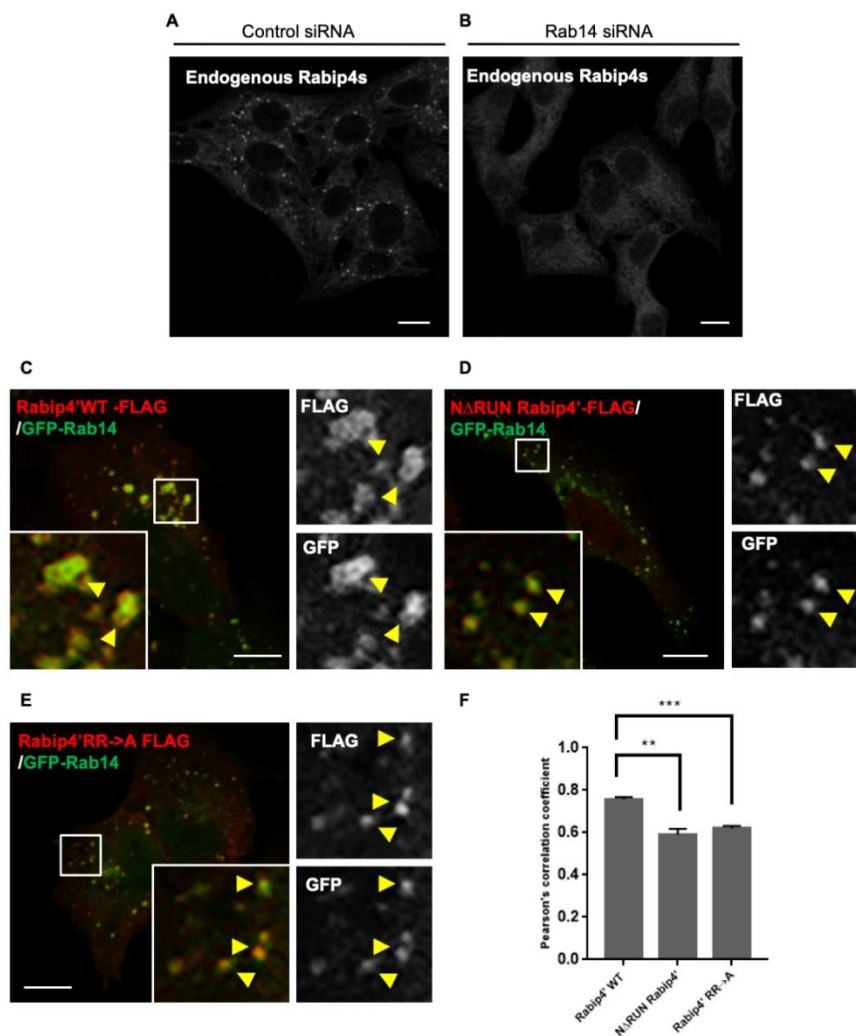
Figure 5.3: Arl8b binding defective mutants of Rabip4' continue to colocalize with Rab14.

A-B) Representative confocal micrographs of HeLa cells treated with Control and Rab14 siRNA respectively and immunostained for endogenous Rabip4s. **C-E**) Immunofluorescence showing HeLa cells co-expressing GFP-Rab14 with either Rabip4'-WT-FLAG, NΔRUN Rabip4'-FLAG or Rabip4' RR→A-FLAG. Insets show colocalized pixels marked by arrowheads. Scale bar=10µm. **F**) Quantification graph showing Pearson's correlation coefficient (Using Coste's randomization) measured using ImageJ for Rabip4'WT and Arl8b binding defective mutants with Rab14. n=3, 30 cells per experiment for each treatment. Values plotted as mean±sem. ** and *** indicates p<0.01 and 0.001

5.2.2 Rabip4' and Arl8b localize to early endosomal structures

Rabip4s have been previously reported to interact with Rab4, and Rab14 and localize to the early endosomes. We confirmed the localization of endogenous Rabip4s in HeLa cells which were co-stained with EEA1 or LAMP1 and the Pearson's correlation coefficient for both was measured using ImageJ (**Fig 5.4 A-C**). The colocalization analysis shows that endogenous Rabip4s and EEA1 have a correlation coefficient (r) value of 0.6, whereas the r-value with LAMP1 is 0.27 (**Fig 5.4 C**). In our steady state confocal microscopy experiments, we observed significant co-localization of co-expressed epitope-tagged Rabip4' and Arl8b (**Fig 5.4 D and Fig 5.2 E and H)**, but the compartment to which these two proteins were localizing was yet to be determined clearly. In order to find out the compartment harboring Rabip4' and Arl8b, HeLa cells were co-transfected with Arl8b-HA and Rabip4' WT-FLAG, followed by co-staining for either EEA1 or LAMP1. Rabip4' continued to significantly localize to EEA1-positive structures as compared to compartments marked by LAMP1 in HeLa cells co-expressing Arl8b (**Fig 5.4 D and E**). Confocal microscopy analysis yielded a significant population of Rabip4' and Arl8b-double positive endosomes that were colocalizing with EEA1 when compared to LAMP1 (**Fig 5.4 F-G**). Out of the numerous Arl8b-positive compartments, only up to 20-30 of them were positive for Rabip4' and EEA1, while the rest of the Arl8b pool was present on endolysosomes marked by LAMP1 (**Fig 5.4 G**). These results suggest that a subset of Arl8b pool colocalizes with Rabip4' on early endosomes, where they interact and contribute to vesicular functioning.

The colocalization of Rabip4' and Arl8b on early endosomal compartments was striking and we wanted to be sure that observed effect was specific. Like Rabip4', Nischarin is another known effector of Rab14 that regulates maturation of early to late endocytic compartments marked by Rab9 (Kuijl et al., 2013). We tested the co-localization of Nischarin and Arl8b in HeLa cells by over-expressing epitope-tagged proteins followed by immunostaining. Myc-Nischarin did not colocalize with Arl8b-HA when co-expressed (**Fig 5.5 B**). Whereas, Myc-Nischarin punctae continued to colocalize with early endosomes marked by GFP-Rab14 (**Fig 5.5 A**). Next we wanted to test whether other late-endosomal small GTP-binding protein such as Rab7 colocalize with Rabip4' or not. Rabip4'WT-FLAG and HA-Rab7 were co-transfected in HeLa cells, and confocal microscopy analysis did not

show any colocalization of the two ((**Fig 5.5 D-F**). These results imply that the colocalization observed for Rabip4' and Arl8b is specific.
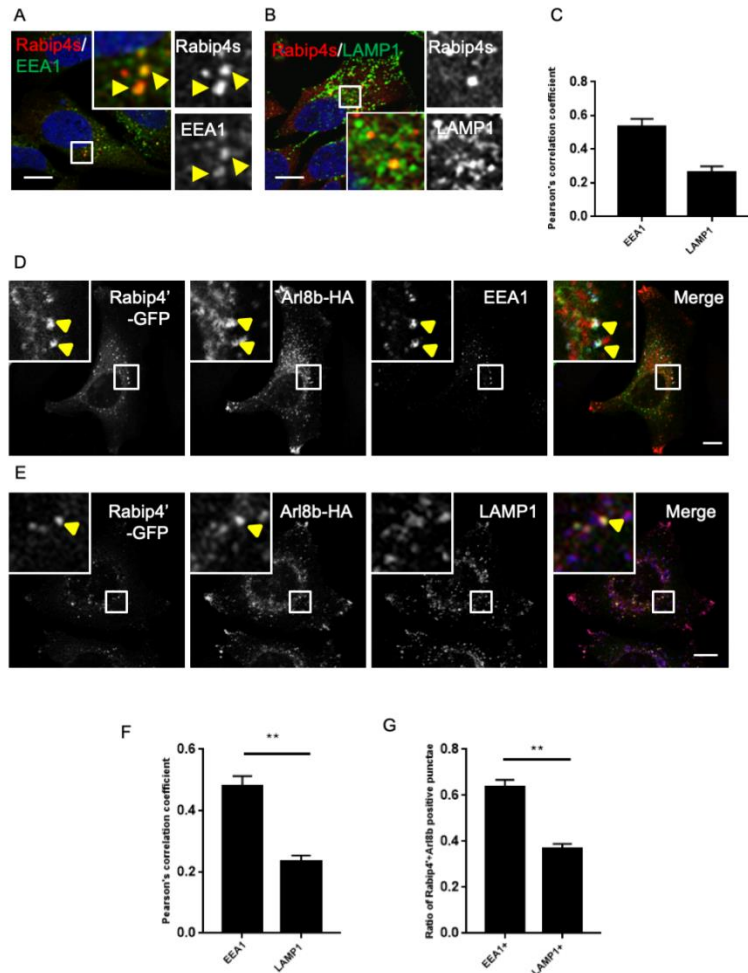
Figure 5.4: Rabip4' and Arl8b colocalize on early endosomal structures.

A-B) Representative confocal micrographs of HeLa cells immunostianed for endogenous Rabip4s and EEA1 or LAMP1. **C**) Colocalization of endogenous Rabip4s with EEA1 and LAMP1 was measured by Pearson's correlation coefficient (Coste's randomization) (n=3, 50 cells per experiment for each treatment). **D-E**) HeLa cells were co-transfected with Rabip4' WT-GFP and Arl8b-HA followed by immunostaining with either **D**) EEA1 or **E**) LAMP1 and were analyzed by confocal microscopy. Insets show co-localized pixels marked by arrowheads. Scale bar=10μm. **F**) Co-localization of Rabip4' with either EEA1 or LAMP1 in cells co-transfected with Arl8b was measured by Pearson's coefficient (Coste's Randomization) (n=3, 30 cells per experiment for each treatment). **G**) The number of Rabip4'-Arl8b double positive were manually counted for being either EEA1+ or LAMP1+ for three independent experiments (n=3, 200 vesicles per experiment for each treatment). Values plotted as mean±sem. ** indicates p>0.01

Previous studies have shown that Rabip4s bind to Rab14 at the C-terminal end and we observed that N-terminal RUN domain binds to Arl8b. To test whether Rabip4' can enhance the colocalization of membranes harboring small GTP-binding proteins Rab14 and Arl8b, we did triple transfection of Rabip4' WT-FLAG and GFP-Rab14 either with Arl8b-HA or HA-Rab7 (taken as a control). Confocal microscopic analysis revealed enhanced colocalization between Rab14- and Arl8b-positive compartments in cells transfected expressing Rabip4', whereas such colocalization was not seen for Rab14 and Rab7 compartments (**Fig 5.5 E-F**). Also Nischarin was unable to bring about colocalization of Rab14+ and Arl8b+ structures (**Fig 5.5 C**). Together these observations further strengthened our results which showed specific colocalization of Rabip4,' and Arl8b to early endosomal structures positive for Rab14 and this occurs via interaction of Rabip4' with Arl8b and Rab14 via separate domains.

It was surprising to find a predominantly endolysosomal protein, Arl8b to be present on a specific pool of early endocytic compartments along with Rabip4'. Previous studies show Arl8b to be localized primarily on lysosomal membranes, and its presence on other organelle membranes remains unknown (Khatter et al., 2015b). A recent study has reported that late endosomal small GTP-binding protein Rab7 localizes to other intracellular compartments such as mitochondria and endoplasmic reticulum (Jimenez-Orgaz et al., 2018). This study raises the possibility that proteins that predominantly localize to a particular organelle can be present on other non-canonical membranes under specific conditions. Intrigued by the idea, we asked the question of whether Arl8b, which primarily localizes to endolysosomal structures, is present on early endocytic compartments as well or not. To test this, we over-expressed GFP-tagged constitutively GTP bound form of Rab5 (Q79L) in HeLa cells, causing enlargement of the early endosomes and Arl8b-HA, followed by immunostaining either with anti-LAMTOR1 (a lysosomal protein) or anti-Rabip4s antibodies. Interestingly, we observed that few of the enlarged early endosomal GFP-Rab5Q79L containing punctate structures were positive for Arl8b-HA and endogenous Rabip4s. However, LAMTOR1 was absent from the enlarged early endosomal structures (**Fig 5.5 G-I**). These results together indicate the presence of Arl8b, though transiently on Rab14-positive early endosomes along with Rabip4'.
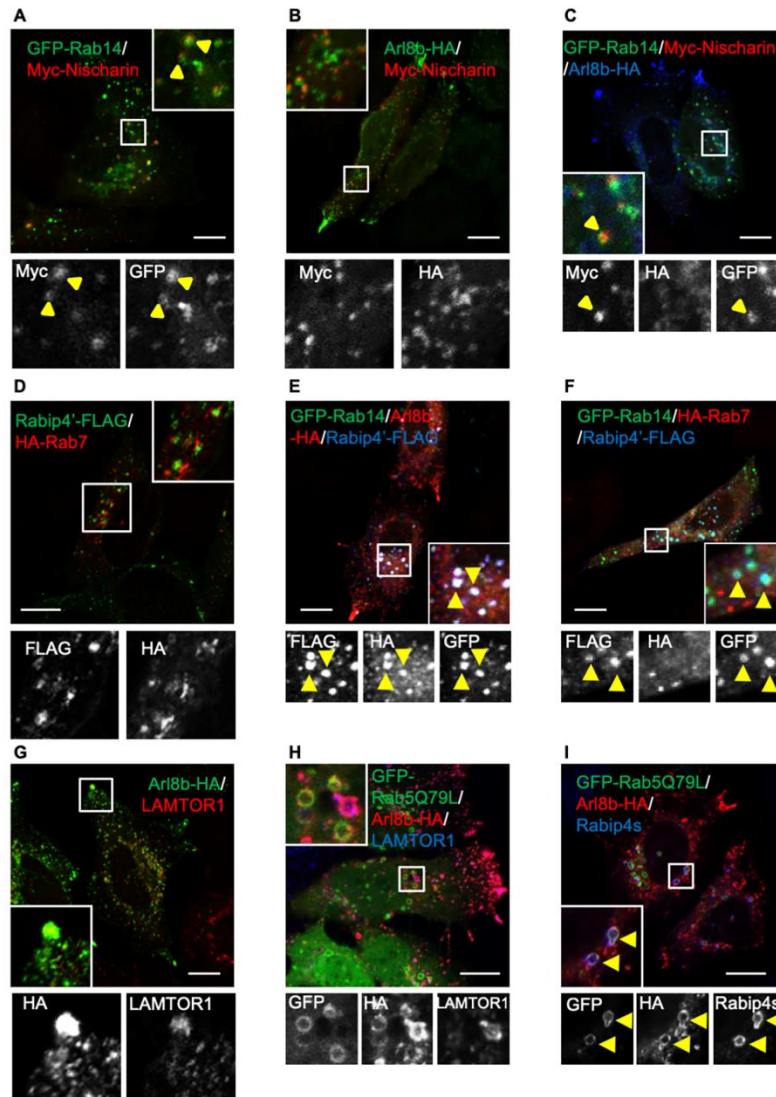
Figure 5.5: Arl8b, not Rab7 is present on a subset of early endosomes positive for Rabip4s and Rab14.

A-C) HeLa cells co-expressing Myc-Nischarin either with GFP-Rab14 or Arl8b-HA and triple transfection of all three were analyzed by confocal microscopy. **D-F**) Representative confocal micrographs of HeLa cells transfected with the indicated plasmids and immunostained. **G-I**) Representative confocal micrographs of HeLa cells transfected with either Arl8b-HA alone or co-transfected with GFP-Rab5Q79L and immunostained with indicated antibodies against endogenous proteins. Insets show co-localized pixels marked by arrowheads. Scale bar=10µm.

5.2.3 Arl8b silencing disrupts association of Rabip4s with endosomal membranes

Till now our binding assays and steady-state confocal microscopy results indicate that Rabip4' binds Arl8b via its N-terminal RUN domain and they are colocalized on a subpopulation of early endosomal structures. It was surprising to find interaction and colocalization between Rabip4' and Arl8b which individually are on distinct endocytic compartments. Next we asked the question that whether the interaction and colocalization of Rabip4' and Arl8b is physiologically relevant or we were observing it due to over-expression approach used up until now for our experiments. To this end, we immunostained for endogenous Rabip4s in control and Arl8b siRNA-treated HeLa cells. The efficiency of Arl8b silencing using two different oligonucleotides was confirmed by qRT-PCR and was found to be >85% (**Fig 5.6 A**). Unlike control siRNA-treated cells, where Rabip4s were present on endosomal structures positive for EEA1, endogenous Rabip4s redistributed to the cytosol upon Arl8b depletion using multiple oligonucleotides. Importantly, while Rabip4s were mostly cytosolic in Arl8b-depleted cells, few endosomes were observed that colocalized with EEA1, indicating that Arl8b is not the only determining factor of Rabip4s membrane association (**Fig 5.6 B-D**). Next, to confirm the specificity of Arl8b depletion, we rescued its effect on Rabip4s localization in HeLa cells expressing siRNA-resistant Arl8b (**Fig 5.6 E**). It was observed that in siRNA-resistant Arl8b-transfected cells, numerous Rabip4s punctae were now present. This effect was quantified by measuring the number of Rabip4s and EEA1 (**Fig 5.6 G-I**) (taken as control) punctae using ImageJ over three independent experiments (**Fig 5.6 F and J**). Rabip4s protein levels were not altered in Arl8b depleted cells (**Fig 5.6 K**). It was noteworthy that, while Arl8b knockdown disrupted the membrane association of Rabip4s, it did not alter the localization of other early endosomal proteins such PI3P binding PX-domain and Rab14 effector Nischarin (**Fig 5.7 A-F**). The effect of Arl8b depletion on Rabip4s membrane localization corroborated with our previous observations showing cytosolic distribution of Arl8b binding defective mutants of Rabip4'. Collectively these results show that Rabip4' and Arl8b interaction is physiologically significant and membrane localization of Rabip4s is partly regulated by interaction with Arl8b.
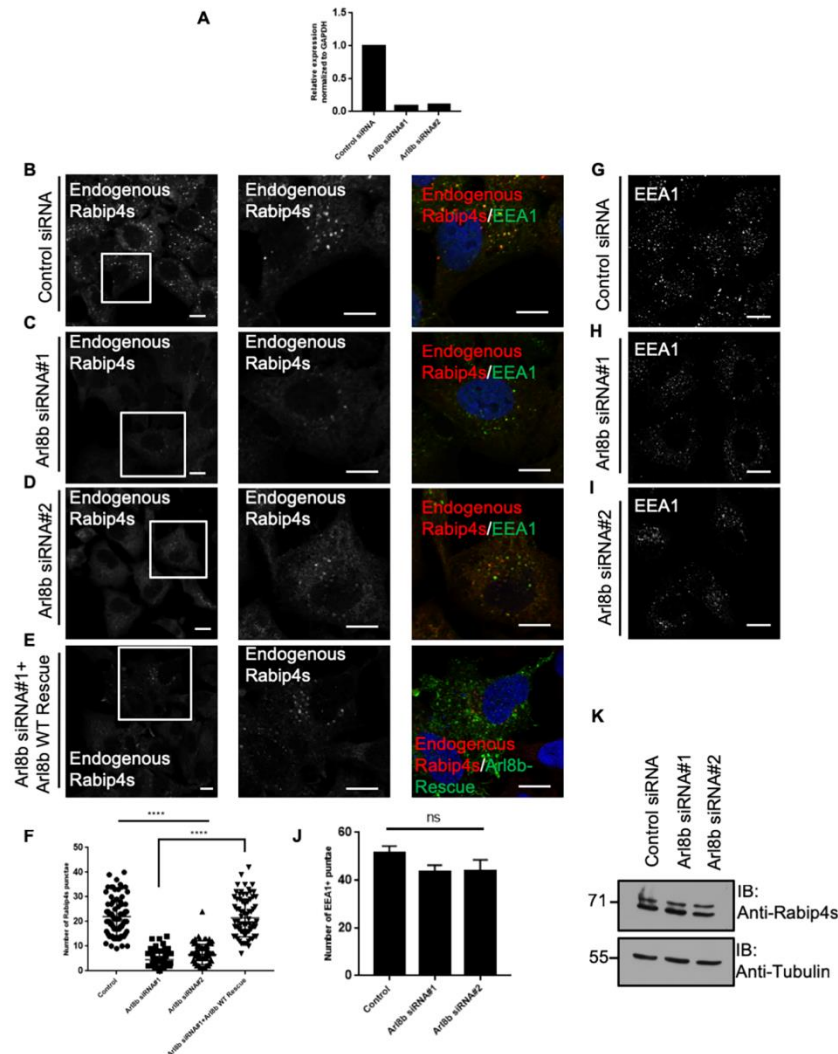
Figure 5.6: Arl8b regulates membrane association of Rabip4s.

A) Graph showing the relative expression of Arl8b normalized to GAPDH in HeLa cells treated with Control-siRNA, Arl8b-siRNA#1 and Arl8b-siRNA#2 analysed by quantitative RT-PCR. **B-D**) Representative confocal micrographs of HeLa cells treated with indicated siRNAs and immunostained for endogenous Rabip4s and EEA1. Loss in punctae number was observed in case of Arl8b depleted cells as compared to Control siRNA treated cells. **E**) siRNA resistant untagged Arl8b-WT was transfected in Arl8b depleted cells, immunostained for endogenous Rabip4s and Arl8 and analyzed by confocal microscopy. Scale bar=10µm. **F**) The graph represents the number of endogenous Rabip4s punctae calculated for Control, Arl8b siRNA#1 and 2 and siRNA resistant Arl8b-WT transfected cells using ImageJ (n=3, 50 cells for each treatment per experiment). **G-I**) Confocal micrographs of HeLa cells treated with indicated siRNAs and immunostained for early endosomal marker EEA1. **J**) Quantification graph of the number of EEA1 punctae in Control vs. Arl8b depleted cells using two different oligonucleotides (n=3, 50 cells per experiment for each treatment). Values plotted are mean±sem. **** indicates p<0.0001, ns-not significant. **K**) HeLa cell lysates from Control siRNA, Arl8b siRNA#1 and 2 were immunoblotted with anti-Rabip4s antibody and anti-tubulin was used as loading control.

102
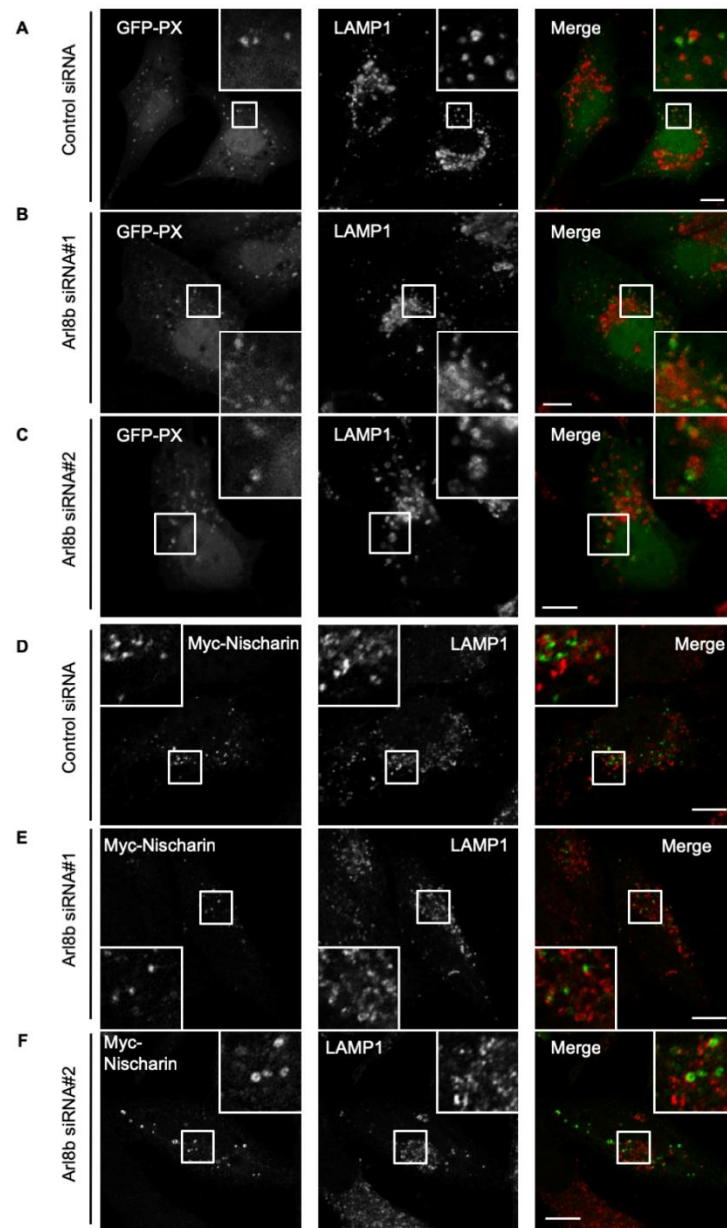
Figure 5.7: Arl8b depletion does not alter membrane association of other early endosomal proteins.

A-C) Control and Arl8b siRNAs treated cells were transfected with GFP-PX and immunostained with LAMP1. **D-F**) Representative confocal micrographs of HeLa cells treated with indicated siRNAs and transfected with Myc-Nischarin and stained with anti-LAMP1. Both GFP-PX and Myc-Nischarin are observed to be punctate. Scale bar=10μm.
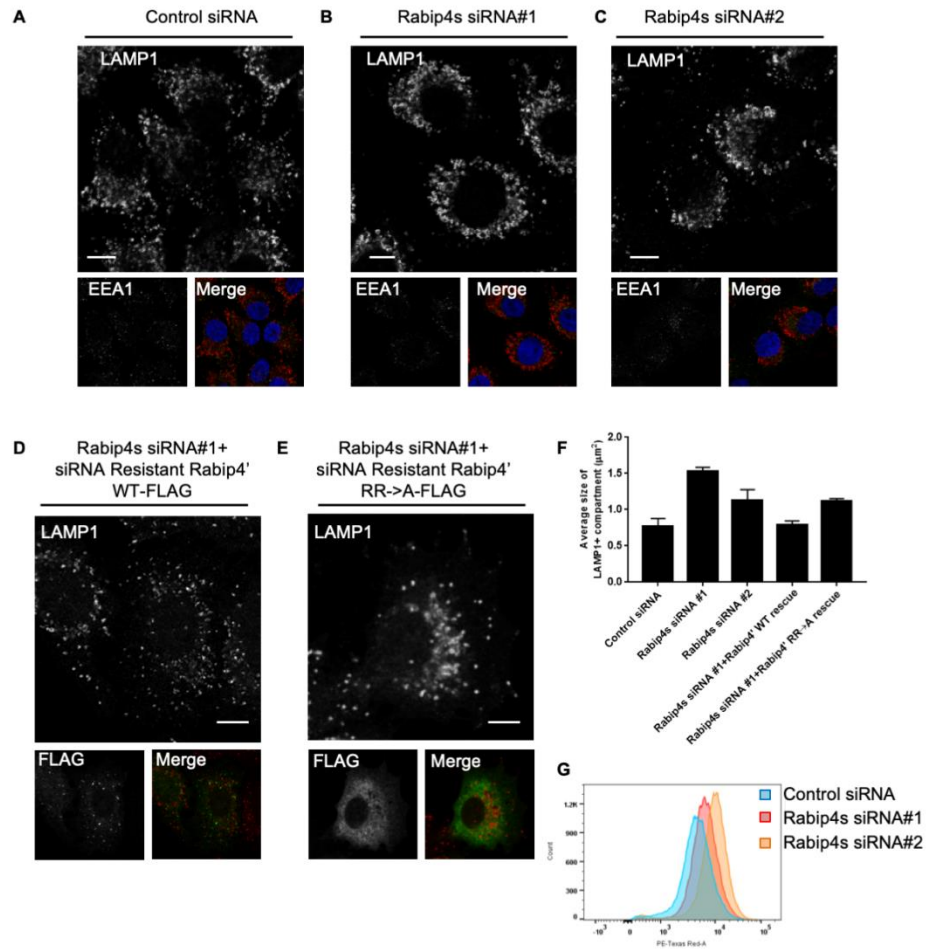
5.2.4 Rabip4s depletion leads to enlargement of endolysosomes

To investigate the physiological function of Rabip4s/Rabip4', we depleted Hela cells of Rabip4s using two different oligonucleotides. The efficiency of knockdown by siRNA was tested by western blotting. Previous studies have reported that Rabip4s affect the degradation of EGF/EGFR and recycling of transferrin in cells (Gosney et al., 2018; Yamamoto et al., 2010). In accordance with the reported function of Rabip4s, we found that siRNA mediated depletion of Rabip4s in HeLa cells led to a delay in EGF degradation (**Fig 5.8 A** and quantification in **D**). Notably, upon siRNA-mediated depletion of Rabip4s we found that the LAMP1+ compartments were not redistributed to cell periphery as previously reported, but instead were enlarged and accumulated in the perinuclear region of the cell (**Fig 5.9 A-C**). The average size of endolysosomes in Control siRNA treated cells was 0.77 µm2 which nearly doubled to 1.53 µm2 and 1.12 µm2 in case of Rabip4s depletion using two different oligonucleotides (**Fig 5.9 F**). The average size of LAMP1-positive compartment was rescued in case of Rabip4'-WT transfected cells, whereas siRNA resistant Arl8b binding defective Rabip4' RR→A-FLAG construct was unable to do so (**Fig 5.9 D-E** and quantification in **F**). Staining of lysotracker, a commonly used dye to see acidic endolysosomes was analyzed by flow cytometry of HeLa cells treated with Control- and Rabip4s –siRNAs and incubated with lysotracker for 2 hours in Fluorobrite DMEM. Flowcytometry analysis showed an increase in the staining of lysotracker for Rabip4s depleted cells as compared to control cells (**Fig 5.9 G**). Increase in lysotracker staining indicates enhanced accumulation of the dye in acidic compartments and corroborates with the enlargement of endolysosome compartment upon Rabip4s depletion. These results suggest that Rabip4s modulates the endolysosome compartment, ensuring typical morphology and it depends upon its interaction with Arl8b.
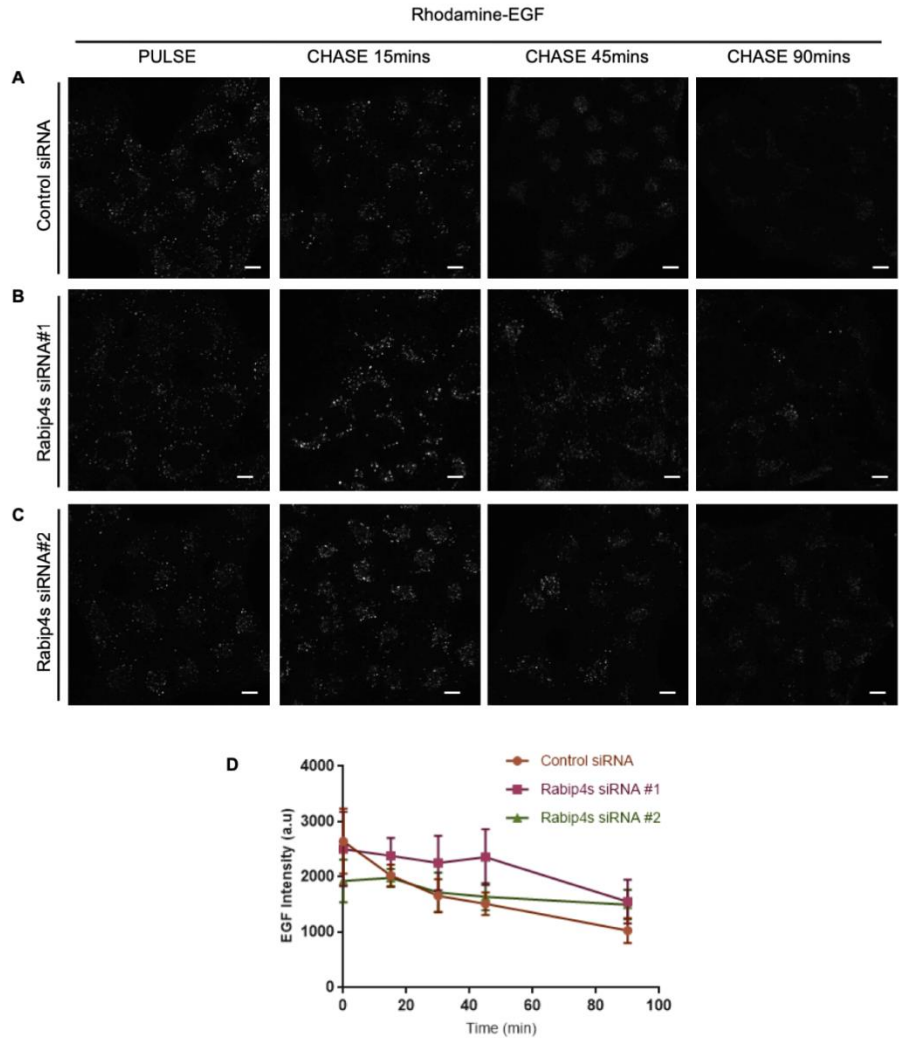
Figure 5.8: EGF degradation is delayed in Rabip4s depleted cells.

A-C) Representative confocal micrographs of HeLa cells treated with Control- and Rabip4s siRNAs , pulsed with Rhodamine-EGF and fixed at indicated time points. Scale bar=10µm. **D)** CTCF (Corrected total cell fluorescence) for Rhodamine-EGF in Control-, Rabip4s-siRNA#1 and 2 at different time points was calculated using ImageJ and plotted as shown. n=3, 50 cells per experiment, for each time point and treatment.

Figure 5.9: Rabip4s depletion leads to enlarged endolysosomes.

A-C) Representative confocal micrographs of HeLa cells treated with Control-siRNA, Rabip4s siRNA#1 and Rabip4s siRNA#2 and immunostained for LAMP1 and EEA1. **D-E**) Rabip4s depleted HeLa cells were transfected with siRNA resistant Rabip4' WT-FLAG or Rabip4' RR→A FLAG, immunostained for LAMP1 and analyzed by confocal microscopy. **F**) Quantification graph showing the average size of endolysosomes marked by LAMP1 measured using ImageJ in indicated treatments (n=3, 50 cells per experiment for each treatment). Values plotted as mean±sem. *,** indicate $p < 0.05$ and $p < 0.001$. **G**) Flow-cytometry analysis of lysotracker staining done in HeLa cells treated with the indicated siRNAs (30,000 cells analyzed for each treatment).

5.2.5 Rabip4s depletion leads to defective *Salmonella* replication and delayed LAMP1 acquisition onto SCVs

Salmonella enterica serovar typhimurium (*Salmonella* typhimurium) is an intracellular pathogen known to extensively interact with the endocytic compartments and utilize the host machinery for its survival and replication. Small GTP-binding protein Arl8b has previously been shown to regulate *Salmonella* pathogenesis in cells as it is crucial for maintaining the replicative niche or *Salmonella*-containing vacuole (SCV) and formation of *Salmonella*-induced filaments (Sifs) (Tuli and Sharma, 2018). Rab14 is also known to mediate early to late SCV transition in Salmonella-infected cells (Kuijl et al., 2013). Our results show that known Rab14 effector, Rabip4' interacts with Arl8b and this interaction is essential for maintaining typical endolysosomal morphology and efficient cargo trafficking to lysosomes. Based on these pieces of evidence, we were prompted to check the role of Rabip4' in *Salmonella* pathogenesis. To this end, we first analyzed the localization of endogenous Rabip4s in *Salmonella*-infected HeLa cells at various time points. Extensive research done previously on *Salmonella* pathogenesis in mammalian cells has shown that after infection the SCV interacts with the endocytic pathway and acquires endocytic marker proteins. At 5-10mins post-infection, the SCV is marked by EEA1, whereas it starts obtaining LAMP1-positive membrane by 1hr post infection. 2hrs post infection majority of the SCVs in cells have acquired the lysosomal membrane, and the bacteria begin replication post 4 to 6 hours of infection (Tuli and Sharma, 2018). HeLa cells infected with GFP expressing SL1344 strain of *Salmonella* (WT strain) were fixed at different time points post infection and immunostained for endogenous Rabip4s. We observed a dramatic enlargement of the endogenous Rabip4s compartment in Salmonella-infected cells at 30mins post-infection, a time point where the SCVs transition from early to late endocytic compartments (**Fig 5.10 A**). It was surprising to note the cytosolic distribution of endogenous Rabip4s at 2hrs post infection (**Fig 5.10 B**). Standard punctate localization of endogenous Rabip4s was restored by 6 hours post infection (**Fig 5.10 C**). The enlargement of Rabip4s-positive compartment upon Salmonella infection was dependent upon Rab14 but not Arl8b as demonstrated in our experiment with cells depleted of these small GTP-binding proteins respectively and analyzed for endogenous Rabip4s staining by confocal microscopy (**Fig 5.10 D-F**).

107
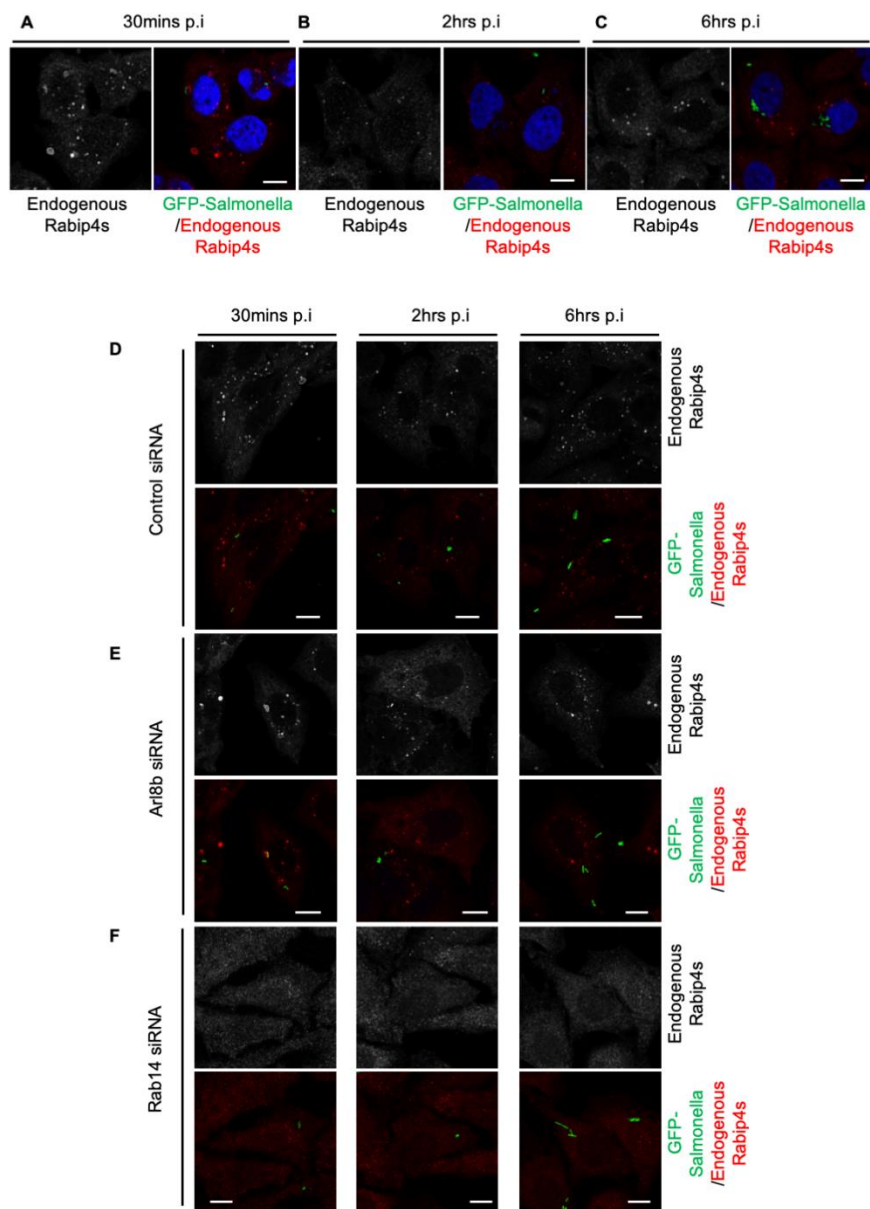
Figure 5.10: Formation of enlarged Rabip4s-positive endosomes in *Salmonella* infected cells is Rab14 dependent.

A-C) Representative confocal micrographs of HeLa cells infected with GFP expresisng *Salmonella* SL1344 strain, fixed at indicated time points and immunostained for endogenous Rabip4s. **D-F)** HeLa cells treated with Control-siRNA, Arl8b siRNA#1 and Rab14 siRNA were infected with GFP expressing *Salmonella* , fixed at indicated time points, immunostained for endogenous Rabip4s and analyzed by confocal microscopy. Scale bar=10µm.
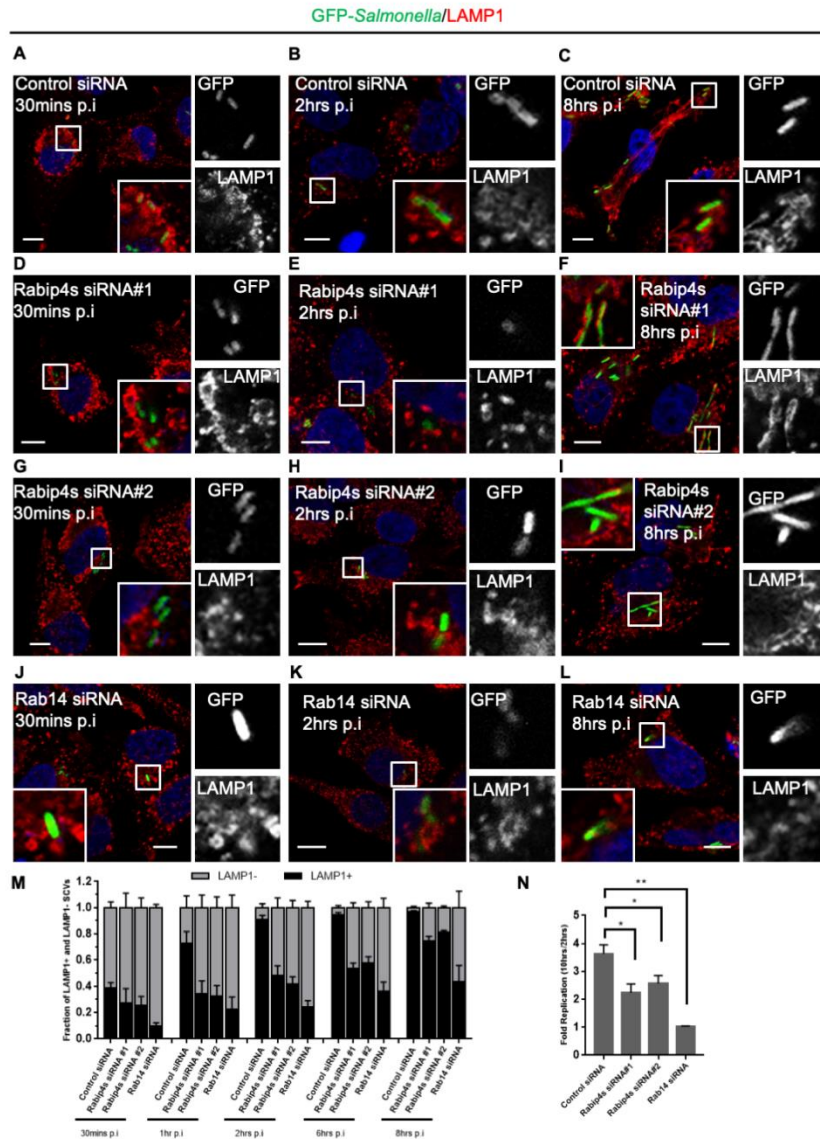
Figure 5.11: Delayed LAMP1 acquisition onto SCVs and defect in *Salmonella* replication is observed in case of Rabip4s and Rab14 depleted cells.

A-L) Representative confocal micrographs of HeLa cells treated with Control-, Rabip4s-#1, Rabip4s-#2 and Rab14-siRNA for 60hrs followed by infection with GFP expressing Salmonella SL1344 strain at an MOI of 1:150 and PFA fixed at the indicated time points post infection. The cells were immunostained with anti-LAMP1 and analyzed by confocal microscopy. **M**) Quantification graph represents fraction of SCVs positive or negative for LAMP1 in indicated siRNA treatments for 30mins, 1hr, 2hrs,6hrs and 8hrs post infection (n=3 ~100 SCVs per experiment for each time point and each treatment). Values plotted as mean±sem. Intracellular replication assay. **N**) HeLa cells treated with indicated siRNA and infected with *Salmonella* were harvested at indicated times p.i. The fold replication is plotted in the graph as mean±sem. Scale bar=10µm.

To investigate the role of Rabip4s in regulating recruitment of the lysosomal membrane to SCVs, we treated HeLa cells with Control-, Rabip4s- and Rab14-siRNA followed by infection with GFP expressing SL1344 strain of *Salmonella* typhimurium and fixation at different time points. Confocal microscopy analysis revealed that in control-siRNA treated cells, SCVs acquired LAMP1 membrane by 2 hours post infection, whereas in case of Rabip4s depleted cells, lysosomal membrane acquisition by SCVs was delayed unto 6 hours post infection. Intriguingly, Rab14 depletion caused severe defect in LAMP1 recruitment to SCVs (**Fig 5.11 A-L** and quanitification shown in **M**). Intracellular replication of *Salmonella* was also tested using the Colony Forming Units (CFU) assay in HeLa cells treated with Control-, Rabip4s- and Rab14-siRNA. In the case of HeLa cells, we observed 3.6 -fold replication for control cells, 2.2 fold replication in cells depleted of Rabip4s and no replication upon Rab14 silencing (**Fig 5.11 N**). These results show that Rabip4s (Rabip4'), Rab14 and Arl8b mediate trafficking or maturation of SCVs and regulate bacteria pathogenesis in cells.

5.3 Discussion

Small GTP-binding protein Arl8b plays a crucial role in regulating lysosome function, and it does so by recruiting its downstream effectors SKIP, PLEKHM1 and HOPS complex known that regulate lysosome positioning and fusion with late-endosomes and autophagosomes (Khatter et al., 2015a; Marwaha et al., 2017; Rosa-Ferreira and Munro, 2011). Recent findings show that SKIP and PLEKHM1 interact with Arl8b via their N-terminal RUN-domain. Previous studies shed light on RUN domain-containing proteins as interaction partners for members of Rab and Rap small GTP-binding proteins. RUN domains are alpha helical in structure, organized into six blocks and have conserved basic/positively charged residues implicated in interaction with small GTP-binding proteins (Callebaut et al., 2001). Member of RUN and FYVE (RUFY) family of proteins, RUFY1/ Rabip4' was recently proposed as a coordinator of lysosome positioning in mammalian cells. Interestingly RUFY1 gene products, which primarily localize to early endosomes, led to lysosome redistribution to the cell periphery (Ivan et al., 2012). A recent study also suggested a role of Rabip4s in EGFR trafficking, a cargo that goes to lysosomes for degradation (Gosney et al., 2018). Rabip4s depletion resulted in longer retention, hence delayed trafficking of EGFR to

lysosomes. However, no mechanism has been elucidated yet for the role of Rabip4s in regulating lysosome positioning and cargo trafficking. Prompted by the presence of RUN domain that is 38% and 35% similar to known Arl8b effectors PLEKHM1 and SKIP/PLEKHM2 respectively and plausible role in lysosome function regulation, we investigated Rabip4s as potential Arl8b binding partner.

Here in this study, we find that Rabip4s interact with Arl8b via their N-terminal RUN domain and conserved arginine residues (R206 and R208) within this domain mediate the binding. We observed binding of Rabip4' with active Arl8b-GTP, whereas reduced interaction with inactive Arl8b-GDP was seen in purified protein interaction assay. Depletion of Rabip4s altered the endolysosomal morphology, leading to the formation of enlarged LAMP1-positive compartments but the distribution remained unaffected. We were unable to observe any peripheral accumulation of lysosome upon Rabip4s depletion as previously reported. The possible reason for this could be that our experiments were done using HeLa cells, whereas the lysosome distribution phenotype is reported using HEK cells. Differences in the cell types and differential expression of Rabip4s can be contributing factors towards the differences we see in our results. The mechanism of enlargement of endolysosomes remains an open question to be further elucidated. AP-3 has been previously shown to regulate packaging and Golgi to endosome trafficking of LAMP-1 in melanocytes (Chapuy et al., 2008). It will be interesting to elucidate if Rabip4' and AP-3 interaction affects efficient delivery of structural and luminal lysosomal proteins in other cell types as well and how does Arl8b contribute to this pathway. Future experiments will be instrumental in determining the mechanism of RUFY1/Rabip4s mediated regulation of endolysosomes.

Interestingly we observed that Arl8b and Rabip4' colocalized on a subset of Rab14-positive early endosomes. Depletion of Arl8b resulted in partial loss of endogenous Rabip4s from endosome membrane as compared to control cells. Typical endogenous Rabip4s localization was restored upon transfection of siRNA resistant Arl8b-WT in cells lacking Arl8b. Together, these results indicate that Arl8b is crucial for maintaining a stable membrane localized pool of Rabip4s at the endogenous level. It is previously known that Rab14 is necessary for recruiting Rabip4s to endosome membrane. It will be interesting to find out the mechanism by which Rab14 and Arl8b coordinate to maintain a stable

111

membrane-bound pool of Rabip4s. Previous studies have shown that Rabip4' is an effector for Rab4 and Rab14. Out of the two Rabs, Rab14 is essential for recruiting Rabip4' onto endosomal membranes, whereas Rab4 is dispensable for the same. The mechanism of Arl8b contribution to membrane localization of Rabip4' remains an open question. Rabip4' is recruited onto the endosomal membranes by small GTP-binding protein Rab14, and is likely that further interaction with Arl8b is crucial for maintaining a stable, functional pool of the protein. Interaction between Arl8b-Rabip4' and Rab4/Rab14 probably allows to form transient contact between endosomes for exchange of cargo or maturation of the vesicles.

It has been suggested previously that RUFY family members can act as docking proteins and mediate crosstalk between multiple small GTP-binding proteins. Increased colocalization of Rab14 and Arl8b positive compartments upon Rabip4' over-expression provides a good starting point to further explore the role of Rabip4' as linker between the two small GTP-binding proteins.

Salmonella infection in Rabip4s depleted cells yielded exciting observations. We observed a delay in LAMP1 acquisition on SCVs and a decreased replication of *Salmonella* typhimurium upon Rabip4s depletion. Salmonella infection led to the formation of enlarged Rabip4s-positive compartments at 30mins post-infection time point. Standard size and localization of endogenous Rabip4s were restored post 2 hours of infection. It is known that 30mins post-infection, the SCV transitions from early to late stage. Maturation of early to late SCV is accompanied by change in lipid and protein composition of the membrane. It will be interesting to know the mechanistic role of RUFY1/Rabip4s in mediating the enlargement of early endosomal compartment/ early SCVs upon *Salmonella* infection. Previous studies suggest differential expression of RUFY1 gene products, with the longer isoform Rabip4' expressing more as compared to the shorter isoform in HeLa cells and an equal expression of both the isoforms is reported in HEK cells. We were only able to detect the expression of Rabip4' (longer isoform) precisely in HeLa cells with endogenous antibody available with us. The contribution of the two isoforms to lysosome function regulation in different cell types remains an interesting question for further exploration. Here, with our findings we propose that binding of Rabip4' to Arl8b via its N-terminal RUN domain is essential for maintaining stable and functional Rabip4s protein pool on endosome membrane. Rabip4' and

Arl8b interaction is essential for ensuring typical endolysosomal morphology and regulates cargo trafficking to lysosomes.

Chapter 6

Bibliography

Andrews, N.W., P.E. Almeida, and M. Corrotte. 2014. Damage control: cellular mechanisms of plasma membrane repair. *Trends Cell Biol*. 24:734-742.

Bagshaw, R.D., J.W. Callahan, and D.J. Mahuran. 2006. The Arf-family protein, Arl8b, is involved in the spatial distribution of lysosomes. *Biochem Biophys Res Commun*. 344:1186-1191.

Balderhaar, H.J., and C. Ungermann. 2013. CORVET and HOPS tethering complexes - coordinators of endosome and lysosome fusion. *J Cell Sci*. 126:1307-1316.

Ballabio, A. 2016. The awesome lysosome. *EMBO molecular medicine*. 8:73-76.

Behar, S.M., M. Divangahi, and H.G. Remold. 2010. Evasion of innate immunity by Mycobacterium tuberculosis: is death an exit strategy? *Nat Rev Microbiol*. 8:668-674.

Bo, T., F. Yan, J. Guo, X. Lin, H. Zhang, Q. Guan, H. Wang, L. Fang, L. Gao, J. Zhao, and C. Xu. 2016. Characterization of a Relatively Malignant form of Osteopetrosis Caused by a Novel Mutation in the PLEKHM1 Gene. *J Bone Miner Res*.

Bonifacino, J.S. 2014. Vesicular transport earns a Nobel. *Trends in cell biology*. 24:3-5.

Boucrot, E., T. Henry, J.P. Borg, J.P. Gorvel, and S. Meresse. 2005. The intracellular fate of Salmonella depends on the recruitment of kinesin. *Science*. 308:1174-1178.

Bucci, C., P. Alifano, and L. Cogli. 2014. The role of rab proteins in neuronal cells and in the trafficking of neurotrophin receptors. *Membranes*. 4:642-677.

Burguete, A.S., T.D. Fenn, A.T. Brunger, and S.R. Pfeffer. 2008. Rab and Arl GTPase family members cooperate in the localization of the golgin GCC185. *Cell*. 132:286-298.

Cabukusta, B., and J. Neefjes. 2018. Mechanisms of lysosomal positioning and movement. *Traffic*. 19:761-769.

Callebaut, I., J. de Gunzburg, B. Goud, and J.P. Mornon. 2001. RUN domains: a new family of domains involved in Ras-like GTPase signaling. *Trends in biochemical sciences*. 26:79-83.

Chapuy, B., R. Tikkanen, C. Muhlhausen, D. Wenzel, K. von Figura, and S. Honing. 2008. AP-1 and AP-3 mediate sorting of melanosomal and lysosomal membrane proteins into distinct post-Golgi trafficking pathways. *Traffic*. 9:1157-1172.

Chia, P.Z., and P.A. Gleeson. 2014. Membrane tethering. *F1000prime reports*. 6:74.

Ciechanover, A. 2005. Intracellular protein degradation: from a vague idea thru the lysosome and the ubiquitin–proteasome system and onto human diseases and drug targeting*. *Cell Death And Differentiation*. 12:1178.

Cormont, M., M. Mari, A. Galmiche, P. Hofman, and Y. Le Marchand-Brustel. 2001. A FYVE-finger-containing protein, Rabip4, is a Rab4 effector involved in early endosomal traffic. *Proceedings of the National Academy of Sciences of the United States of America*. 98:1637-1642.

Corona, A.K., Y. Mohamud, W.T. Jackson, and H. Luo. 2018. Oh, SNAP! How enteroviruses redirect autophagic traffic away from degradation. *Autophagy*. 14:1469-1471.

Del Fattore, A., R. Fornari, L. Van Wesenbeeck, F. de Freitas, J.P. Timmermans, B. Peruzzi, A. Cappariello, N. Rucci, G. Spera, M.H. Helfrich, W. Van Hul, S. Migliaccio, and A. Teti. 2008. A new heterozygous mutation (R714C) of the osteopetrosis gene, pleckstrin homolog domain containing family M (with run domain) member 1 (PLEKHM1), impairs vesicular acidification and increases TRACP secretion in osteoclasts. *Journal of bone and mineral research : the official journal of the American Society for Bone and Mineral Research*. 23:380-391.

Deshar, R., S. Moon, W. Yoo, E.B. Cho, S.K. Yoon, and J.B. Yoon. 2016. RNF167 targets Arl8B for degradation to regulate lysosome positioning and endocytic trafficking. *FEBS J*. 283:4583-4599.

Divangahi, M., M. Chen, H. Gan, D. Desjardins, T.T. Hickman, D.M. Lee, S. Fortune, S.M. Behar, and H.G. Remold. 2009. Mycobacterium tuberculosis evades macrophage defenses by inhibiting plasma membrane repair. *Nat Immunol*. 10:899-906.

Doray, B., P. Ghosh, J. Griffith, H.J. Geuze, and S. Kornfeld. 2002. Cooperation of GGAs and AP-1 in packaging MPRs at the trans-Golgi network. *Science*. 297:1700-1703.

Dykes, S.S., A.L. Gray, D.T. Coleman, M. Saxena, C.A. Stephens, J.L. Carroll, K. Pruitt, and J.A. Cardelli. 2016a. The Arf-like GTPase Arl8b is essential for three-dimensional invasive growth of prostate cancer in vitro and xenograft formation and growth in vivo. *Oncotarget*. 7:31037-31052.

Dykes, S.S., A.L. Gray, D.T. Coleman, M. Saxena, C.A. Stephens, J.L. Carroll, K. Pruitt, and J.A. Cardelli. 2016b. The Arf-like GTPase Arl8b is essential for three-dimensional invasive growth of prostate cancer in vitro and xenograft formation and growth in vivo. *Oncotarget*.

Falcon-Perez, J.M., R. Nazarian, C. Sabatti, and E.C. Dell'Angelica. 2005. Distribution and dynamics of Lamp1-containing endocytic organelles in fibroblasts deficient in BLOC-3. *J Cell Sci*. 118:5243-5255.

Farias, G.G., C.M. Guardia, R. De Pace, D.J. Britt, and J.S. Bonifacino. 2017. BORC/kinesin-1 ensemble drives polarized transport of lysosomes into the axon. *Proceedings of the National Academy of Sciences of the United States of America*. 114:E2955-E2964.

Filipek, P.A., M.E.G. de Araujo, G.F. Vogel, C.H. De Smet, D. Eberharter, M. Rebsamen, E.L. Rudashevskaya, L. Kremser, T. Yordanov, P. Tschaikner, B.G. Furnrohr, S. Lechner, T. Dunzendorfer-Matt, K. Scheffzek, K.L. Bennett, G. Superti-Furga, H.H. Lindner, T. Stasyk, and L.A. Huber. 2017. LAMTOR/Ragulator is a negative regulator of Arl8b- and BORC-dependent late endosomal positioning. *The Journal of cell biology*. 216:4199-4215.

Flannagan, R.S., V. Jaumouillé, and S. Grinstein. 2012. The Cell Biology of Phagocytosis. *Annual Review of Pathology: Mechanisms of Disease*. 7:61-98.

Fu, M.M., and E.L. Holzbaur. 2014. Integrated regulation of motor-driven organelle transport by scaffolding proteins. *Trends in cell biology*. 24:564-574.

Fujiwara, T., S. Ye, T. Castro-Gomes, C.G. Winchell, N.W. Andrews, D.E. Voth, K.I. Varughese, S.G. Mackintosh, Y. Feng, N. Pavlos, T. Nakamura, S.C. Manolagas, and H. Zhao. 2016. PLEKHM1/DEF8/RAB7 complex regulates lysosome positioning and bone homeostasis. *JCI insight*. 1:e86330.

Fukuda, M., H. Kobayashi, K. Ishibashi, and N. Ohbayashi. 2011. Genome-wide investigation of the Rab binding activity of RUN domains: development of a novel tool that specifically traps GTP-Rab35. *Cell structure and function*. 36:155-170.

Garg, S., M. Sharma, C. Ung, A. Tuli, D.C. Barral, D.L. Hava, N. Veerapen, G.S. Besra, N. Hacohen, and M.B. Brenner. 2011. Lysosomal trafficking, antigen presentation, and microbial killing are controlled by the Arf-like GTPase Arl8b. *Immunity*. 35:182-193.

Geuze, H.J., W. Stoorvogel, G.J. Strous, J.W. Slot, J.E. Bleekemolen, and I. Mellman. 1988. Sorting of mannose 6-phosphate receptors and lysosomal membrane proteins in endocytic vesicles. *J Cell Biol*. 107:2491-2501.

Gosney, J.A., D.W. Wilkey, M.L. Merchant, and B.P. Ceresa. 2018. Proteomics reveals novel protein associations with early endosomes in an epidermal growth factor-dependent manner. *The Journal of biological chemistry*. 293:5895-5908.

Guardia, C.M., G.G. Farias, R. Jia, J. Pu, and J.S. Bonifacino. 2016. BORC Functions Upstream of Kinesins 1 and 3 to Coordinate Regional Movement of Lysosomes along Different Microtubule Tracks. *Cell Rep*. 17:1950-1961.

Guerra, F., and C. Bucci. 2016. Multiple Roles of the Small GTPase Rab7. *Cells*. 5.

Hamalisto, S., and M. Jaattela. 2016. Lysosomes in cancer-living on the edge (of the cell). *Curr Opin Cell Biol*. 39:69-76.

Hartel-Schenk, S., A. Gratchev, M.L. Hanski, D. Ogorek, G. Trendelenburg, M. Hummel, M. Hopfner, H. Scherubl, M. Zeitz, and C. Hanski. 2001. Novel adapter protein AP162 connects a sialyl-Le(x)-positive mucin with an apoptotic signal transduction pathway. *Glycoconjugate journal*. 18:915-923.

Heuser, J. 1989. Changes in lysosome shape and distribution correlated with changes in cytoplasmic pH. *J Cell Biol*. 108:855-864.

Hofmann, I., and S. Munro. 2006. An N-terminally acetylated Arf-like GTPase is localised to lysosomes and affects their motility. *Journal of cell science*. 119:1494-1503.

Hutagalung, A.H., and P.J. Novick. 2011. Role of Rab GTPases in membrane traffic and cell physiology. *Physiol Rev*. 91:119-149.

Ihrke, G., A. Kyttala, M.R. Russell, B.A. Rous, and J.P. Luzio. 2004. Differential use of two AP-3-mediated pathways by lysosomal membrane proteins. *Traffic*. 5:946-962.

Ivan, V., E. Martinez-Sanchez, L.E. Sima, V. Oorschot, J. Klumperman, S.M. Petrescu, and P. van der Sluijs. 2012. AP-3 and Rabip4' coordinately regulate spatial distribution of lysosomes. *PloS one*. 7:e48142.

Jeyakumar, M., R.A. Dwek, T.D. Butters, and F.M. Platt. 2005. Storage solutions: treating lysosomal disorders of the brain. *Nat Rev Neurosci*. 6:713-725.

Jiang, P., T. Nishimura, Y. Sakamaki, E. Itakura, T. Hatta, T. Natsume, and N. Mizushima. 2014. The HOPS complex mediates autophagosome-lysosome fusion through interaction with syntaxin 17. *Mol Biol Cell*. 25:1327-1337.

Jimenez-Orgaz, A., A. Kvainickas, H. Nagele, J. Denner, S. Eimer, J. Dengjel, and F. Steinberg. 2018. Control of RAB7 activity and localization through the retromer-TBC1D5 complex enables RAB7-dependent mitophagy. *The EMBO journal*. 37:235-254.

Johnson, D.E., P. Ostrowski, V. Jaumouille, and S. Grinstein. 2016. The position of lysosomes within the cell determines their luminal pH. *J Cell Biol*. 212:677-692.

Jordens, I., M. Fernandez-Borja, M. Marsman, S. Dusseljee, L. Janssen, J. Calafat, H. Janssen, R. Wubbolts, and J. Neefjes. 2001. The Rab7 effector protein RILP controls lysosomal transport by inducing the recruitment of dynein-dynactin motors. *Current biology : CB*. 11:1680-1685.

Kaksonen, M., and A. Roux. 2018. Mechanisms of clathrin-mediated endocytosis. *Nature reviews. Molecular cell biology*. 19:313-326.

Kaniuk, N.A., V. Canadien, R.D. Bagshaw, M. Bakowski, V. Braun, M. Landekic, S. Mitra, J. Huang, W.D. Heo, T. Meyer, L. Pelletier, H. Andrews-Polymenis, M. McClelland, T. Pawson, S. Grinstein, and J.H. Brumell. 2011. Salmonella exploits Arl8B-directed kinesin activity to promote endosome tubulation and cell-to-cell transfer. *Cell Microbiol*. 13:1812-1823.

Khatter, D., V.B. Raina, D. Dwivedi, A. Sindhwani, S. Bahl, and M. Sharma. 2015a. The small GTPase Arl8b regulates assembly of the mammalian HOPS complex on lysosomes. *J Cell Sci*. 128:1746-1761.

Khatter, D., A. Sindhwani, and M. Sharma. 2015b. Arf-like GTPase Arl8: Moving from the periphery to the center of lysosomal biology. *Cellular logistics*. 5:e1086501.

Kimura, S., T. Noda, and T. Yoshimori. 2007. Dissection of the autophagosome maturation process by a novel reporter protein, tandem fluorescent-tagged LC3. *Autophagy*. 3:452-460.

Kinchen, J.M., and K.S. Ravichandran. 2010. Identification of two evolutionarily conserved genes regulating processing of engulfed apoptotic cells. *Nature*. 464:778-782.

Kitagishi, Y., and S. Matsuda. 2013. RUFY, Rab and Rap Family Proteins Involved in a Regulation of Cell Polarity and Membrane Trafficking. *International journal of molecular sciences*. 14:6487-6498.

Klassen, M.P., Y.E. Wu, C.I. Maeder, I. Nakae, J.G. Cueva, E.K. Lehrman, M. Tada, K. Gengyo-Ando, G.J. Wang, M. Goodman, S. Mitani, K. Kontani, T. Katada, and K. Shen. 2010. An Arf-like small G protein, ARL-8, promotes the axonal transport of presynaptic cargoes by suppressing vesicle aggregation. *Neuron*. 66:710-723.

Klionsky, D.J., K. Abdelmohsen, A. Abe, M.J. Abedin, H. Abeliovich, A. Acevedo Arozena, H. Adachi, C.M. Adams, P.D. Adams, K. Adeli, P.J. Adhihetty, S.G. Adler, G. Agam, R. Agarwal, M.K. Aghi, M. Agnello, P. Agostinis, P.V. Aguilar, J. Aguirre-Ghiso, E.M. Airoldi, S. Ait-Si-Ali, T. Akematsu, E.T. Akporiaye, M. Al-Rubeai, G.M. Albaiceta, C. Albanese, D. Albani, M.L. Albert, J. Aldudo, H. Algul, M. Alirezaei, I. Alloza, A. Almasan, M. Almonte-Beceril, E.S. Alnemri, C. Alonso, N. Altan-Bonnet, D.C. Altieri, S. Alvarez, L. Alvarez-Erviti, S. Alves, G. Amadoro, A. Amano, C. Amantini, S. Ambrosio, I. Amelio, A.O. Amer, M. Amessou, A. Amon, Z. An, F.A. Anania, S.U. Andersen, U.P. Andley, C.K. Andreadi, N. Andrieu-Abadie, A. Anel, D.K. Ann, S. Anoopkumar-Dukie, M. Antonioli, H. Aoki, N. Apostolova, S. Aquila, K. Aquilano, K. Araki, E. Arama, A. Aranda, J. Araya, A. Arcaro, E. Arias, H. Arimoto, A.R. Ariosa, J.L. Armstrong, T. Arnould, I. Arsov, K. Asanuma, V. Askanas, E. Asselin, R. Atarashi, S.S. Atherton, J.D. Atkin, L.D. Attardi, P. Auberger, G. Auburger, L. Aurelian, R. Autelli, L. Avagliano, M.L. Avantaggiati, L. Avrahami, S. Awale, N. Azad, T. Bachetti, J.M. Backer, D.H. Bae, J.S. Bae, O.N. Bae, S.H. Bae, E.H. Baehrecke, S.H. Baek, S. Baghdiguian, A. Bagniewska-Zadworna, et al. 2016. Guidelines for the use and interpretation of assays for monitoring autophagy (3rd edition). *Autophagy*. 12:1-222.

Korolchuk, V.I., and D.C. Rubinsztein. 2011. Regulation of autophagy by lysosomal positioning. *Autophagy*. 7:927-928.

Korolchuk, V.I., S. Saiki, M. Lichtenberg, F.H. Siddiqi, E.A. Roberts, S. Imarisio, L. Jahreiss, S. Sarkar, M. Futter, F.M. Menzies, C.J. O'Kane, V. Deretic, and D.C. Rubinsztein. 2011. Lysosomal positioning coordinates cellular nutrient responses. *Nat Cell Biol*. 13:453-460.

Kuijl, C., M. Pilli, S.K. Alahari, H. Janssen, P.S. Khoo, K.E. Ervin, M. Calero, S. Jonnalagadda, R.H. Scheller, J. Neefjes, and J.R. Junutula. 2013. Rac and Rab GTPases dual effector Nischarin regulates vesicle maturation to facilitate survival of intracellular bacteria. *The EMBO journal*. 32:713-727.

Kukimoto-Niino, M., T. Takagi, R. Akasaka, K. Murayama, T. Uchikubo-Kamo, T. Terada, M. Inoue, S. Watanabe, A. Tanaka, Y. Hayashizaki, T. Kigawa, M. Shirouzu, and S. Yokoyama. 2006. Crystal structure of the RUN domain of the RAP2-interacting protein x. *The Journal of biological chemistry*. 281:31843-31853.

Kumari, S., S. Mg, and S. Mayor. 2010. Endocytosis unplugged: multiple ways to enter the cell. *Cell research*. 20:256-275.

Langemeyer, L., F. Frohlich, and C. Ungermann. 2018. Rab GTPase Function in Endosome and Lysosome Biogenesis. *Trends in cell biology*. 28:957-970.

Li, X., N. Rydzewski, A. Hider, X. Zhang, J. Yang, W. Wang, Q. Gao, X. Cheng, and H. Xu. 2016. A molecular mechanism to regulate lysosome motility for lysosome positioning and tubulation. *Nat Cell Biol*. 18:404-417.

Lim, C.Y., and R. Zoncu. 2016. The lysosome as a command-and-control center for cellular metabolism. *The Journal of cell biology*. 214:653-664.

Lin, X., T. Yang, S. Wang, Z. Wang, Y. Yun, L. Sun, Y. Zhou, X. Xu, C. Akazawa, W. Hong, and T. Wang. 2014. RILP interacts with HOPS complex via VPS41 subunit to regulate endocytic trafficking. *Sci Rep*. 4:7282.

Luzio, J.P., P.R. Pryor, and N.A. Bright. 2007. Lysosomes: fusion and function. *Nature reviews. Molecular cell biology*. 8:622-632.

Mari, M., E. Macia, Y. Le Marchand-Brustel, and M. Cormont. 2001. Role of the FYVE finger and the RUN domain for the subcellular localization of Rabip4. *The Journal of biological chemistry*. 276:42501-42508.

Marwaha, R., S.B. Arya, D. Jagga, H. Kaur, A. Tuli, and M. Sharma. 2017. The Rab7 effector PLEKHM1 binds Arl8b to promote cargo traffic to lysosomes. *The Journal of cell biology*. 216:1051-1070.

McEwan, D.G., and I. Dikic. 2015. PLEKHM1: Adapting to life at the lysosome. *Autophagy*. 11:720-722.

McEwan, D.G., D. Popovic, A. Gubas, S. Terawaki, H. Suzuki, D. Stadel, F.P. Coxon, D. Miranda de Stegmann, S. Bhogaraju, K. Maddi, A. Kirchof, E. Gatti, M.H. Helfrich, S. Wakatsuki, C. Behrends, P. Pierre, and I. Dikic. 2015a. PLEKHM1 regulates autophagosome-lysosome fusion through HOPS complex and LC3/GABARAP proteins. *Mol Cell*. 57:39-54.

McEwan, D.G., B. Richter, B. Claudi, C. Wigge, P. Wild, H. Farhan, K. McGourty, F.P. Coxon, M. Franz-Wachtel, B. Perdu, M. Akutsu, A. Habermann, A. Kirchof, M.H. Helfrich, P.R. Odgren, W. Van Hul, A.S. Frangakis, K. Rajalingam, B. Macek, D.W. Holden, D. Bumann, and I. Dikic. 2015b. PLEKHM1 regulates Salmonella-containing vacuole biogenesis and infection. *Cell host & microbe*. 17:58-71.

Michelet, X., S. Garg, B.J. Wolf, A. Tuli, P. Ricciardi-Castagnoli, and M.B. Brenner. 2015. MHC class II presentation is controlled by the lysosomal small GTPase, Arl8b. *J Immunol*. 194:2079-2088.

Michelet, X., A. Tuli, H. Gan, C. Geadas, M. Sharma, H.G. Remold, and M.B. Brenner. 2018. Lysosome-Mediated Plasma Membrane Repair Is Dependent on the Small GTPase Arl8b and Determines Cell Death Type in Mycobacterium tuberculosis Infection. *J Immunol*. 200:3160-3169.

Mohamud, Y., J. Shi, J. Qu, T. Poon, Y.C. Xue, H. Deng, J. Zhang, and H. Luo. 2018. Enteroviral Infection Inhibits Autophagic Flux via Disruption of the SNARE Complex to Enhance Viral Replication. *Cell reports*. 22:3292-3303.

Mori, T., T. Wada, T. Suzuki, Y. Kubota, and N. Inagaki. 2007. Singar1, a novel RUN domain-containing protein, suppresses formation of surplus axons for neuronal polarity. *The Journal of biological chemistry*. 282:19884-19893.

Mrakovic, A., J.G. Kay, W. Furuya, J.H. Brumell, and R.J. Botelho. 2012. Rab7 and Arl8 GTPases are necessary for lysosome tubulation in macrophages. *Traffic*. 13:1667-1679.

Nag, S., S. Rani, S. Mahanty, C. Bissig, P. Arora, C. Azevedo, A. Saiardi, P. van der Sluijs, C. Delevoye, G. van Niel, G. Raposo, and S.R.G. Setty. 2018. Rab4A organizes endosomal domains for sorting cargo to lysosome-related organelles. *Journal of cell science*. 131.

Nakae, I., T. Fujino, T. Kobayashi, A. Sasaki, Y. Kikko, M. Fukuyama, K. Gengyo-Ando, S. Mitani, K. Kontani, and T. Katada. 2010. The arf-like GTPase Arl8 mediates delivery of endocytosed macromolecules to lysosomes in Caenorhabditis elegans. *Molecular biology of the cell*. 21:2434-2442.

Nakamura, S., and T. Yoshimori. 2017. New insights into autophagosome-lysosome fusion. *Journal of cell science*. 130:1209-1216.

Naslavsky, N., J. Rahajeng, M. Sharma, M. Jovic, and S. Caplan. 2006. Interactions between EHD proteins and Rab11-FIP2: a role for EHD3 in early endosomal transport. *Mol Biol Cell*. 17:163-177.

Nguyen, T.N., B.S. Padman, J. Usher, V. Oorschot, G. Ramm, and M. Lazarou. 2016. Atg8 family LC3/GABARAP proteins are crucial for autophagosome-lysosome fusion but not autophagosome formation during PINK1/Parkin mitophagy and starvation. *The Journal of cell biology*. 215:857-874.

Nishikiori, M., M. Mori, K. Dohi, H. Okamura, E. Katoh, S. Naito, T. Meshi, and M. Ishikawa. 2011. A host small GTP-binding protein ARL8 plays crucial roles in tobamovirus RNA replication. *PLoS Pathog*. 7:e1002409.

Niwa, S., D.M. Lipton, M. Morikawa, C. Zhao, N. Hirokawa, H. Lu, and K. Shen. 2016. Autoinhibition of a Neuronal Kinesin UNC-104/KIF1A Regulates the Size and Density of Synapses. *Cell Rep*. 16:2129-2141.

Okai, T., Y. Araki, M. Tada, T. Tateno, K. Kontani, and T. Katada. 2004. Novel small GTPase subfamily capable of associating with tubulin is required for chromosome segregation. *Journal of cell science*. 117:4705-4715.

Pankiv, S., E.A. Alemu, A. Brech, J.A. Bruun, T. Lamark, A. Overvatn, G. Bjorkoy, and T. Johansen. 2010. FYCO1 is a Rab7 effector that binds to LC3 and PI3P to mediate microtubule plus end-directed vesicle transport. *The Journal of cell biology*. 188:253-269.

Platt, F.M., B. Boland, and A.C. van der Spoel. 2012. The cell biology of disease: lysosomal storage disorders: the cellular impact of lysosomal dysfunction. *J Cell Biol*. 199:723-734.

Pu, J., C.M. Guardia, T. Keren-Kaplan, and J.S. Bonifacino. 2016. Mechanisms and functions of lysosome positioning. *Journal of cell science*. 129:4329-4339.

Pu, J., T. Keren-Kaplan, and J.S. Bonifacino. 2017. A Ragulator-BORC interaction controls lysosome positioning in response to amino acid availability. *The Journal of cell biology*. 216:4183-4197.

Pu, J., C. Schindler, R. Jia, M. Jarnik, P. Backlund, and J.S. Bonifacino. 2015. BORC, a multisubunit complex that regulates lysosome positioning. *Developmental cell*. 33:176-188.

Reddy, A., E.V. Caler, and N.W. Andrews. 2001. Plasma membrane repair is mediated by Ca(2+)-regulated exocytosis of lysosomes. *Cell*. 106:157-169.

Reinecke, J.B., D. Katafiasz, N. Naslavsky, and S. Caplan. 2015. Novel functions for the endocytic regulatory proteins MICAL-L1 and EHD1 in mitosis. *Traffic*. 16:48-67.

Rocha, N., C. Kuijl, R. van der Kant, L. Janssen, D. Houben, H. Janssen, W. Zwart, and J. Neefjes. 2009. Cholesterol sensor ORP1L contacts the ER protein VAP to control Rab7-RILP-p150 Glued and late endosome positioning. *J Cell Biol*. 185:1209-1225.

Rogov, V.V., A. Stolz, A.C. Ravichandran, D.O. Rios-Szwed, H. Suzuki, A. Kniss, F. Lohr, S. Wakatsuki, V. Dotsch, I. Dikic, R.C. Dobson, and D.G. McEwan. 2017. Structural and functional analysis of the GABARAP interaction motif (GIM). *EMBO reports*. 18:1382-1396.

Rosa-Ferreira, C., and S. Munro. 2011. Arl8 and SKIP act together to link lysosomes to kinesin-1. *Dev Cell*. 21:1171-1178.

Sandvig, K., S. Pust, T. Skotland, and B. van Deurs. 2011. Clathrin-independent endocytosis: mechanisms and function. *Current opinion in cell biology*. 23:413-420.

Schiefermeier, N., J.M. Scheffler, M.E. de Araujo, T. Stasyk, T. Yordanov, H.L. Ebner, M. Offterdinger, S. Munck, M.W. Hess, S.A. Wickstrom, A. Lange, W. Wunderlich, R. Fassler, D. Teis, and L.A. Huber. 2014. The late endosomal p14-MP1 (LAMTOR2/3) complex regulates focal adhesion dynamics during cell migration. *J Cell Biol*. 205:525-540.

Settembre, C., A. Fraldi, D.L. Medina, and A. Ballabio. 2013. Signals from the lysosome: a control centre for cellular clearance and energy metabolism. *Nature reviews. Molecular cell biology*. 14:283-296.

Sharma, M., S.S. Giridharan, J. Rahajeng, N. Naslavsky, and S. Caplan. 2009. MICAL-L1 links EHD1 to tubular recycling endosomes and regulates receptor recycling. *Mol Biol Cell*. 20:5181-5194.

Shi, A., and B.D. Grant. 2013. Interactions between Rab and Arf GTPases regulate endosomal phosphatidylinositol-4,5-bisphosphate during endocytic recycling. *Small GTPases*. 4:106-109.

Sindhwani, A., S.B. Arya, H. Kaur, D. Jagga, A. Tuli, and M. Sharma. 2017. Salmonella exploits the host endolysosomal tethering factor HOPS complex to promote its intravacuolar replication. *PLoS Pathog*. 13:e1006700.

Sobacchi, C., A. Schulz, F.P. Coxon, A. Villa, and M.H. Helfrich. 2013. Osteopetrosis: genetics, treatment and new insights into osteoclast function. *Nat Rev Endocrinol*. 9:522-536.

Tabata, K., K. Matsunaga, A. Sakane, T. Sasaki, T. Noda, and T. Yoshimori. 2010. Rubicon and PLEKHM1 negatively regulate the endocytic/autophagic pathway via a novel Rab7-binding domain. *Molecular biology of the cell*. 21:4162-4172.

Takeuchi, H., A. Takada, M. Kuboniwa, and A. Amano. 2016. Intracellular periodontal pathogen exploits recycling pathway to exit from infected cells. *Cellular microbiology*. 18:928-948.

Terawaki, S., V. Camosseto, P. Pierre, and E. Gatti. 2016. RUFY4: Immunity piggybacking on autophagy? *Autophagy*. 12:598-600.

Terawaki, S., V. Camosseto, F. Prete, T. Wenger, A. Papadopoulos, C. Rondeau, A. Combes, C. Rodriguez Rodrigues, T.P. Vu Manh, M. Fallet, L. English, R. Santamaria, A.R. Soares, T. Weil, H. Hammad, M. Desjardins, J.P. Gorvel, M.A. Santos, E. Gatti, and P. Pierre. 2015. RUN and FYVE domain-containing protein 4 enhances autophagy and lysosome tethering in response to Interleukin-4. *The Journal of cell biology*. 210:1133-1152.

Tuli, A., and M. Sharma. 2018. How to do business with lysosomes: Salmonella leads the way. *Current opinion in microbiology*. 47:1-7.

Tuli, A., J. Thiery, A.M. James, X. Michelet, M. Sharma, S. Garg, K.B. Sanborn, J.S. Orange, J. Lieberman, and M.B. Brenner. 2013. Arf-like GTPase Arl8b regulates lytic granule polarization and natural killer cell-mediated cytotoxicity. *Molecular biology of the cell*. 24:3721-3735.

van der Kant, R., A. Fish, L. Janssen, H. Janssen, S. Krom, N. Ho, T. Brummelkamp, J. Carette, N. Rocha, and J. Neefjes. 2013. Late endosomal transport and tethering are coupled processes controlled by RILP and the cholesterol sensor ORP1L. *J Cell Sci*. 126:3462-3474.

Van Wesenbeeck, L., P.R. Odgren, F.P. Coxon, A. Frattini, P. Moens, B. Perdu, C.A. MacKay, E. Van Hul, J.P. Timmermans, F. Vanhoenacker, R. Jacobs, B. Peruzzi, A. Teti, M.H. Helfrich, M.J. Rogers, A. Villa, and W. Van Hul. 2007. Involvement of PLEKHM1 in osteoclastic vesicular transport and osteopetrosis in incisors absent rats and humans. *The Journal of clinical investigation*. 117:919-930.

Vazquez-Martinez, R., and M.M. Malagon. 2011. Rab proteins and the secretory pathway: the case of rab18 in neuroendocrine cells. *Frontiers in endocrinology*. 2:1.

Vukmirica, J., P. Monzo, Y. Le Marchand-Brustel, and M. Cormont. 2006. The Rab4A effector protein Rabip4 is involved in migration of NIH 3T3 fibroblasts. *The Journal of biological chemistry*. 281:36360-36368.

Wang, G., Q. Zhang, Y. Song, X. Wang, Q. Guo, J. Zhang, J. Li, Y. Han, Z. Miao, and F. Li. 2015. PAK1 regulates RUFY3-mediated gastric cancer cell migration and invasion. *Cell death & disease*. 6:e1682.

Wang, T., Z. Ming, W. Xiaochun, and W. Hong. 2011. Rab7: role of its protein interaction cascades in endo-lysosomal traffic. *Cell Signal*. 23:516-521.

Wei, Z., M. Sun, X. Liu, J. Zhang, and Y. Jin. 2014. Rufy3, a protein specifically expressed in neurons, interacts with actin-bundling protein Fascin to control the growth of axons. *Journal of neurochemistry*. 130:678-692.

Wijdeven, R.H., H. Janssen, L. Nahidiazar, L. Janssen, K. Jalink, I. Berlin, and J. Neefjes. 2016. Cholesterol and ORP1L-mediated ER contact sites control autophagosome transport and fusion with the endocytic pathway. *Nat Commun*. 7:11808.

Witwicka, H., H. Jia, A. Kutikov, P. Reyes-Gutierrez, X. Li, and P.R. Odgren. 2015. TRAFD1 (FLN29) Interacts with Plekhm1 and Regulates Osteoclast Acidification and Resorption. *PLoS One*. 10:e0127537.

Wu, Y.E., L. Huo, C.I. Maeder, W. Feng, and K. Shen. 2013. The balance between capture and dissociation of presynaptic proteins controls the spatial distribution of synapses. *Neuron*. 78:994-1011.

Xie, R., J. Wang, X. Liu, L. Wu, H. Zhang, W. Tang, Y. Li, L. Xiang, Y. Peng, X. Huang, Y. Bai, G. Liu, A. Li, Y. Wang, Y. Chen, Y. Ren, G. Li, W. Gong, S. Liu, and J. Wang. 2017. RUFY3 interaction with FOXK1 promotes invasion and metastasis in colorectal cancer. *Scientific reports*. 7:3709.

Xu, H., and D. Ren. 2015. Lysosomal physiology. *Annual review of physiology*. 77:57-80.

Yamamoto, H., H. Koga, Y. Katoh, S. Takahashi, K. Nakayama, and H.W. Shin. 2010. Functional cross-talk between Rab14 and Rab4 through a dual effector, RUFY1/Rabip4. *Molecular biology of the cell*. 21:2746-2755.

Yang, J., O. Kim, J. Wu, and Y. Qiu. 2002. Interaction between tyrosine kinase Etk and a RUN domain- and FYVE domain-containing protein RUFY1. A possible role of ETK in regulation of vesicle trafficking. *The Journal of biological chemistry*. 277:30219-30226.

Ye, S., T.W. Fowler, N.J. Pavlos, P.Y. Ng, K. Liang, Y. Feng, M. Zheng, R. Kurten, S.C. Manolagas, and H. Zhao. 2011. LIS1 regulates osteoclast formation and function through its interactions with dynein/dynactin and Plekhm1. *PloS one*. 6:e27285.

Yoshida, H., N. Okumura, Y. Kitagishi, N. Shirafuji, and S. Matsuda. 2010. Rab5(Q79L) interacts with the carboxyl terminus of RUFY3. *International journal of biological sciences*. 6:187-189.

Zhang, M., L. Chen, S. Wang, and T. Wang. 2009. Rab7: roles in membrane trafficking and disease. *Bioscience reports*. 29:193-209.

Zhao, Y.G., and H. Zhang. 2018. Autophagosome maturation: An epic journey from the ER to lysosomes. *The Journal of cell biology*.

Zhi, Q., H. Chen, F. Liu, Y. Han, D. Wan, Z. Xu, Y. Kuang, and J. Zhou. 2019. Podocalyxin-like protein promotes gastric cancer progression through interacting with RUN and FYVE domain containing 1 protein. *Cancer science*. 110:118-134.